Chapter 3 Results of the Survey

3-1 Seafloor Topography

The survey area, including the Island of Niue at the center, occupies southwestern part of the Samoa Basin in the north and northern part of the Southwest Pacific Basin in the south and the Tonga Trench bound its western edge (Fig.3-1-1). The water depth of the both basins is approximately 5,500 to 5,600m and the Tonga Trench reaches to water depth of 8,000m. The Niue Island, with many seamounts and knolls in its vicinity, is one of the largest atolls on the north-south trending sea plateau of 5,000m deep extending continuously southward from the Samoa Island in the north. In the southeast of the Niue Island, several isolated seamounts occur and one of them rises above the sea level forming a lagoon (20° S, 168° W). Other than that, at 120 nm west of the Niue Island, the Capricorn Table Mount occurs close to the Tonga Trench.

(1) Seafloor Topography by MBES

The bathymetric survey in the area was conducted only during the cruising from one sampling station to another and did not cover a whole of survey area (Appendix Fig.1) Therefore, it was not possible to produce bathymetric map of the whole area. The bathymetric map of swath width along track lines was drawn and it was superimposed on the existing map based on the satellite gravity data (Fig. 3-1-2). The topographic profile is shown in Appendix Fig. 2.

Although there are some discrepancies in water depth, the MBES bathymetric map of swath width and the existing map by satellite data, generally correspond well. Particularly, the locations of seamounts and knolls correspond well. The new findings by the MBES survey, not shown on the map by satellite data, are a seamount of 3,800m deep at latitude 19° S and longitude 168 ° 10′ W and a topographic high of 4,000m deep at latitude 18° 40′ S and longitude 167° 15′ W

Concerning topographic division of the area, the topographic high consisting of seamounts and knolls including the Niue Island is classified into the Hilly Province. This region intermittently continue to the hilly region of the western end of the Cook Islands Sea area(166° W) where survey was carried out in fiscal year 1990. The other region except the Hilly Province is classified into the Plain Province.

The classification of topographic types and their definition are given in Table 3-1-1.

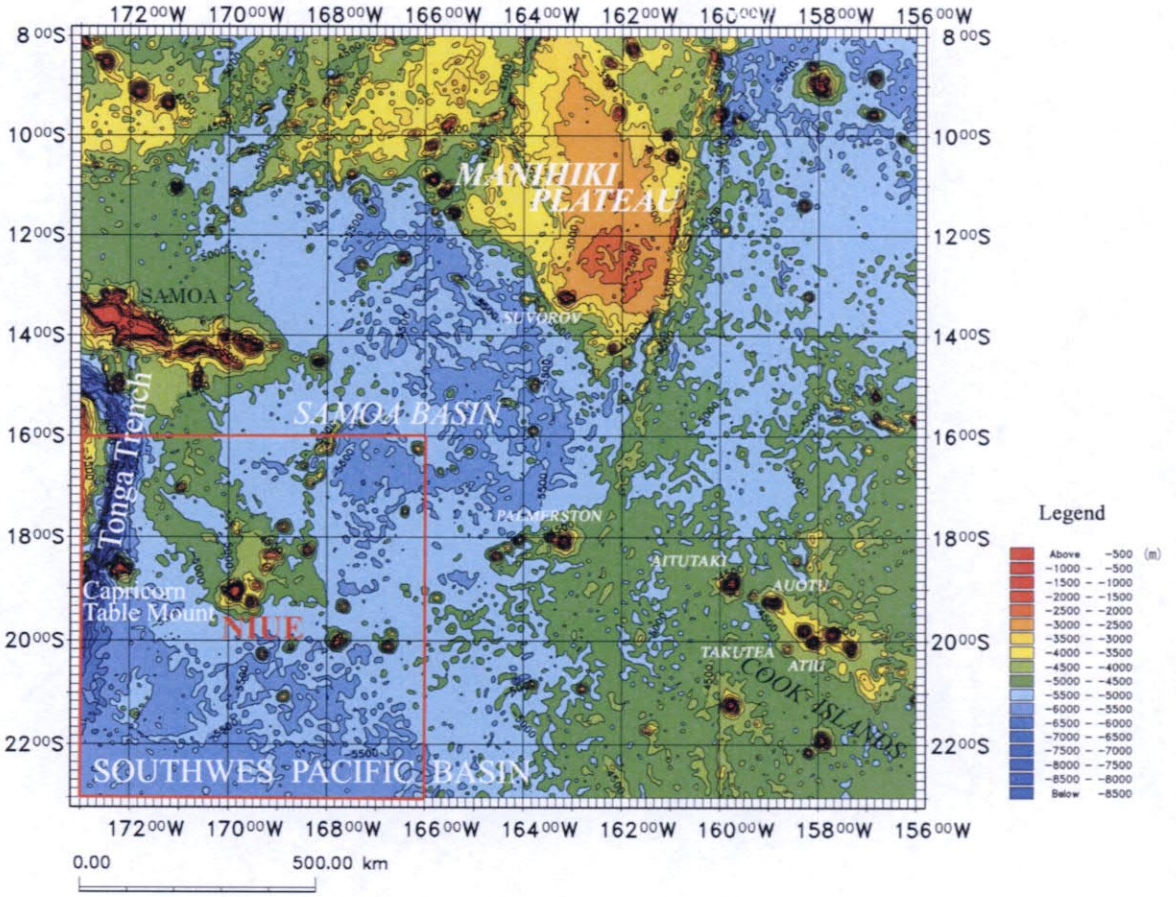

Fig. 3-1-1 Bathymetric Map of Southwest Pacific area

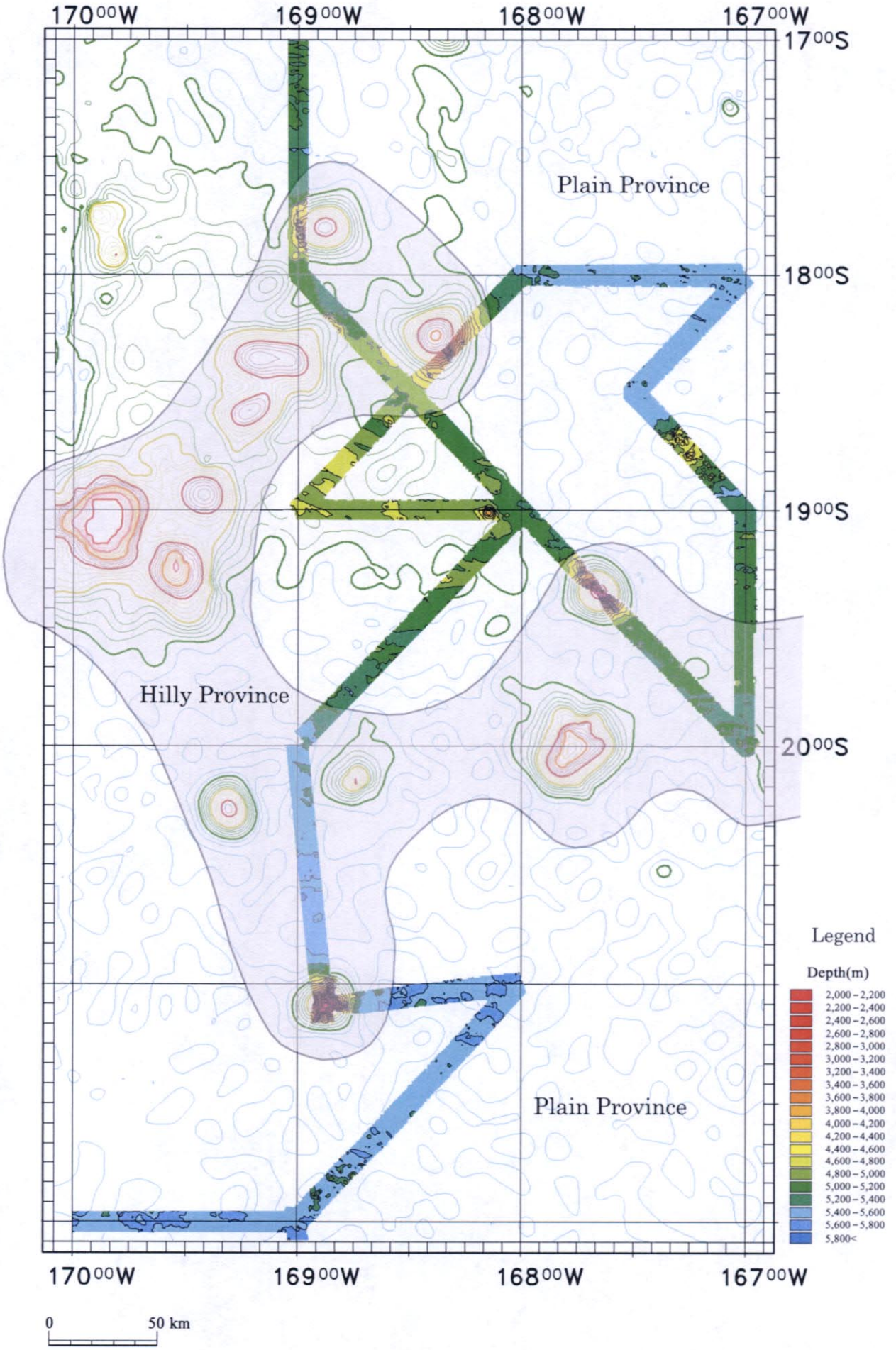

Fig. 3-1-2 Bathymetric map based on MBES

Table 3-1-1 Seafloor Topographic Division

Topographic Division	Definition
Plain Province	Seafloor is generally flat and it includes isolated seamounts and knolls.
Hilly Province	The area mainly consists of seamounts and knolls.

3-2 Survey of Surface Sediments

(1) SBP Survey

1) Classification of SBP records

The SBP records in this area are classified into three types according to the mode of acoustic reflection layers. The types with acoustically transparent layer (hereafter, "transparent layer" is used.) developing at the uppermost part of SBP records are classified as type a and type b, and ones with intercalating transparent layer at intermediate part are classified as type ac and type ec. The other group is composed only of acoustically opaque layers (opaque layers) and is subdivided into type d1, d2, and ds.

The definition of each type is given below and examples of SBP records of each type are shown in Fig. 3-2-1.

i. Types with transparent layer at the uppermost part

- Type a: consists of two layers, a transparent and an opaque layers
  Transparency is high and the boundary with the opaque layer is clear. Thickness of the transparent layer is 10m to 20m.
- Type-b : consists of two layers, transparent and an opaque layers
  Transparency is low (translucent) and the boundary of the opaque layer is not so clear as type a. Thickness is similar to type a, 10m to 20m.

ii. Types with intercalating transparent layer at intermediate part

- Type ac: It has three-layer structure, opaque-transparent-opaque layer.
  It consists of uppermost opaque layer of about 10m thick and the lower opaque layer, and they are intercalated by transparent layer in the middle.
- Type ec: It has three-layers structure, opaque-transparent-opaque layer.
  The uppermost layer shows striped pattern indicating a little low acoustic reflectance compared with that of type ac.

iii. Types formed by only opaque layer

- Type d1: The layer is composed solely of an opaque layer.

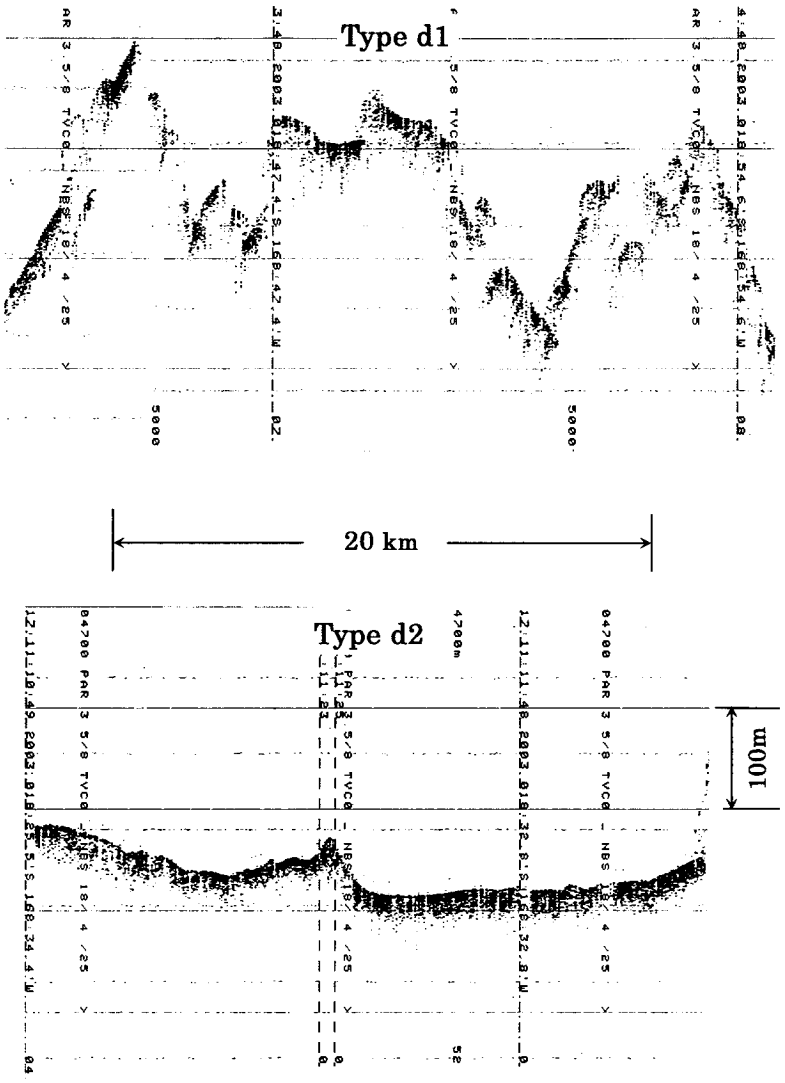

(1) One layer type, opaque layer

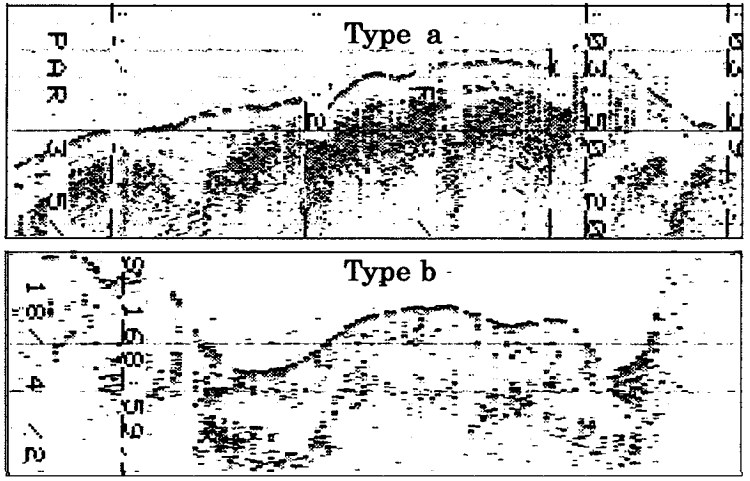

(2) Two layers type, transparent layer - opaque layer

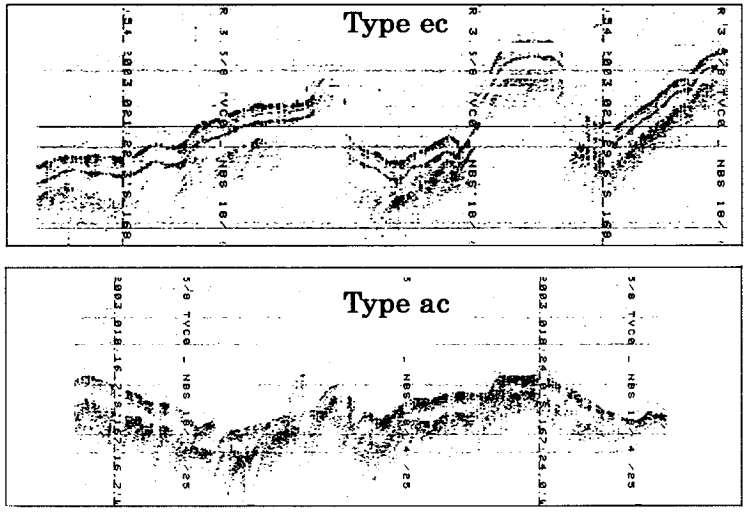

(3) Three layers type, opaque layer - transparent layer - opaque layer

Fig. 3-2-1 Types of SBP Record

This type is observed at seamounts and knolls and it suggests exposed rock.

- Type d2: The layer is composed solely of an opaque layer.
  This type is observed in flat seafloor areas (the Plain Province) and it is not always attributed to exposed rock.
- Type ds: The layer is composed solely of an opaque layer.
  This type suggests an exposure of bedrock same as Type d1. The records of this type do not clearly show multiple hyperbolic reflection patterns because of scattering of waves by seafloor and topographic profile is not clear.

2) SBP type and distribution of acoustically transparent layer

The distribution of SBP types together with thickness of transparent layer is shown in Fig.3-2-2. In case transparent layer is intercalated by upper and lower opaque layer such as types ac and ec, the thickness means the distance from seafloor to the bottom of intermediate transparent layer or the thickness from seafloor surface to acoustic basement.

One of the acoustic characteristics of the area in view from SBP types is the dominant distribution of SBP types without uppermost transparent layer. Particularly in the area north of latitude 20° S, types d1 and d2, composed only of opaque layer, are widely distributed, suggesting very poor distribution of unconsolidated sediments on the seafloor surface (Appendix Fig. 3).

The distribution of each type in the area is as follows.

Type d1: The distribution corresponds with seamounts and knolls. No development of transparent layer (0m)

Type d2: Widely distributed in the comparatively flat sea floor area north of 20° S latitude. The development of unconsolidated sediments is assumed very poor in the area north of 20° S. The seafloor is considered to be composed of exposed rocks or consolidated sediments. As mentioned later, acoustic reflection intensity of MBES is rather high in the area. Thickness of the transparent layer is 0m as same as d1.

Type ds: The distribution is local and is observed at rugged topographic area adjacent to the type d1 area
Thickness of the transparent layer is 0m.

Type ac: This type is widely distributed in the northeast of the area and in the area between the latitudes of 20° S and 21° S. In the area north of 20° S latitude, this type is observed gradually changing from type d2. The uppermost layer of

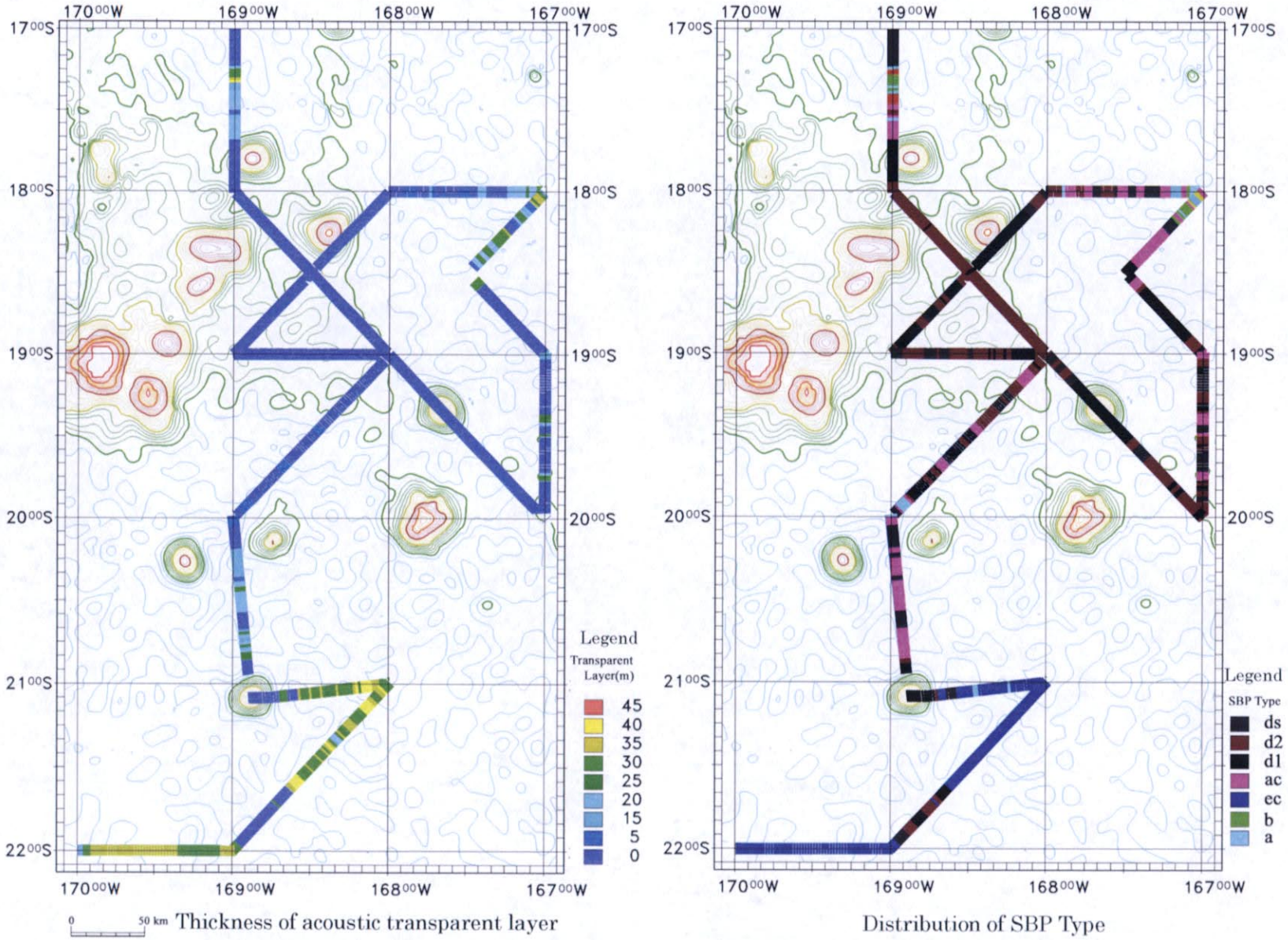

Fig. 3-2-2 Thickness of Acoustic Transparent Layer and Distribution of SBP Type

this type shows opaque layer and this may indicate the seafloor being covered by semi-consolidated sediments or coarse materials.

Thickness of the transparent layer is 10m in the northeast of the area and 10m to 20m in the area between 20° to 21° S latitude.

Type ec: It is widely distributed in the area south of 21 ° S latitude. The stripe patterned opaque layer of the uppermost part may indicate coarse, unconsolidated sediments but the acoustic reflection intensity is not so strong as type ac. Thickness of the transparent layer is 20m to 40m.

Type a: It is locally distributed at certain areas; one is at 18° S latitude and 167° W longitude and the other at 20° S latitude and 169° W longitude. The uppermost transparent layer seems to show comparatively fine-grained unconsolidated sediments. Thickness of the transparent layer is 10m to 20m.

Type b: Locally distributed at the area of 18° S latitude and 167° W longitude. It gradually changes to type a, and the uppermost transparent layer seems to suggest unconsolidated sediments, same as type a. Thickness of the transparent layer is 10m to 20m.

(2) MBES Acoustic Survey

Acoustic reflection intensity data from the seafloor by Multi-Narrow Beam Echo Sounder (MBES) is processed to produce MBES acoustic reflection intensity distribution map. The modification of obtained data was done using the factors such as change of output level, time variable gain (TVG), extent of attenuation caused by different path lengths. Further, the compensation of signal level caused by different incident angle of acoustic waves to the seafloor was done. The results are shown as the Distribution Map of Acoustic Reflection Intensity by MBES in Fig. 3-2-3. In the figure, distribution of SBP Types is shown for correlation.

The acoustic reflection intensity, generally, shows information on the distribution of surface materials such as exposed rock or unconsolidated sediments of the seafloor. Exposed rocks show strong reflection intensity, thus the area composed of such rocks is expressed as dark color (black) on the MBES image. On the contrary, weak reflection intensity coming from unconsolidated sediments is shown as pale color (light gray) on the image. The intensity of reflection for unconsolidated sediments varies affected by other parameters such as grain size, extent of compaction.

General characteristics of MBES distribution pattern mentioned above are applicable in this area and it is conformable with the distribution pattern of SBP types. That is, areas of SBP Type d1 and d2, dominantly distributed in the area north of 20° S

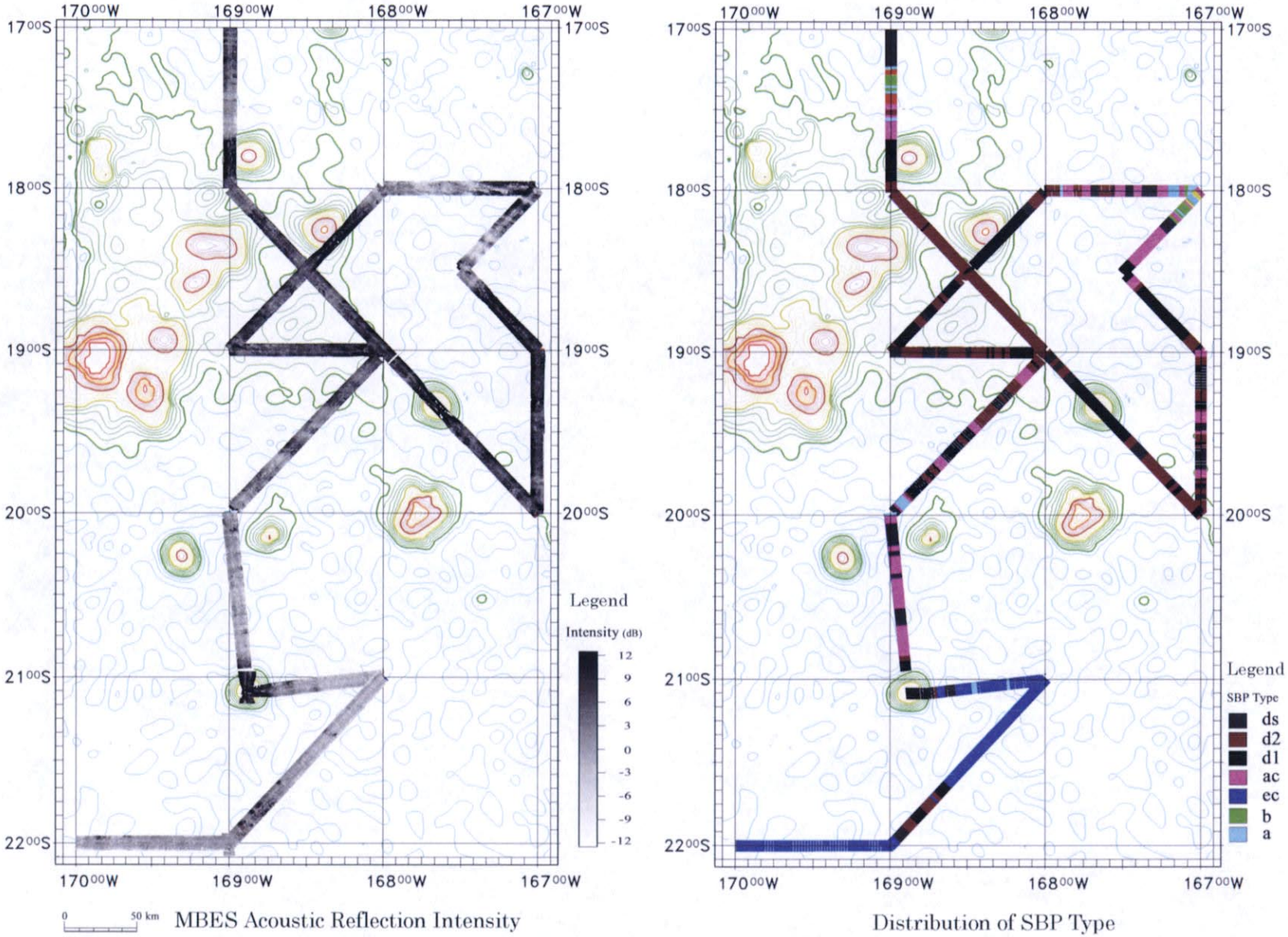

Fig. 3-2-3 MBES Acoustic Reflection Intensity and Distribution of SBP Type

latitude, represented by acoustically opaque layers, are shown as dark colors on the MBES image.

Similarly, three-layer types, such as Type ac represented by the uppermost opaque layer, transparent intermediate layer, and acoustic basement, or Type ec represented by striped uppermost layer, which are distributed in the area south of 20° S latitude and the northeastern edge of the area, appear comparatively pale color (light gray) on the MBES image.

The relations of SBP types and acoustic reflection intensity of MBES are given below.

Type d1: It corresponds to seamounts and knolls. Reflection intensity is high due to exposed rocks and represented by dark color on the MBES image. No distribution of unconsolidated sediments.

Type d2: It consists of totally opaque layer by SBP type and represented by dark color same as type d1 on the MBES image. Acoustic reflection intensity is quite high and the seafloor is assumed to consist of exposed rocks or compact sediments. No unconsolidated sediments or thin if any.

Type ac: It is shown as solely opaque layer in SBP records, however, acoustic reflection intensity is slightly low and it is represented by pale color pattern on the MBES image. Thin, soft sediments seem to cover the seafloor surface. Soft sediments are too thin to appear in SBP records.

Type ec: SBP records show opaque with striped pattern in the upper portion. It is represented by pale color on the MBES image like Type ac. Thin unconsolidated sediments are assumed to cover on the top of the opaque layer with stripes.

Type a: Top transparent layer of SBP is shown as low acoustic reflection intensity and it is represented by pale color on the image. A distribution of clayey soft sediments is assumed on the seafloor surface to the depth of acoustic basement.

Type b: Same as the type a.

3-3 Bottom Sediments

As the results of the sampling of this year, unconsolidated sediments were collected from 16 sampling points (FG: 13 points, SC: 3 points).

Collection of bottom sediments by FG was done using tube sampler attached to FG and undisturbed columnar sediments of maximum length of approximately 40cm were collected by SC. Description and examination of collected sediments, such as grain size, color and tests by hydrochloric acid and hydrogen peroxide were done soon after

collection of sediments. The smear slides of sediments were prepared for microscopic observation. Fossil identification and chemical analysis were done using samples collected by SC.

(1) Classification of Bottom Sediments

Description and classification of the bottom sediments collected at 16 sampling points were done by microscopic observation of smear slide. The content of terrigenous materials and volcanogenic clastic grains in the sediments are less than 10% and all of the samples are considered to be pelagic origin. They were classified based upon the classification of pelagic sediment shown in Table 3-3-1.

Table 3-3-1 Classification Bottom Sediments

	Total Fossil (%)	Siliceous Fossil*1 (%)	Calcareous Fossil *2 (%)	Remarks
Brown clay	<10			
Insoluble brown clay	<10			Impermeable clay
Zeolitic clay	<10			Contain 5 to 10% zeolite
Siliceous clay	10 to 30		<5	
Silic-calcareous clay	10 to 30		>5	Siliceous fossil> Calcareous fossil
Calc-siliceous clay	10 to 30	>5		Calcareous fossil> Siliceous fossil
Calcareous clay	10 to 30	<5		
Foraminiferal ooze	>30			Calcareous fossil> Siliceous fossil Mainly foraminifer fossils
Cocolith ooze	>30			Calcareous fossil> Siliceous fossil Mainly coccolith
Silic-calcareous ooze	>30			Siliceous fossil>calcareous fossil
Siliceous ooze	>30			

*1 radiolaria, siliceous algae, spines of sponge, siliceous flagella

*2 foraminifer, calcareous nannoplankton

(2) Characteristics of Bottom Sediments

Among 36 sampling points by FG and SC (FG: 29 points, SC: 7 points), sediments were collected at 16 sampling points and they are all fall into insoluble brown clay. The content of organic materials is comparatively small and there is no ooze sample with the content of organic remains over 30%. Contained siliceous fossil are radiolaria and

sponge spines, and they are observed in almost all samples but the amount is not more than 5%. Foraminiferal remains are, except few examples (excluding samples collected from shallower than 5,000m deep), rarely observed. Contrary to a small amount of organic fossil remains, some samples contain volcanogenic clastics as much as 10% and most of the samples contain a few %.

A color tone of brown clay is, in order of abundance, moderate brown, grayish brown, and dark gray, and they correspond to 10YR 3/4, 10YR3/3 to 4/3, 10YR2/2 to 3/2 on Munsell Soil Color Charts.

Main constituents of brown clay, under microscope observation of smear slides, are clay minerals, volcanic clastics and siliceous organic remains, and a small amount of amorphous materials, zeolites, micro-nodules (ferro manganese oxides) and others are contained. Micro-nodules associated with subcompact muddy concretion occur in all samples and almost all of them are minute grains.

(3) Bottom Sediments Samples of SC

The sampling by SC at 7 points was conducted to obtain the information of vertical variation of sediments and buried manganese nodules. Unconsolidated sediments with thickness ranging from 30cm to 38cm were collected at three points and their columnar profiles are shown in Appendix Fig. 5. The collected sediments are clay with color of dark grayish brown to dark gray (10YR2/2 to 19YR 3/1), and all the surface sediments fall into insoluble brown clay under the microscopic observation of smear slides. At the point 03S2327SC01, buried manganese nodules were confirmed associated with thin manganese oxides film at depth of 23cm to 26cm. A covering ration of 3 % to 6% was estimated to the buried manganese nodules.

(4) CCD (Carbonate Compensation Depth)

The smear slide observation and the occurrences of radiolarian fossils and foraminiferal fossil suggest that almost all sediments samples are obtained from the depths close to CCD or deeper than CCD. Take into the account of the fact that identifiable foraminiferal fossils were obtained from the sample of 03S2027SC01(water depth: 4,754m), CCD of this area is assumed to be about 4,800m to 5,000m deep.

(5) Distribution of Bottom Sediments

All the sediments samples collected at 16 sampling points are classified into insoluble brown clay. This suggests a wide distribution of insoluble brown clay over the whole area. While, in previously surveyed area of the Cook Islands, the eastern

vicinity of Niue area, brown clay is dominantly distributed over the whole area with rare occurrences (several sampling points) of insoluble clay.

(6) Analyses of Bottom Sediments

1) Constituent Minerals (X-ray diffraction analysis)

For identification of minerals not identifiable by microscope and obtaining the information of vertical variation of constituent minerals, 10 samples of sediments collected by SC were selected for X-ray diffraction analyses. The analyses of bulk samples were done on the non-orientation method and the conditions of analyses are given below.

X-ray diffraction device	Rigaku Corp.Geigerflx RAD-2C Type
Cathode	Cu
Filter	Ni
Cathode Tube Voltage	30kv
Current	15mA
Full-scale of count	1,000cps
Time constant	1 sec
Scanning speed	2° /min.
Recording paper speed	2cm/min.
Slit condition	1° −1° − 0.3mm
Scan range	2θ =2° ~70°

The results of X-ray diffraction analysis are shown in Table 3-3-2. The characteristics of bottom sediments in the area are summarized as follows.

i. The identified minerals are plagioclase, quarts, clinopyroxene, potassium feldspar, tridymite, hornblende, and calcite is rarely included. Particularly, 03S2327SC01XR01 (Depth 0 to 1cm) is rich in calcite, suggesting that the sediments are derived from limestone or calcareous fossil remains. This is agreeable with topographic characteristics of the area with scattered small-scale seamounts and knolls.

ii. 03S2027SC01XR01 is relatively high in zeolite (phillipsite).

iii. Almost all samples contain rare amount of illite, illite-smectite mixed layer and chlorite. However, clay minerals were not found in the samples, 03S2027SC01XR02 (Depth 20 to 25cm) and 03S2326SC01XR02 (Depth 0 to 3cm).

Table 3-3-2 Result of X-ray Diffraction Analysis of Seafloor Sediments

No.	Sea Area	Station No.	Sample No.		Depth(m)	Core Depth(m)	Silicate minerals										Sulfate		Carbonate		Others			Remarks
							Quartz	Tridymite	Plagioclase	Potash feldspar	Hornblende	Clinopyroxine	Phillipsite	Illite/smectite	Illite	Chlorite	Gypsum		Calcite		Pyrite	Geothite	Halite	
1	Niue	03503	03S2027SC01	XR01	4,754	0.00 ~ 0.05	4.7	0.6	>11.1	1.1	0.2		4.1	0.3	0.8	0.6			0.1				2.2	
2				XR02	4,754	0.20 ~ 0.25	0.4	0.6	5.7	1.0		1.7											0.7	
4		03513	03S2327SC01	XR01	5,569	0.00 ~ 0.01	2.7	0.3	1.6	0.6	0.1	0.4		0.2	0.3	0.3			4.8				3.2	
5				XR02	5,569	0.15 ~ 0.20	4.3		2.7	1.1	0.2	0.9		0.2	0.7	0.7	0.2				0.2		3.1	
6				XR03	5,569	0.23 ~ 0.26	2.6	0.3	3.9	1.0		1.3		0.2	0.3	0.2					0.1		2.0	Albitized plagioclase
7				XR04	5,569	0.30 ~ 0.33	7.1		3.1		0.1			0.2	1.1	0.8			0.2				2.8	Albitized plagioclase
8		03514	03S2326SC01	XR01	5,620	0.00 ~ 0.03	0.4	0.8	4.4	1.1	0.2	1.6							0.3		0.1		1.2	
9				XR02	5,620	0.10 ~ 0.15	2.9		1.7	0.4		0.8		0.2	0.3	0.4						0.3	2.1	
10				XR03	5,620	0.15 ~ 0.20	5.2	0.3	2.6	0.6	0.1	0.9		0.2	0.7	0.6	0.2						3.1	
11				XR04	5,620	0.26 - 0.30	4.6	0.3	3.9	0.7	0.2	0.8		0.1	0.7	0.6							2.6	

Showing by Quartz Index

iv. The samples, 03S2327SC01XR02 and XR03, 03S2326SC01XR01 and XR02 contain pyrite and goethite but diffraction peaks of these are weak and these minerals may be contained also in other samples.

2) Chemical Composition (Major and Trace elements)

The chemical analyses of major and trace elements were conducted for 10 sediments samples of X-ray diffraction analyses. Before the chemical analyses the samples are sufficiently desalinized. The analytical methods and detection limit of each element are given below (Table3-3-3)

Table 3-3-3 List of Analysis Method

Element	Analysis Method	Detection Limit
SiO_2, TiO_2, Al_2O_3, Fe_2O_3 MnO, MgO, CaO, BaO Na_2O, K_2O, P_2O_5	ICP mass spectrometry	0.01%
FeO	Titration	0.01%
LOI	Weight method	0.01%
CO_2, H_2O^+, H_2O^-	Induction furnace infrared absorption method (LECO Corp)	0.01%
Pb, Zn, Ni, Cu, Co, Sr, V Mo	ICP mass spectrometry	1ppm
B	Neutron activation analysis	1ppm
As	Atomic Absorption spectrometry	1ppm
Y	ICP mass spectrometry	1ppm

The results of chemical analyses of the area, together with results of the Cook Islands area and typical deep-sea bottom sediments of the world, are shown in Tables 3-3-4 (1) and (2). The results of principal component analysis are given in Tables 3-3-5 to 3-3-8. The followings are the chemical characteristics of the sediments of the area.

i. Surface sediments (0 to 5cm deep): Compared with typical deep-sea sediments of red clay, SiO_2 is about the same value ranging from 49.21% to 54.90% , Al_2O_3 is slightly low value of 11.98% to 14.91%. TiO_2, Fe_2O_3 and MnO are 0.62% to 0.64%, 4.56% to 5.38%

Table 3-3-4 (1) Results of Chemical Analysis (Niue Area)

Sample Name	Depth	SiO_2	TiO_2	Al_2O_3	Cr_2O_3	Fe_2O_3	FeO	MnO	MgO	CaO	Na_2O	K_2O	P_2O_5	CO_2	H_2O^-	H_2O^+	LOI	Total
		%	%	%	%	%	%	%	%	%	%	%	%	%	%	%	%	%
03S2027SC01 CS01	0–5cm	49.21	0.62	11.98	0.03	5.37	3.41	0.50	3.41	5.15	3.90	1.29	0.18	2.13	3.44	1.47	12.55	97.60
03S2027SC01 CS02	20–25cm	45.59	0.59	11.43	0.01	5.49	2.57	0.44	2.92	8.29	3.45	1.33	0.16	8.58	3.56	2.55	15.55	97.82
03S2327SC01 CS01	0–1cm	54.60	0.64	14.69	0.04	4.56	5.92	0.19	3.94	8.91	2.11	0.71	0.10	0.51	0.25	0.40	1.27	97.68
03S2327SC01 CS02	15–20cm	51.72	0.63	13.35	0.02	5.22	3.15	0.35	3.59	4.46	3.54	1.67	0.12	1.25	3.04	2.64	10.05	97.87
03S2327SC01 CS03	23–26cm	51.84	0.66	14.11	0.02	5.16	4.05	0.30	4.15	5.93	3.47	1.44	0.11	0.81	2.26	1.85	7.19	98.43
03S2327SC01 CS04	30–33cm	50.49	0.67	13.99	0.01	6.12	1.67	0.50	3.28	2.28	4.02	2.30	0.14	1.69	3.32	3.55	12.50	97.97
03S2326SC01 CS01	0–3cm	54.90	0.64	14.91	0.02	4.75	5.79	0.18	3.87	8.99	2.02	0.60	0.09	0.22	0.17	0.26	0.91	97.67
03S2326SC01 CS02	10–15cm	53.07	0.63	13.26	0.02	5.31	3.09	0.45	3.18	4.32	3.67	1.63	0.14	1.54	2.56	2.58	9.00	97.77
03S2326SC01 CS03	15–20cm	52.58	0.63	13.21	0.03	4.79	3.34	0.35	3.32	4.18	3.79	1.76	0.12	1.17	2.80	2.52	9.74	97.84
03S2326SC01 CS04	26–30cm	52.13	0.64	13.96	0.02	5.02	3.73	0.31	3.67	4.82	3.38	1.67	0.11	1.17	2.73	2.39	8.67	98.13

Sample Name	Depth	Pb	Zn	Ni	Cu	Co	Sr	V	Mo	Ba	As	Y
		ppm	ppm	ppm	ppm	ppm	ppm	ppm	ppm	ppm	ppm	ppm
03S2027SC01 CS01	0–5cm	29.7	168	46.9	262	43.3	266	205	9.2	390	74.6	24.8
03S2027SC01 CS02	20–25cm	27.6	89	47.9	178	41.2	419	176	2.0	390	12.1	27.2
03S2327SC01 CS01	0–1cm	3.8	58	24.8	152	33.9	269	322	1.8	150	5.0	15.3
03S2327SC01 CS02	15–20cm	21.8	67	46.3	143	41.2	232	206	1.5	370	7.9	18.1
03S2327SC01 CS03	23–26cm	17.0	68	41.3	150	40.0	249	257	1.3	310	6.0	17.7
03S2327SC01 CS04	30–33cm	37.7	87	72.1	136	46.8	231	160	2.1	540	10.1	23.8
03S2326SC01 CS01	0–3cm	2.5	67	20.3	168	34.3	265	336	1.5	150	5.2	15.4
03S2326SC01 CS02	10–15cm	23.7	75	44.7	275	41.6	226	189	1.9	350	12.0	21.5
03S2326SC01 CS03	15–20cm	26.6	95	43.5	181	36.9	213	194	1.8	350	21.7	18.4
03S2326SC01 CS04	26–30cm	25.3	76	44.5	179	37.4	218	210	2.5	340	36.8	17.6

Table 3-3-4(2) Chemical Analysis (Cook Islands Area and published data)

Sample Name	Depth	SiO_2	TiO_2	Al_2O_3	Cr_2O_3	Fe_2O_3	FeO	MnO	MgO	CaO	Na_2O	K_2O	P_2O_5	CO_2	H_2O^-	H_2O^+	LOI	Total	
		%	%	%	%	%	%	%	%	%	%	%	%	%	%	%	%	%	
00S1934SC04	0–5cm	38.69	1.03	11.60	–	8.94	0.25	1.69	3.09	4.88	4.91	1.92	0.57	3.19	2.20	1.16	22.59	100.16	Cook Islands Area
00S1736SC31	5–10cm	37.65	1.59	12.05	–	10.87	0.17	2.08	3.33	2.95	5.45	1.87	0.63	1.14	6.10	2.63	21.83	100.47	Cook Islands Area
00S1636SC19	0–10cm	34.20	1.46	10.89	–	9.99	0.15	1.85	2.97	7.66	4.78	1.72	0.59	5.02	4.28	2.24	24.56	100.82	Cook Islands Area
00S1636SC37	0–10cm	35.81	1.58	11.55	–	11.95	0.15	2.38	3.24	2.75	5.34	1.82	0.61	1.25	7.63	3.85	23.38	100.56	Cook Islands Area
00S1338SC01	0–5cm	41.32	0.98	12.39	–	8.14	0.18	1.84	2.26	2.75	5.30	3.16	1.18	0.92	12.80	4.46	20.49	99.99	Cook Islands Area
Clarke Steiger Synthetic sample of Pacific, Atlantic and Indian Ocean*	—	54.48	0.98	15.94	–	8.66	0.84	1.21	3.31	1.96	2.05	2.85	0.30	–	7.04		–	99.62	Pacific Ocean 51samples Atlantic 8 samples Indian Ocean 2 samples
R/V Challenger*	—	54.28	–	16.41	–	13.58	1.26	1.62	1.76	0.74	1.37	1.61	0.35	–	7.02		–	100.00	
R/V Meteor*	—	55.16	0.96	16.79	–	5.65	1.38	4.13	2.76	0.27	2.41	1.09	0.32	–	9.08		–	100.00	
Red clay of SW area in Northern Pacific Ocean (Ishibashi and Harada)*	—	50.77	–	20.75	–	10.94	–	2.01	3.08	1.72	1.39	2.78	0.28	–	9.75		–	103.49	
Red clay of North Pacific Ocean (Hamaguchi)*	—	52.45	0.84	16.05	–	8.26	–	1.12	3.35	2.44	4.98	2.57	0.34	–	7.34		–	99.84	

* 'Chemistry of sediments' (1972, Tokai Univ. Press)

Sample Name	Depth	Pb	Zn	Ni	Cu	Co	Sr	V	Mo	BaO	As	Y
		ppm	ppm	ppm	ppm	ppm	ppm	ppm	ppm	%	ppm	ppm
00S1934SC04	0–5cm	66	120	256	224	196	320	170	6	0.11	33	127
00S1736SC31	5–10cm	58	120	240	288	192	328	185	9	0.19	11	120
00S1636SC19	0–10cm	58	128	223	342	177	501	191	10	0.15	16	113
00S1636SC37	0–10cm	64	146	263	365	199	365	238	19	0.14	25	117
00S1338SC01	0–5cm	48	86	270	271	162	238	128	12	0.04	12	258

Table 3-3-5 Correlation Coefficient

Correlation	SiO_2	Al_2O_3	Fe_2O_3	FeO	CaO	MgO	Na_2O	K_2O	Cr_2O_3	TiO_2	MnO	P_2O_5	CO_2	LOI	H_2O^-	H_2O^+	Pb	Zn	Ni	Cu	Co	Sr	V	Mo	Ba	As	Y
SiO_2	1.000																										
Al_2O_3	0.870	1.000																									
Fe_2O_3	−0.636	−0.413	1.000																								
FeO	0.684	0.604	−0.863	1.000																							
CaO	0.107	0.131	−0.598	0.753	1.000																						
MgO	0.654	0.757	−0.551	0.735	0.324	1.000																					
Na_2O	−0.572	−0.605	0.707	−0.911	−0.841	−0.570	1.000																				
K_2O	−0.339	−0.250	0.714	−0.891	−0.927	−0.467	0.874	1.000																			
Cr_2O_3	0.520	0.238	−0.730	0.641	0.272	0.426	−0.385	−0.493	1.000																		
TiO_2	0.555	0.773	0.123	0.086	−0.391	0.576	−0.027	0.275	0.000	1.000																	
MnO	−0.703	−0.731	0.840	−0.897	−0.654	−0.768	0.878	0.700	−0.442	−0.205	1.000																
P_2O_5	−0.798	−0.883	0.649	−0.676	−0.323	−0.729	0.688	0.359	−0.234	−0.486	0.903	1.000															
CO_2	−0.885	−0.789	0.396	−0.465	0.218	−0.693	0.256	0.079	−0.489	−0.741	0.460	0.603	1.000														
LOI	−0.885	−0.848	0.753	−0.919	−0.531	−0.777	0.866	0.692	−0.535	−0.394	0.896	0.835	0.681	1.000													
H_2O^-	−0.780	−0.771	0.724	−0.927	−0.673	−0.675	0.940	0.782	−0.489	−0.272	0.881	0.769	0.513	0.972	1.000												
H_2O^+	−0.499	−0.408	0.744	−0.948	−0.809	−0.622	0.858	0.958	−0.621	0.050	0.738	0.433	0.321	0.794	0.841	1.000											
Pb	−0.667	−0.617	0.802	−0.956	−0.790	−0.698	0.941	0.878	−0.486	−0.067	0.912	0.729	0.387	0.915	0.941	0.883	1.000										
Zn	−0.497	−0.652	0.315	−0.333	−0.254	−0.386	0.507	0.133	0.127	−0.319	0.632	0.802	0.215	0.533	0.523	0.077	0.518	1.000									
Ni	−0.577	−0.410	0.906	−0.948	−0.811	−0.570	0.866	0.920	−0.576	0.173	0.847	0.593	0.292	0.815	0.840	0.906	0.939	0.316	1.000								
Cu	−0.110	−0.476	0.041	−0.118	−0.126	−0.408	0.286	−0.044	0.172	−0.414	0.456	0.573	0.090	0.226	0.235	−0.025	0.210	0.584	−0.016	1.000							
Co	−0.623	−0.506	0.958	−0.878	−0.688	−0.537	0.819	0.737	−0.577	0.081	0.912	0.744	0.321	0.795	0.801	0.745	0.840	0.450	0.903	0.186	1.000						
Sr	−0.695	−0.562	0.145	−0.063	0.605	−0.378	−0.153	−0.340	−0.304	−0.694	0.120	0.382	0.890	0.324	0.120	−0.107	−0.023	0.099	−0.071	−0.029	0.043	1.000					
V	0.670	0.677	−0.745	0.971	0.751	0.783	−0.929	−0.870	0.514	0.206	−0.894	−0.705	−0.471	−0.931	−0.951	−0.931	−0.963	−0.389	−0.888	−0.247	−0.791	−0.034	1.000				
Mo	−0.347	−0.505	0.189	−0.122	−0.129	−0.182	0.318	−0.049	0.280	−0.260	0.476	0.698	0.072	0.336	0.341	−0.126	0.327	0.943	0.150	0.599	0.334	0.046	−0.187	1.000			
Ba	−0.647	−0.529	0.895	−0.977	−0.804	−0.637	0.916	0.906	−0.587	0.049	0.897	0.673	0.356	0.886	0.910	0.911	0.972	0.409	0.985	0.075	0.914	−0.026	−0.934	0.224	1.000		
As	−0.323	−0.498	0.114	−0.173	−0.242	−0.201	0.404	0.078	0.254	−0.266	0.448	0.617	0.043	0.380	0.428	−0.008	0.414	0.903	0.180	0.599	0.252	−0.075	−0.287	0.935	0.265	1.000	
Y	−0.892	−0.845	0.776	−0.767	−0.273	−0.814	0.653	0.423	−0.505	−0.459	0.893	0.932	0.771	0.882	0.773	0.547	0.759	0.611	0.679	0.383	0.778	0.542	−0.749	0.456	0.738	0.380	1.000

Test of non-correlation * Significance level >5% ** Significance level >1%

Determination	SiO2	Al2O3	Fe2O3	FeO	CaO	MgO	Na2O	K2O	Cr2O3	TiO2	MnO	P2O5	CO2	LOI	H2O−	H2O+	Pb	Zn	Ni	Cu	Co	Sr	V	Mo	Ba	As	Y
SiO_2	−																										
Al_2O_3	**	−																									
Fe_2O_3	*		−																								
FeO	*		**	−																							
CaO				*	−																						
MgO	*	*		*		−																					
Na_2O			*	**	**		−																				
K_2O			*	**	**		**	−																			
Cr_2O_3			*	*					−																		
TiO_2		**								−																	
MnO	*	*	**	**	*	*	**	*			−																
P_2O_5	**	**	*	*		*	*				**	−															
CO_2	**	**				*				*			−														
LOI	**	**	*	**		**	**	*			**	**	*	−													
H_2O^-	**	**	*	**	*	*	**	**			**	**		**	−												
H_2O^+			*	**	**		**	**			*			**	**	−											
Pb	*		**	**	**	*	**	**			**	*		**	**	**	−										
Zn		*										**						−									
Ni			**	**	**		**	**			**			**	**	**	**		−								
Cu																				−							
Co			**	**	*		**	*			**	*		**	**	*	**		**		−						
Sr	*									*			**									−					
V	*	*	*	**	*	**	**	**			**	*		**	**	**	**		**		**		−				
Mo												*						**						−			
Ba	*		**	**	**	*	**	**			**	*		**	**	**	**		**		**		**		−		
As																		**						**		−	
Y	**	**	**	**		**	*				**	**	**	**	**		*		*		**		*		*		−

Table 3-3-6 Eigenvalue

Principal component	Eigenvalue	Contribution rate	Cumulative Contribution rate
First principal component	16.00858	59.29%	59.29%
Second principal component	4.95472	18.35%	77.64%
Third principal component	3.34667	12.40%	90.04%
Fourth principal component	1.14877	4.25%	94.29%

Table 3-3-7 Principal Loading

Component	First principal component	Second principal component	Third principal component	Fourth principal component
SiO_2	-0.79642	-0.41523	0.32528	0.17093
Al_2O_3	-0.76300	-0.58982	0.06223	-0.17887
Fe_2O_3	0.84366	-0.24426	-0.14257	-0.40080
FeO	-0.95783	0.24977	0.12148	-0.06381
CaO	-0.65543	0.63681	-0.37374	-0.14919
MgO	-0.77822	-0.25419	0.21050	-0.33428
Na_2O	0.91007	-0.23015	0.21306	0.13748
K_2O	0.76772	-0.61332	0.03838	0.14697
Cr_2O_3	-0.54518	0.25167	0.58189	0.22310
TiO_2	-0.24436	-0.82636	0.24840	-0.40140
MnO	0.96566	0.04043	0.14162	-0.03983
P_2O_5	0.85063	0.44952	0.17790	-0.10227
CO_2	0.55590	0.55418	-0.60658	0.02119
LOI	0.97239	0.11412	-0.11310	0.05865
H_2O^-	0.95921	-0.02706	0.02477	0.11269
H_2O^+	0.83022	-0.47250	-0.18229	0.22301
Pb	0.96193	-0.18524	0.10319	0.04643
Zn	0.55931	0.49042	0.60071	-0.18461
Ni	0.89249	-0.40255	-0.01906	-0.13974
Cu	0.29419	0.47177	0.52205	0.29678
Co	0.88754	-0.20249	0.04935	-0.31416
Sr	0.18315	0.70656	-0.64453	-0.20381
V	-0.95405	0.15980	0.02942	-0.24390
Mo	0.37274	0.53018	0.69969	-0.27810
Ba	0.94637	-0.30297	0.00528	-0.08019
As	0.39871	0.43744	0.72975	-0.06989
Y	0.88711	0.36001	-0.13864	-0.16389

Table 3-3-8 Principal Component Score

Sample number	First principal component	Second principal component	Third principal component	Fourth principal component
03S2027SC01 CS01	3.834	3.581	3.858	-1.002
03S2027SC01 CS02	4.355	3.753	-3.999	0.064
03S2327SC01 CS01	-6.906	0.985	0.023	-0.171
03S2327SC01 CS02	0.563	-1.485	-0.600	0.514
03S2327SC01 CS03	-1.721	-1.600	-0.320	-1.029
03S2327SC01 CS04	5.084	-3.798	-0.481	-1.542
03S2326SC01 CS01	-6.849	0.777	-0.590	-0.785
03S2326SC01 CS02	1.560	-0.406	0.531	1.403
03S2326SC01 CS03	0.401	-0.711	0.897	1.952
03S2326SC01 CS04	-0.321	-1.097	0.681	0.596

and 0.18% to 0.50%, respectively, and lower than those of red clay. On the other hand, CaO is, 5.15% to 8.99%, higher than red clay. This high CaO content is explained by the reason that the sampling depth (4,754m to 5,620m) is near carbonate compensation depth (CCD) or slightly shallower, and calcareous remains such as foraminifer are not completely dissolved and are left to some extent in the sediments.

ii. Compared to unconsolidated sediments of the Cook Islands area, SiO_2, FeO and LOI are apparently high and Fe_2O_3 is low. The analytical results of Niue sediments reflect the evidence that volcanogenic clastic grains escaped from post-deposition alteration are comparatively abundant in the sediments. The chemical compositions of the sediments are strongly affected by constituent minerals of volcanogenic clstics, and this agrees with the results that many rock- forming minerals are detected by X-ray diffraction analysis.

iii. The vertical profile of chemical compositions of the sampling point 03503 (03S2027SC01) shows rather uniform value except CaO. The CaO content is low at the surface, and this strongly suggests dissolution of carbonates after deposition. The tendency of this chemical difference at the surface is, similarly, admitted at the sample point 03514(03S2326SC01). This fact strongly suggests that both seafloor surfaces have been exposed to the seawater longer enough to show the present chemical composition.

iv. The vertical chemical variation is not so simple as iii at 03513 (03S2327SC01). There is a compositional gap between the samples CS02 (Depth 15-20cm) and CS03 (Depth 23-26cm). For example, major elements such as SiO_2, Al_2O_3, FeO, CaO, and MgO decrease toward depths but it increases between CS02 and CS03. On the contrary, CO_2, LOI, Na_2O, and MnO tend to increase toward depths but they decrease once between CS02 and CS03. This agrees with facies change of the sediments and explains the existence of buried manganese nodules at CS03. The vertical chemical variation, also, suggests an existence of hiatus between CS02 and CS03.

Principal Component Analysis: Brown clay (red clay) deposited on the deep seafloor of pelagic environment is multi-source sediments mainly consist of such as terrigenous grains of clay transported by wind, volcanogenic clastics, organic skeletons, autochtonous minerals and cosmic materials. For the purpose of estimating sedimentary environment of each sample, principal component analysis was conducted using the analytical results of sediments.

As first, each components were standardized on the base of mean value=0 and standard deviation =1, and then correlation coefficient of each component was calculated (Table 3-3-5). Non-correlation test was done for obtained correlation coefficients. Principal component analysis was conducted using correlation matrix, and obtained results of eigenvalues, contribution rate and cumulative contribution rate are shown in Table 3-3-6. The principal loading and principal component scores are given in Tables 3-3-7 and 3-3-8, respectively.

As the result of analysis, the first principal component covers about 60% of the variance, and the cumulative variance at the second principal component reaches about 78%, and also the cumulative variance from the first through third becomes more than 90%. The correlation of components in the samples can be mostly explained by the first to third principal components.

The characteristics of each principal component are given below and depositional environment of the sediments is considered.

i. First Principal Component

The first principal component consists of groups elements: LOI, MnO, Pb, H_2O^-, Ba, Na_2O, Ni, Co, Y, P_2O_5, Fe_2O_3, H_2O^+, K_2O with high positive loading value and FeO, V, SiO_2, MgO, Al_2O_3 with high negative loading value.

Among the elements with high positive value, metal elements such as Pb, Ba, Ni, Co are included, and they have a high correlation with Mn, so that the first principal component is attributed to enrichment of Mn. The eigenvalue of the first principal component is as high as 59.29%.

Among core samples, sample CS04 (0.30-0.33m depth) of the 03S2327SC01 sampling point at 03513 station shows a high principal component score of 5.084. The occurrence of manganese nodules at depth of 0.26m to 0.30m, just above 03S2327SC01CS04 sample, suggests that the high principal component score of this sample is related to Mn enrichment. Other samples with high scores are 03S2027SC01CS01 and CS02, showing respectively 3.834 and 4.355, and Mn enrichment around these samples is expected.

As the contrary cases, the sample 03S2327SC01CS01 and 03S2326SC01CS01are poor in Mn content and negative principal component of, respectively, −6.906 and −6.848. These samples do not seem to be affected by Mn enrichment.

ii.Second Principal Component

The second principal component includes groups of elements: Sr, CaO, CO_2, Mo, Zn, Cu, P_2O_5, As with high positive loading value, and TiO_2, K_2O, Al_2O_3, H_2O^+, SiO_2 with high negative loading value.

Among core samples, 03S2027SC01CS01 and CS02 of the same sampling point have high principal component scores, respectively, 3.753 and 3.581. The abundant foraminifer found by microscopic observation in these samples suggests that this principal component is related to carbonates material such as foraminifer fossils.

iii. Third Principal Component

The third principal component includes groups of elements: As, Mo, Zn, Al_2O_3, Cu with high positive loading value and Sr, CO_2, CaO with high negative loading value. The metallic elements such as As, Mo, Zn, Cr, Cu show high loading value of this component, and these elements are generally associated with hydrothermal mineralization. However, the sample showing high principal component score is only the CS01 of 03S2027SC01 point and beneath this, 03S2027SC01 CS02 shows low score. The third principal component is related to terrigenous material transported from distant location to the present site.

As the reference, the map of clay mineral distribution of the Pacific Ocean (Griffin et al., 1968) is shown in Fig. 3-3-1. According to this, the sampling locations of this survey fall in the area of montmorillonite 50%, chloride 20 to 30%, illite 20%, and Kaolinite 10%. A detail work of X-ray diffraction analyses is necessary for further discussed of this, however, all the clay minerals given above were detected by X-ray diffraction analysis. Concerning chemical composition, the CaO content is rather high compared with that of typical deep-sea sediments of red clay.

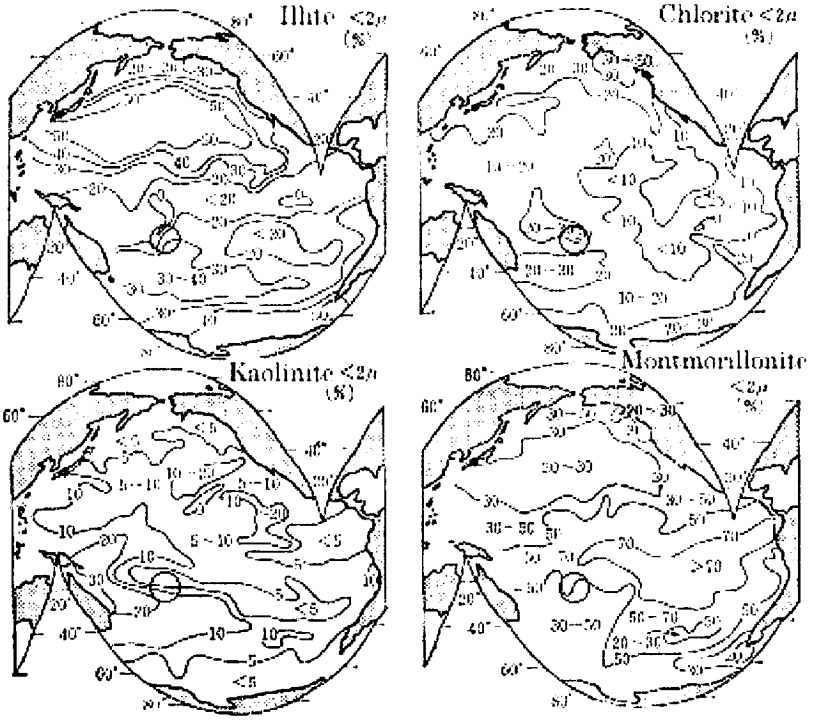

Fig.3-3-1 Distribution of Clay Minerals in the Pacific Ocean

(Griffin et al., 1968)

top left: illite <2 μ (%)　　top right: chlorite <2 μ (%)

bottom left: kaolinite <2 μ (%)　　bottom right montmorillonite<2 μ (%)

○ : approximate position of the survey area

(7) Fossil Identification of Bottom Sediments

Fossil species (foraminifer, radiolaria, Ichtyolith) in the collected bottom sediments by SC were identified, and geologic age of the bottom sediments and sedimentation environment were estimated. Samples used for the work are as follow.

Sample no.	Location	Water Depth
03S2027SC01	18° 59.96′ S 169° 00.01′ W	4,754m
03S2327SC01	21° 59.99′ S 169° 00.01′ W	5,569m
03S2326SC01	22° 00.01′ S 169° 59.98′ W	5,620m

The age and sedimentation environment of the bottom sediments at each sampling point are summarized as follows. The details of the fossil identification are given in the Appendix Document 1.

a. 03S2027SC01 FS01 – FS04 at 03503 Station

From the inspection of radiolarian fossil, sedimentation age of all of the FS01 to FS04 sample was determined to be 0 – 0.18Ma, and from Ichtyolith, 0 – 0.32Ma. Foraminiferal fossils found in samples FS01 and F03 show the age younger than 0.65Ma.

Concerning the environment of inhabitation and sedimentation, it was assumed from the inspection of radiolarian fossils that the area had been in tropical surface water and cool deep to bottom water with almost no upwelling current. The bottom environment, also, has been the one with weak bottom current. From the inspection of foraminifer, the sedimentation environment was assumed to be tropical to subtropical geographic province, same as present location.

The rate of sedimentation is assumed from the determined ages and core length, and it is about 2.1mm/1,000 years or greater (faster).

b. 03S2327SC01 FS01 – FS04 at 03513 Station

From the inspection of radiolarian fossils, the ages of all of FS01 to FS04 samples are 0 – 0.18Ma, and for ichtyolith, the type specie representing range of 0 – 0.19Ma were found in FS02 sample.

Concerning the environment of inhabitation and sedimentation, it was assumed from the inspection of radiolarian fossils that the area had been in tropical surface water and cool deep to bottom water with almost no upwelling current. The bottom environment, also, has been the one with weak bottom current

The rate of sedimentation, assumed from the determined ages and core length, is about 0.8 to 1.9mm/1,000 years.

c. 03S2326SC01 FS01 – FS04 at 03514 Station

The radiolarian fossils suggest the sedimentation ages of 0 – 0.42Ma and 0.42 – 0.54Ma, respectively, for three samples of FS01 to FS03 and FE04. While from the inspection of Ichtyolith fossils in the FS01 sample, the type species to represent time ranges of 0 – 63.9Ma and 0 – 0.19Ma were found, and in FS03 and FS04, the type species to represent time range of 0 – 32.5Ma were confirmed.

Concerning the environment of inhabitation and sedimentation, it was assumed from the inspection of radiolarian fossils that the area had been in tropical surface water and cool deep to bottom water with almost no upwelling current. The proliferation of radiolaria is considered to be smaller than at the other two stations. The bottom environment has been the one with weak bottom current

The sedimentation environment between sample FS01 and samples FS02 to FS04 is quite different. The depositional environment of the former had been the environment where terrigenous materials had flown in and that of the latter had been the pelagic environment.

The rate of sedimentation, assumed from the determined ages and core length, is about 0.6 to 1.9mm/1,000 years.

3-4 Manganese Nodules Survey by MFES

The Multi Frequency Exploration System (MFES) used in the survey utilizes three acoustic frequency bands, 30kHz (NBS), 12kHz (PDR), and 3.5kHz (SBP). The transmitted acoustic waves from these acoustic instruments are received as reflection intensity of compound acoustic waves of three frequencies (Rt). This reflection intensity (Rt) is assumed to be proportional to the covering ration of manganese nodules. The assessment is based on the following linear relation that the spatial occupancy-ratio of manganese nodules (S) in terms of spatial occupancy-ratio of unit area (m^2) is expressed as the next relation.

$$S = a \times Rt + b$$

where a and b are local parameters determined independently depending on survey area.

S is, normally, obtained as the occupancy ratio of manganese nodules by actual sampling and, using the measured Rt of the sampling site, parameter a and b, is determined by first regression equation. Once a and b are given, when Rt is measured along a track line without sampling data, S (spatial occupancy ratio of manganese nodules) is estimated using the above equation.

The distribution density (abundance) of manganese nodules is obtained multiplying S and weight factor (fo), which is obtained by the results of actual sampling.

$$\text{Assumed distribution density (abundance)} = S \times fo$$

Where fo =distribution density of manganese nodules/ spatial occupation ratio of manganese nodules.

For the survey of this year, however, only one measurement of occupancy-ratio of manganese nodules has been made at the northeastern edge of the area, and no other

measurement results was available. For this reason, it was impossible to determine parameters (a and b) and coefficient fo of this area. Consequently, spatial occupancy-ratio of manganese nodules (S) and assumed distribution density (S ×fo) of manganese nodules could not be obtained by the MFES data in this area. In this report, therefore, the MFES survey results are shown only as a distribution of compound acoustic reflection intensity, Rt. In Figure 3-4-1, the distribution of Rt is shown on the map together with SBP results.

As is described above, the assessment of abundance of manganese nodules by the MFES survey is made based upon measuring the intensity of backscattering acoustic waves from the seafloor covered by manganese nodules. Manganese nodules are good backscattering objects and when they are distributed on the surface of low acoustic reflection intensity such as unconsolidated sediments, the assumption of abundance is possible. However, in case the circumstances of seafloor is such that composed of exposed rocks or clastic materials with high scattering coefficient, or even unconsolidated sediments composed of coarse materials and having comparatively high back scattering nature, the discrimination of backscattered signal of manganese nodules becomes difficult hidden by reflected signals from compact, high scattering surface materials.

As seen from SBP and MBES acoustic reflection intensity described in the former section, the seafloors in this area, generally, lack acoustically transparent uppermost layer, predominated by Types d1 and d2. It means that most of MFES cruising data are affected by high acoustic reflection intensity materials such as exposed rocks or compact sediments, and the data are shown as quasi-anomaly. Therefore, the seafloor of the area is shown as the area of high occupancy of manganese nodules, disregarding actual distribution of manganese nodules. The areas, represented by low acoustic reflection intensity by MBES and classified as SBP Types as and ec with opaque uppermost layer (presumable existence of soft sediments near the top surface), are, also, shown as the area of high occupancy of manganese nodules by MFES. This means that acoustic waves of PDR and SBP penetrate into thin, soft, top sediments to some depths and the recorded signals contain reflected waves from the opaque layer laying beneath soft sediment layer (There were some cases where the abundance of buried-type manganese nodules were assumed by MFES survey.).

By these reasons stated above, except local areas with SBP Types a and b, in all other areas represented by SBP types other than Types a and b, the MFES data are expressed as high acoustic reflection intensity of "quasi-anomaly" regardless of distribution of manganese nodules. Consequently, MFES was not efficiently used for

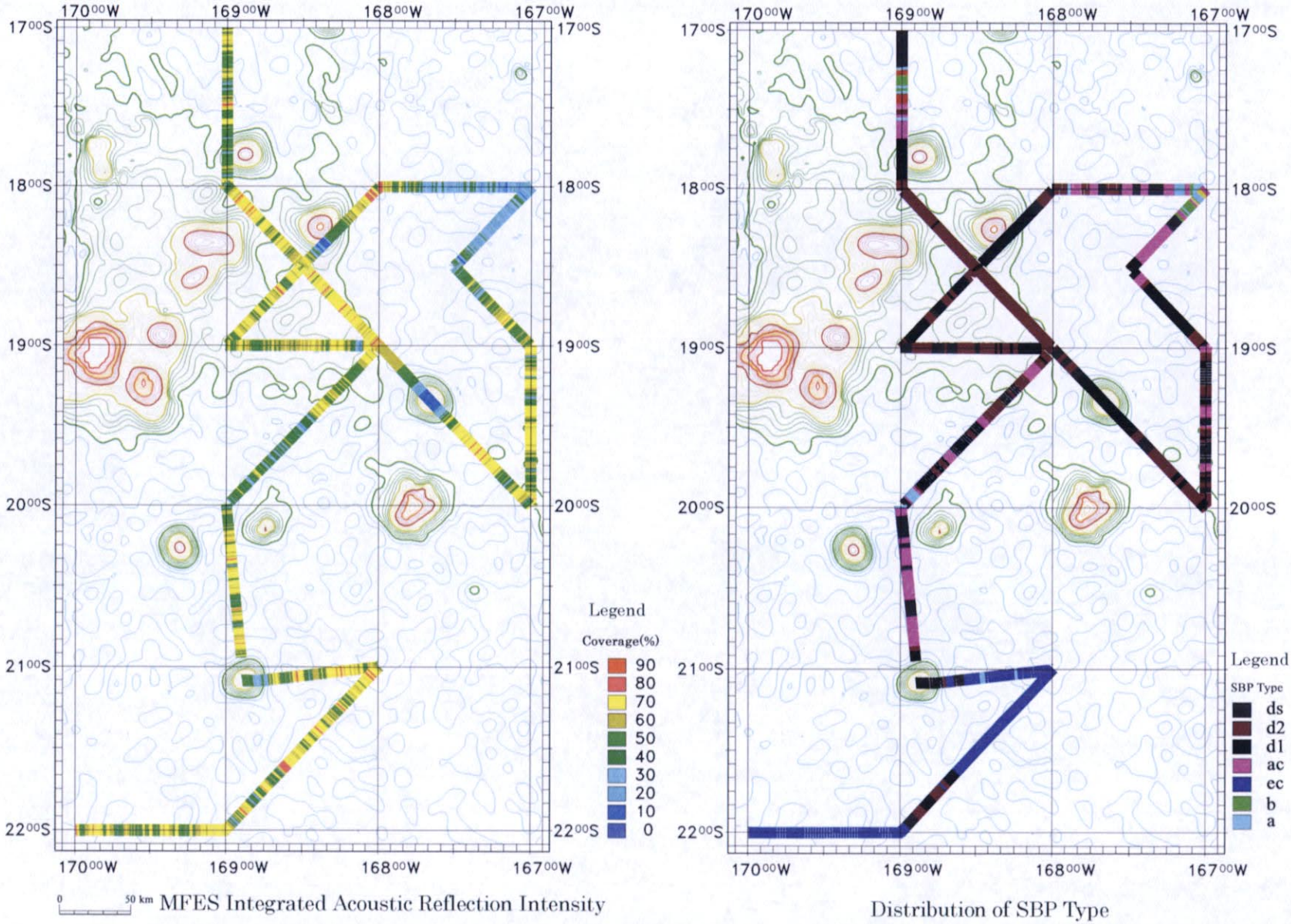

Fig. 3-4-1 MFES Integrated Acoustic Reflection Intensity and Distribution of SBP Type

assessing the distribution of manganese nodules in the area lacking soft, top sediments like brown clay.

3-5 Results of Sampling and Occurrence of Manganese Nodules

(1) Results of Sampling

The samplings at 36 sampling points (12 stations) were carried out in the manganese nodule survey of the Niue area ((Appendix Fig.4). They consist of FG sampling at 29 points and SC sampling at 7 points.

Among these samplings, manganese nodule sample and bottom sediments were collected at one station (3 sampling points) of FG and 3 sampling points of SC. As described in the later section, the collected nodules are mainly pebble type and the amounts of nodules collected by FG at each sampling site are less than 200g

At the FG sampling station 3504, although manganese nodules were not collected, the photographs taken by camera mounted on the sampler revealed a distribution of manganese nodules together with manganese crust (sampling points 03S2028FG 01, 02, 03 at 03504 station).

To confirm the occurrences of these, an Arm Dredge (AD) sampling (03S2028AD01) was conducted at the vicinity of FG sampling points (03509 station). As the results of the sampling, 2.4kg of manganese crust (average thickness of 15mm) and 158kg of manganese nodules (pebble type) were collected at near the point where FG sampling was not successful. The sea-bottom photographs of FG sampling, towing line of AD sampling and photographs of collected samples are shown in Fig. 3-5-1.

The collected crust shows smooth to granular surface texture, and has a two layers stricture.

The first layer is hard and compact, and shows brownish black color containing fine-grained phosphatic clay. The second layer is black to brown in color with patchy texture, and the cavities are filled with white to brownish clay. The substrate is dark brown phosphatized muddy limestone (partly phosphatized). The photographs of collected manganese nodules and crust by AD sampling are shown in Fig. 3-5-2.

The finding of manganese crust at 03S2028AD01 led to another AD sampling (03S2227AD01) to confirm the distribution of manganese crust on the northern slope of the seamount located in the south of the area (21° 04′ S, 168° 52′ W), and manganese crust of 9kg (average thickness of 18mm), consisting of crust and boulder crust, were collected. The towing line of AD sampler and photographs of crust sample are given in Fig. 3-5-3. The collected crust is single layer crust with surface of coarse granulated texture. Brownish phosphatic clay patches (0.1mm to 1mm across) occur on

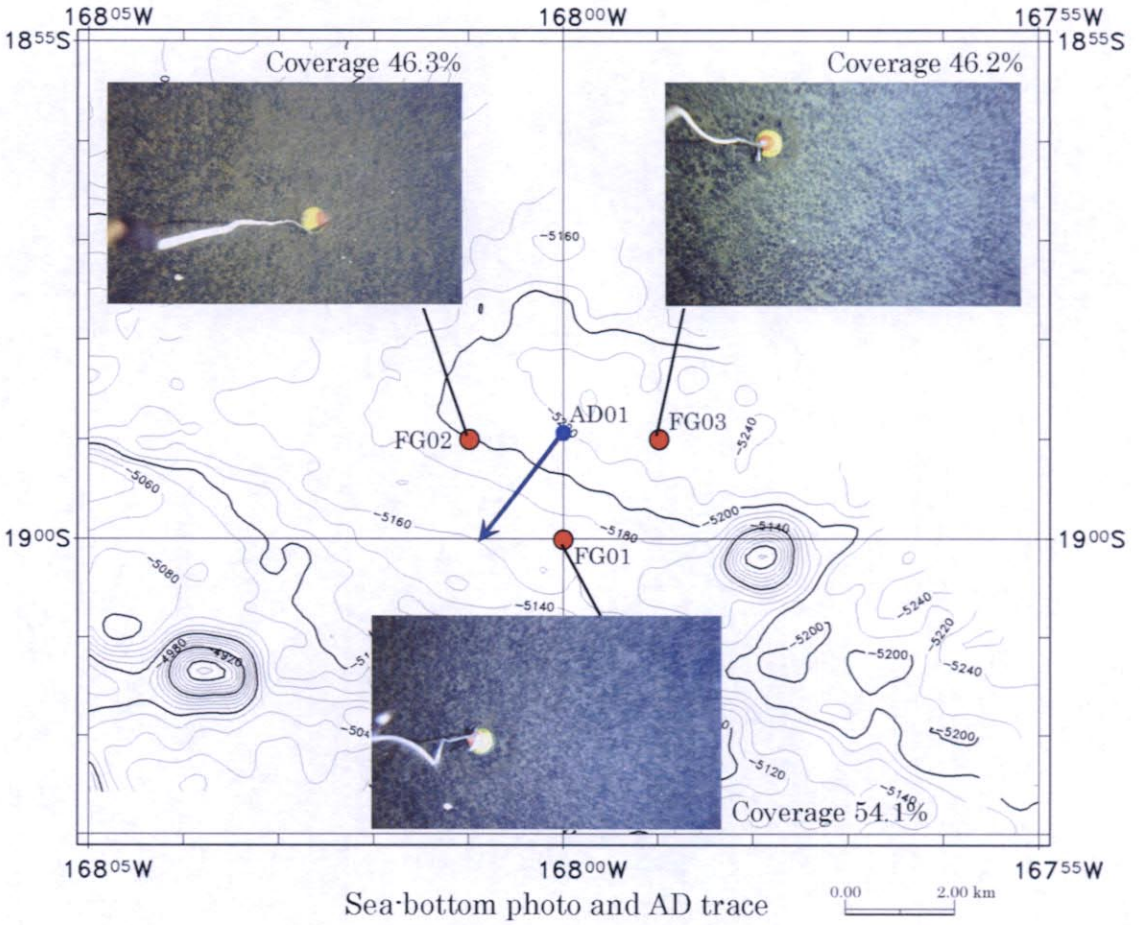

Sea-bottom photo and AD trace

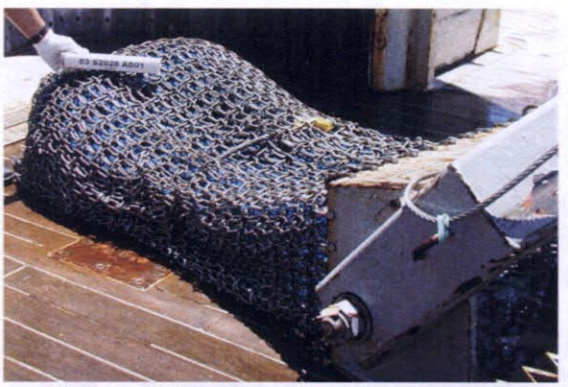

AD equipment

Manganese nodules and crusts

Fig. 3-5-1 03S2028AD01 AD trace and Samples

Obverse side

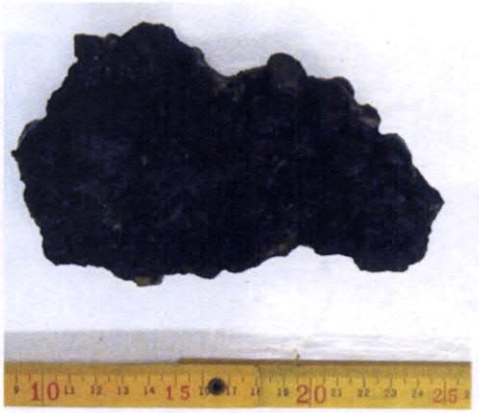

Reverse side

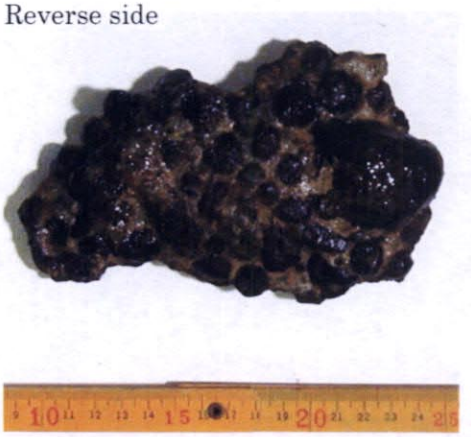

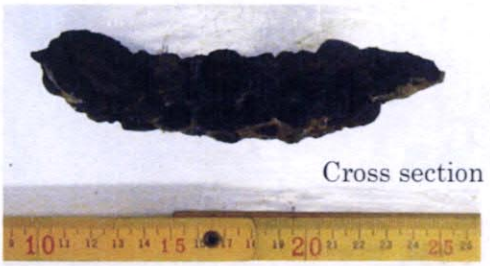

Cross section

03S2028AD01(Station No.03509)

Manganese nodule with phosphatized limestone

Obverse side

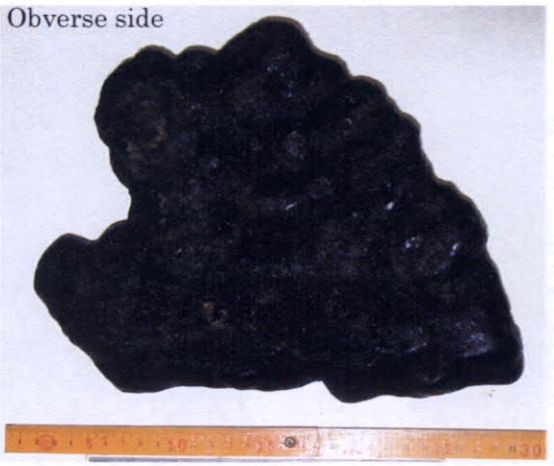

Reverse side

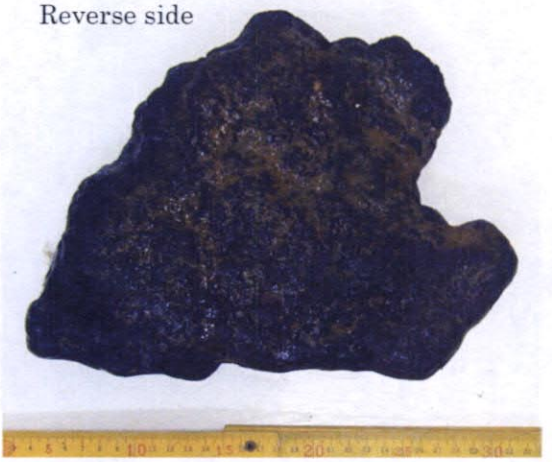

Cross section

03S2028AD01(Station No.03509)

Cobalt crust, mean thickness:15mm, 2-layers structure, basement is phosphatized muddy limestone

Fig. 3-5-2 Sample Photo of AD(03S2028AD01)

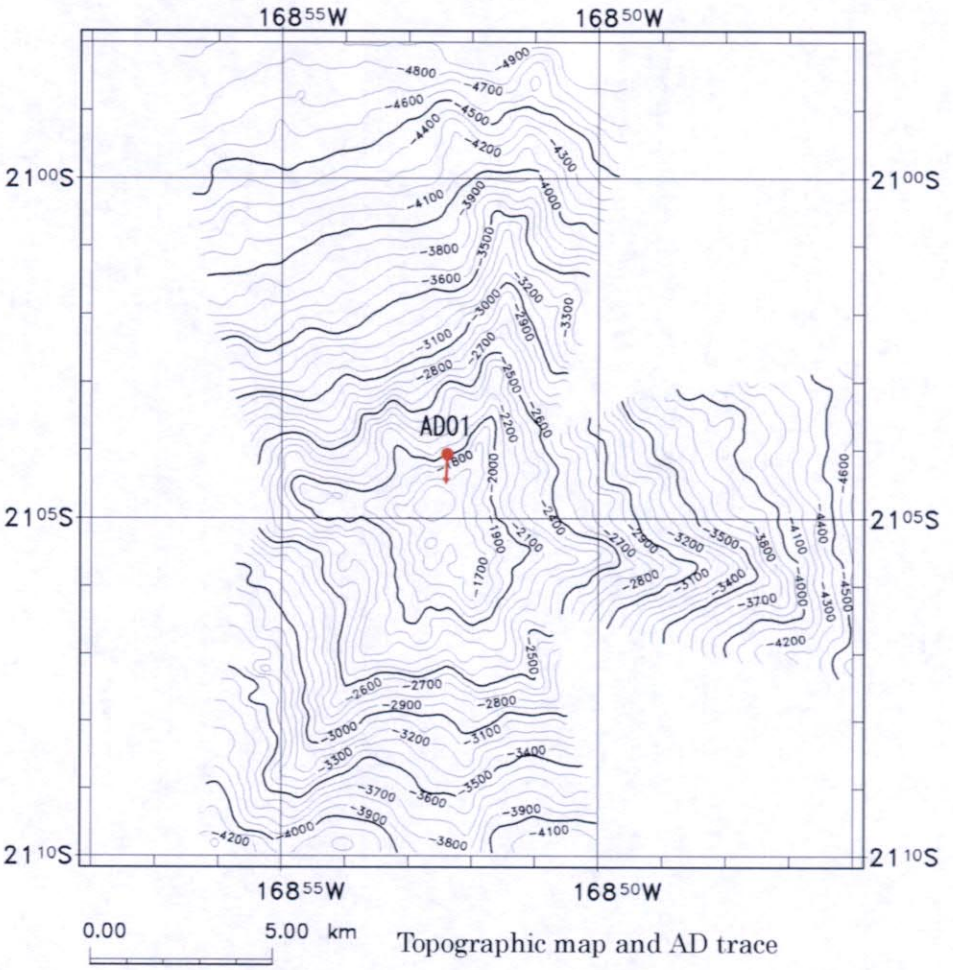

Topographic map and AD trace

AD equipment(Station N0.03511)

Crust

Fig. 3-5-3 03S2227AD01 AD trace and Samples

the surface and inside crust, and it shows patchy texture with cavities filled with clay. The substrate is massive, aphyric basaltic andesite with vesicles of 2 to 5mm across. The boulder crust (21×24cm) is 18 to 20mm thick, and it has three layers stricture with surface of granular texture. The substrate is porous basalt (detailed description of the rock is given in the Appendix Document 2). The photographs of plane view and cross section of the crust at the seamount (03511 station) are shown in Fig. 3-5-4.

The results of spade corer sampling (SC) carried out for the environmental survey is described in later section.

(2) Occurrence, Morphology, Size and Distribution of Manganese Nodules

1) Occurrence

Most of the manganese nodules in this area are pebble type, and they show smooth to slightly rough (granular) surface and more commonly smooth surface. It falls into S type (smooth surface type) category of general classification of manganese nodule (Mizuno, 1985). Nuclei of manganese nodules are mostly silts and siltstone. Almost all samples have neither fractures nor breaks.

2) Morphology and Size

In the previous survey conducted in the sea of the Cook Islands, the morphology of manganese nodules are classified into eight types (massive, discoidal, spheroidal, angular, globular, platy, pebble, and others), however, only pebble type nodules are seen in the area.

Pebble nodules resemble pebble stones seen on beach or river, whose diameters are less than 4cm and shapes are sub angular to sub rounded. Nodule size of the area is mostly 1cm to 4cm, reflecting small amount of nodule collected in the area. The classification of nodule morphology based on size shows that all of the nodules with major axis less than 2cm are pebble type, and 95% of nodules with major axis of 2 to 4cm are pebble type. The photographs of typical example of manganese nodules are shown in Fig. 3-5-5.

(3) Abundance of Manganese Nodules

The abundance of manganese nodules (kg/m^2) on the base of each sampling station (obtained as the average of 3 sampling points) is calculated as follows. At first, correction coefficient (= occupancy ratio of photograph / occupancy ratio of collected samples) is calculated based upon seafloor photographs Then, modified abundance (kg/m^2) (= abundance of collected samples × correction coefficient) is obtained. The

Obverse side

Reverse side

Cross section

03S2227AD01(Station No.03511)

Crushed cobalt crust, thickness:25mm,
one layer crust showing granule like surface,
basaltic andesite basement

Obverse side

Reverse side

Cross section

Conglomeratic crust, size:21x24x1.8-2.0cm,
three layers crust showing granule
like surface, basaltic andesite basement

Fig. 3-5-4 Sample Photo of AD(03S2227AD01)

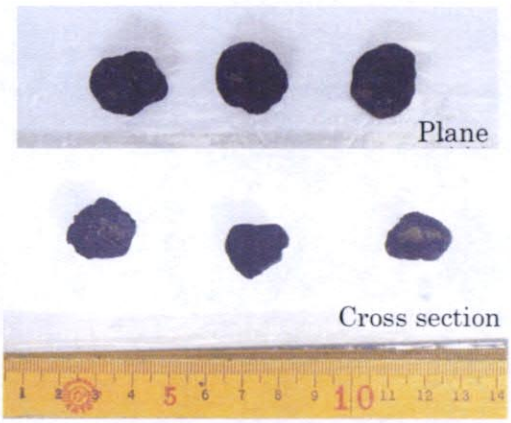

03S1929FG01 0 - 2cm

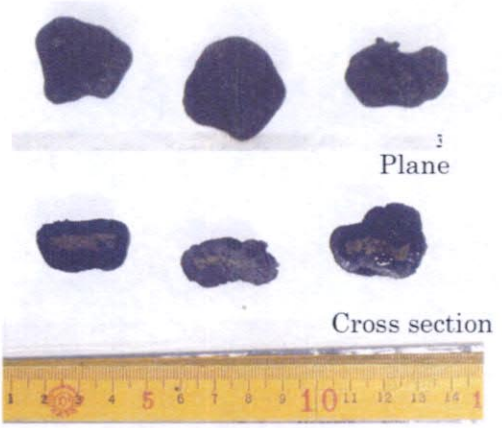

03S1929FG01 2 - 4cm

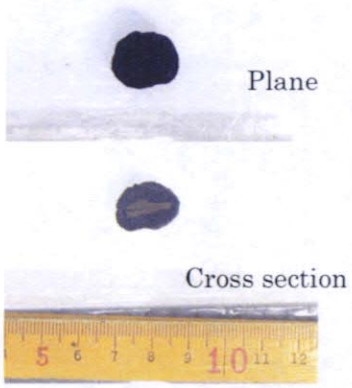

03S1929FG02 0 - 2cm

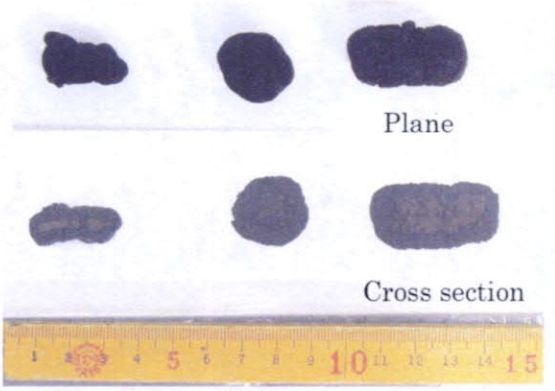

03S1929FG02 2 - 4cm

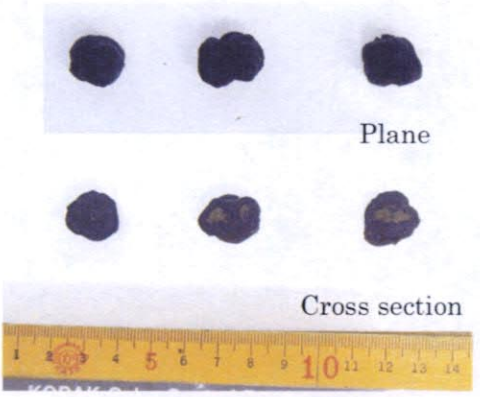

03S1929FG03 0 - 2cm

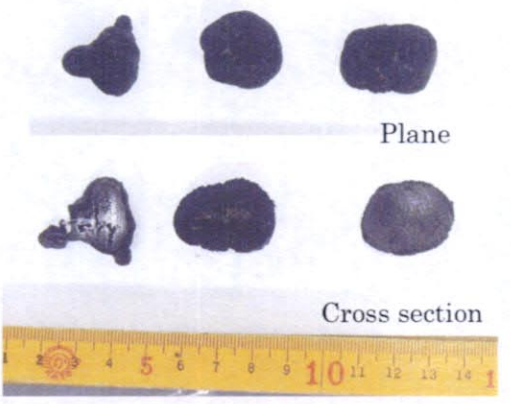

03S1929FG03 2 - 4cm

Samples of FG (Station No. 03506)

Fig. 3-5-5 Shape of Manganese Nodule (1)

Pebble like manganese nodule

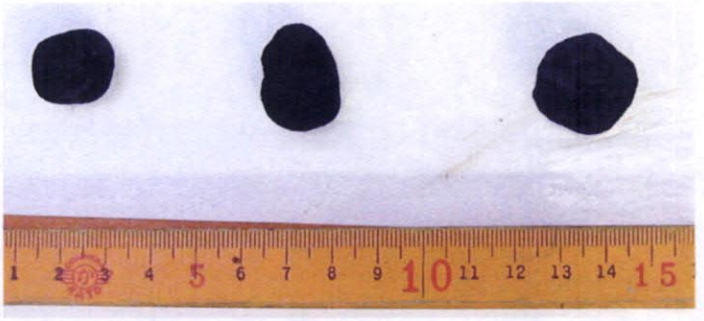

0 - 2cm Plane

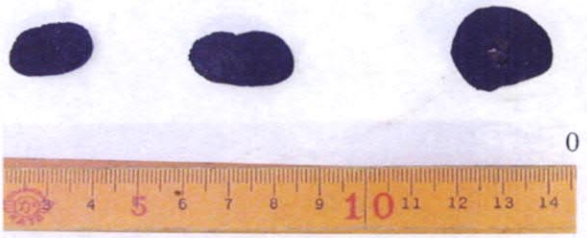

0 - 2cm Cross section

2 -4cm Plane

2 - 4cm Cross section

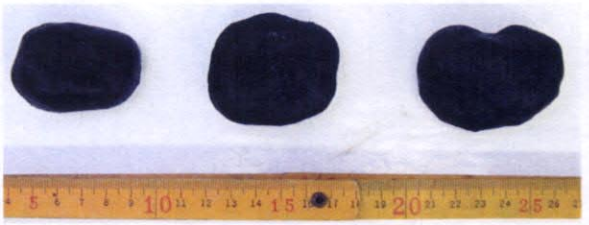

4 - 6cm Plane

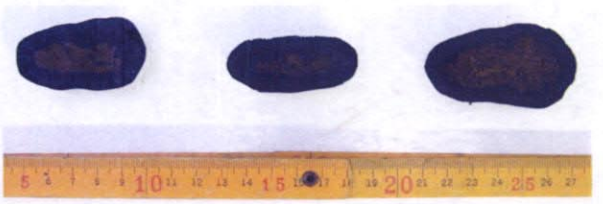

4 - 6cm Cross section

Samples of AD (Station No. 03509)

Fig. 3-5-5 Shape of Manganese Nodule (2)

4 - 6cm(Stick like)　Plane

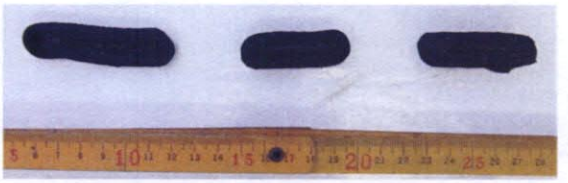

4 - 6cm　Cross section

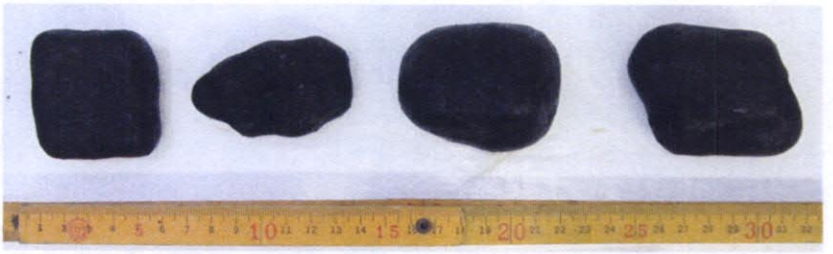

6 - 8cm(Ellipsoidal)　Plane

6 - 8cm　Cross section

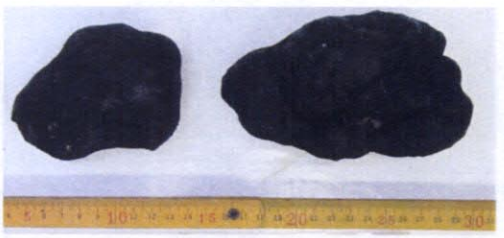

Over 8cm(Ellipsoidal)　Plane

Over 8cm　Reverse side

Over 8cm　Cross section

Samples of AD (Station No.03509)

Fig. 3-5-5 Shape of Manganese Nodule (3)

average of three modified abundances obtained from three sampling points of one sampling station is considered as the modified abundance of each sampling station. In this report, the "modified abundance" of manganese nodules is simply described as the "abundance". The weight of manganese nodule used to acquire "abundance" is wet weight.

Among 12 FG sampling stations, manganese nodules were collected at only one sampling station(03506), and average abundance was calculated to be 1.02 kg/㎡ (abundance of each point are: FG01: 1.25 kg/㎡, FG02: 0.69 kg/㎡, FG03 :1.13 kg/㎡, actual amount of samples collected are: FG01: 162g/1,295 c ㎡, FG02: 48g/1,295 c ㎡, FG03: 146g/1,295 c ㎡). The area of 1,295 c ㎡ is the opening of the free fall grab(37cm x 35cm) that used for the sampling. The seafloor photographs at the station 03506 and collected samples are shown in Fig. 3-5-6.

Additionally, at the sampling station 03504 where manganese nodules were not collected by FG sampling, the average seafloor occupancy-rate was calculated from seafloor photographs as 48.9% (FG01=54.1%, FG02=46.3%, FG03=46.2%). If this is converted to the abundance of manganese nodules, it corresponds to approximately 8 to 10kg/㎡.

From the obtained abundances of manganese nodules in this area together with that of the Cook Islands area, a distribution map of the abundance of manganese nodules was drawn (Fig. 3-5-7). The survey area falls in the area with abundance lower than 2.5kg/㎡, and distribution of manganese nodules seems to be expected only in the east part of the area adjacent to the Cook Islands area.

(4) Chemical Composition of Manganese Nodules

The chemical analyses of 20 manganese nodule samples and 2 crust samples were conducted. The samples of manganese nodules were prepared based on size classification and nuclei were excluded. In case separation of manganese oxides and nucleus is difficult, bulk analysis including nucleus part was done. For the comparison, duplicate analyses, one with nucleus and other without nucleus, were done for several samples.

For manganese nodules samples with nuclei, the chemical analyses of eight components such as Co, Ni, Cu, Mn, Fe, LOI, H_2O^+, H_2O^- were conducted. For the samples without nuclei, chemical analyses of 36 components, adding minor elements and rare earth elements to the above eight components were conducted, and components are: Co, Ni, Cu, Mn, Fe, Pb, Zn, Ti, Mo, V, Si, Al, Ca, Na, K, P, Ba, Sr, Pt, LOI, H_2O^+, H_2O, La, Ce, Pr, Nd, Sm, Eu, Gd, Tb, Dy, Ho, Er, Tm, Yb, Lu. Analytical

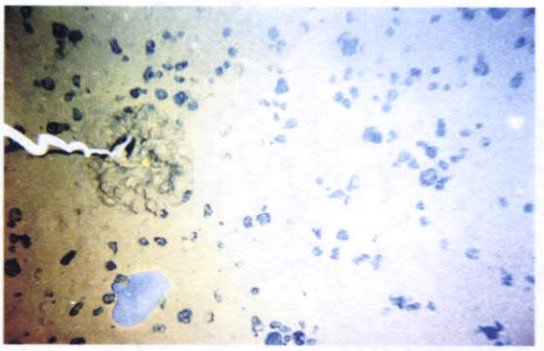

03S1929FG01(Sea-bottom)
Depth 5,412m
Covering surface ratio 7.9%

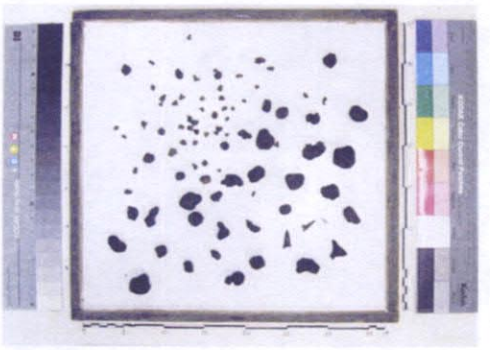

03S1929FG01(Collected samples)
Insoluble brown clay, pebble
Recollected samples ratio 8.0%
Abundance 1.3kg/m^2

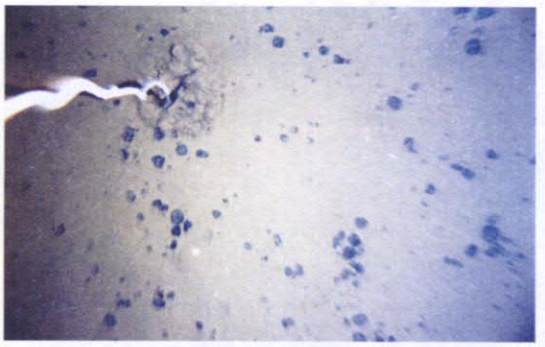

03S1929FG02(Sea-bottom)
Depth 5,396m
Covering surface ratio 4.5%

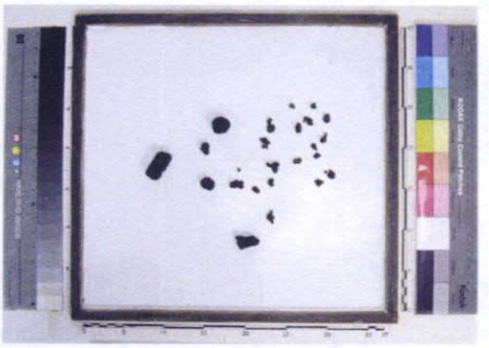

03S1929FG02(Collected samples)
Insoluble brown clay,pebble
Recollected samples ratio 2.5%
Abundance 0.7kg/m^2

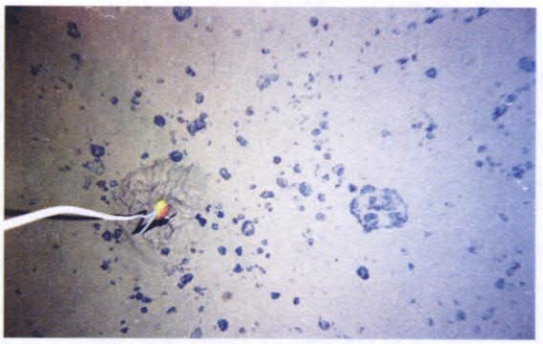

03S1929FG03(Sea-bottom)
Depth 5,391m
Covering surface ratio 6.6%

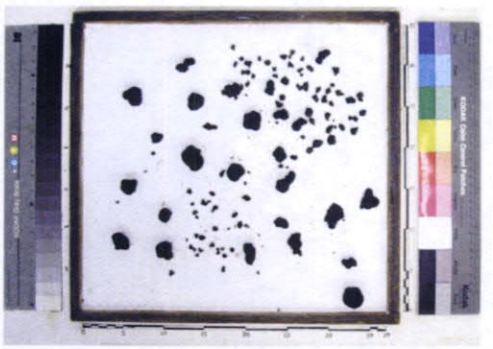

03S1929FG03(Collected samples)
Insoluble brown clay, pebble
Recollected samples ratio 7.9%
Abundance 1.1kg/m^2

Fig. 3-5-6 Sea-bottom Photos and Collected Samples Photos

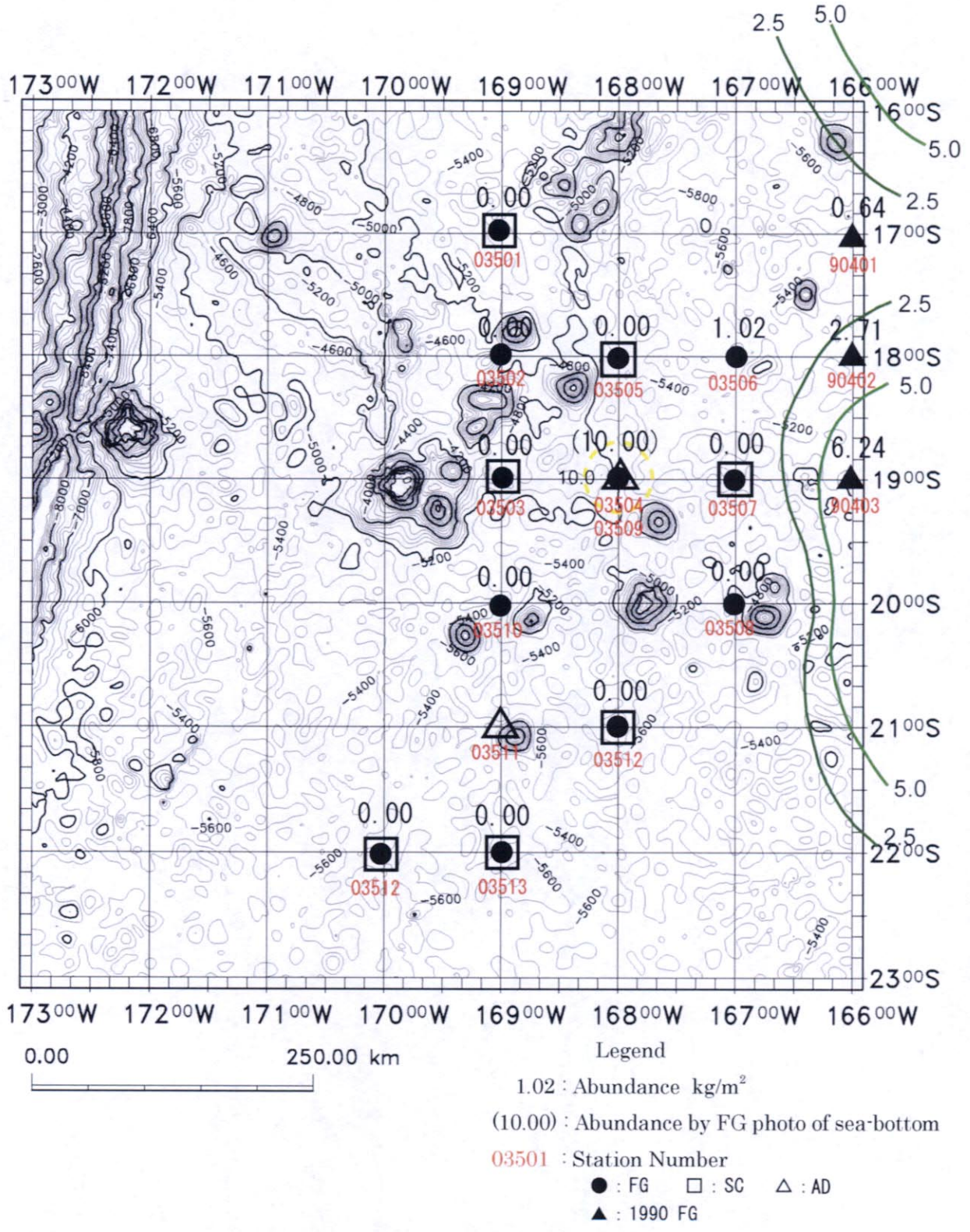

Fig. 3-5-7 Abundance Map of Manganese Nodule

method and other related information such as detection limit are shown in Appendix Document 2. The results of analyses and basic statistical figures are given in Table 3-5-1 and Table 3-5-2.

1) Five Major Elements

For the samples of 03S1929FG02 and 03S2327SC01, using the same manganese nodule sample, two types of samples were analyzed: with-nucleus and without-nucleus. For 03S1929FG02 sample, CM02 is with-nucleus and CM03 is without-nucleus, and for 03S2327SC01 sample, CM 01 is with-nucleus and CM02 is without-nucleus.

Comparing analytical results of two types, the samples without-nucleus shows slightly high value of Co, Ni, and Cu, however, there was no significant difference observed between them. For this reason, data analyses of manganese nodule samples were conducted without distinguishing two types.

Distribution of average content of Co, Ni, Cu on each station is shown in Fig. 3-5-8. The analyzed samples were collected from six sampling stations. Of them, three sampling stations, 03506, 03507, 03513 are located in the Plain Province, east and south of the survey area, and manganese nodules are solely distributed on the seafloor. While, other three sampling stations, 03504, 03509, and 03511, are located in the western Hilly Province associated with seamounts, and manganese nodules occur together with manganese crust. The chemical differences in manganese nodules of both areas are as follows.

- There is significant difference in Co content, 0.30 to 0.37% in the Plain Province, 0.68 to 0.78 in the Hilly Province.
- Ni is 0.21 to 0.53% in the Plain Province, slightly higher content than in the Hilly Province of 0.24 to 0.28%.
- Cu is definitely high in the Plain Province showing 0.19～0.28%, and it is 0.07 to 0.08% in the Hilly Province.

The basic statistical figures were obtained independently for three groups of samples, manganese nodules of the Plain Province, those of the Hilly Province and manganese crust of the Hilly Province. There was no clear compositional difference observed among manganese nodules of different size and thus size was not considered for calculation of basic statistical figures.

The characteristics of five major elements are as follows.

- Co of all the samples ranges form 0.28 to 0.89% with an average of 0.54%.

Table 3-5-1 Results of Chemical Analysis

No.	Station No.	Topography	Sample No.		Depth (m)	Lithology	Remarks	Co (%)	Ni (%)	Cu (%)	Mn (%)	Fe (%)	Mn/Fe	Pb (%)	Zn (%)	Ti (%)	Mo (%)	V (ppm)	Si (%)	Al (%)	Ca (%)	Na (%)	K (%)	P (%)	Ba (ppm)	Ba (ppm)	Sr (ppm)	Pt (ppm)	LOI (%)	H_2O^+ (%)	H_2O^- (%)
1	03504	hill	03S2028FG01	CM01	5,149	Manganes nodule	pebble,2×3.5cm,balk	0.78	0.28	0.07	21.27	19.00	1.12	***	***	***	***	***	***	***	***	***	***	***	***	***	***	***	14.77	7.36	6.33
2	03506	flat	03S1929FG01	CM01	5,412	Manganes nodule	0-2cm,balk	0.33	0.49	0.29	18.86	15.39	1.23	***	***	***	***	***	***	***	***	***	***	***	***	***	***	***	13.01	7.18	4.60
3				CM02	5,412	Manganes nodule	2-4cm,balk	0.36	0.45	0.24	18.56	16.66	1.11	***	***	***	***	***	***	***	***	***	***	***	***	***	***	***	13.66	8.23	4.03
4			03S1929FG02	CM01	5,396	Manganes nodule	0-2cm,balk	0.31	0.48	0.28	17.28	15.72	1.10	***	***	***	***	***	***	***	***	***	***	***	***	***	***	***	13.83	8.45	4.41
5				CM02	5,396	Manganes nodule	2-4cm,balk	0.39	0.40	0.22	18.37	17.07	1.08	***	***	***	***	***	***	***	***	***	***	***	***	***	***	***	13.93	8.10	4.92
6				CM03	5,396	Manganes nodule	2-4cm,core-less	0.40	0.45	0.24	19.56	16.88	1.16	0.10	0.06	1.29	0.03	514	6.58	3.17	1.91	1.84	0.59	0.35	1173.5	1170	899	0.2	14.78	8.86	4.97
7			03S1929FG03	CM01	5,391	Manganes nodule	0-2cm,balk	0.37	0.45	0.24	18.37	16.88	1.09	***	***	***	***	***	***	***	***	***	***	***	***	***	***	***	14.85	13.39	4.30
8				CM02	5,391	Manganes nodule	2-4cm,balk	0.41	0.39	0.21	17.97	17.84	1.01	***	***	***	***	***	***	***	***	***	***	***	***	***	***	***	14.07	9.08	4.01
9	03507	flat	03S2029FG02	CM01	5,260	Manganes nodule	0-2cm,balk	0.37	0.53	0.28	19.56	14.85	1.32	***	***	***	***	***	***	***	***	***	***	***	***	***	***	***	16.01	9.65	5.40
10	03509	hill	03S2028AD01	CM01	5,165	Manganes nodule	0-2cm,balk	0.69	0.24	0.08	19.26	19.00	1.01	***	***	***	***	***	***	***	***	***	***	***	***	***	***	***	15.49	9.80	4.68
11				CM02	5,165	Manganes nodule	2-4cm,core-less	0.74	0.26	0.08	20.06	18.90	1.06	0.12	0.04	1.27	0.04	588	5.78	2.07	2.03	1.91	0.60	0.40	1091.8	1090	1133	0.1	16.06	9.86	4.25
12				CM03	5,165	Manganes nodule	4-6cm,core-less	0.89	0.34	0.07	22.94	17.55	1.31	0.12	0.04	1.26	0.04	600	4.96	1.69	2.29	2.00	0.55	0.39	929.6	930	1133	0.1	16.38	9.82	5.06
13				CM04	5,165	Manganes nodule	6-8cm,core-less	0.73	0.25	0.08	19.95	18.80	1.06	0.12	0.04	1.25	0.04	586	5.77	2.04	2.10	1.89	0.59	0.41	864.0	860	1082	0.1	16.18	9.95	4.34
14				CM05	5,165	Manganes nodule	8cm<,core-less	0.60	0.22	0.08	19.95	19.09	1.05	0.13	0.04	1.23	0.04	627	5.77	2.10	2.18	1.83	0.54	0.42	893.4	890	1154	<0.1	16.39	9.95	4.40
15				CM06	5,165	Manganes nodule	cylinder-shape,core-less	0.75	0.25	0.07	20.45	18.32	1.12	0.13	0.04	1.27	0.04	579	5.82	1.95	2.17	1.96	0.56	0.41	800.0	800	1109	0.1	17.31	10.50	4.26
16				CM07	5,165	Manganes nodule	crust-type	0.65	0.23	0.08	22.51	18.80	1.20	0.13	0.04	1.24	0.04	635	5.48	2.07	1.99	1.95	0.57	0.41	926.3	930	1166	0.1	17.03	10.77	4.31
17				CM08	5,165	Manganes nodule	polysynthetic.nodul.balk	0.39	0.14	0.05	19.06	19.09	1.00	***	***	***	***	***	***	***	***	***	***	***	***	***	***	***	14.55	9.02	3.36
18	03511	hill	03S2227AD01	CM01	1,791	Manganes nodule	0-2cm,core-less	0.69	0.24	0.08	19.86	19.19	1.03	0.12	0.04	1.25	0.03	554	5.60	2.12	2.07	1.89	0.53	0.41	811.2	810	1064	0.1	18.47	11.05	5.94
19				CM02	1,791	Cobble-type crust	core-less	0.61	0.35	0.11	19.85	18.52	1.07	0.13	0.06	1.27	0.03	583	4.81	1.51	4.04	1.90	0.48	0.46	1525.3	1530	1415	0.2	19.45	10.75	4.42
20				CM03	1,791	Crust		0.89	0.37	0.11	21.14	18.42	1.15	0.14	0.07	1.47	0.03	597	4.16	1.13	3.93	1.89	0.56	0.53	1677.2	1680	1404	0.3	17.68	9.56	4.20
21	03513	flat	03S2327SC01	CM01	5,569	Manganes nodule	0-2cm.balk,buried-type	0.28	0.20	0.19	14.03	19.38	0.72	***	***	***	***	***	***	***	***	***	***	***	***	***	***	***	13.09	9.14	3.98
22				CM02	5,569	Manganes nodule	0-2cm,core-less,buried-type	0.32	0.22	0.20	15.01	19.76	0.76	0.09	0.05	1.35	0.01	596	8.45	3.51	1.72	1.91	0.60	0.39	1208.1	1210	877	0.1	13.62	9.62	4.45

No.	Position No.	tophography	Sample No.		Depth	Lithology	Remarks	La (ppm)	Ce (ppm)	Pr (ppm)	Nd (ppm)	Sm (ppm)	Eu (ppm)	Gd (ppm)	Tb (ppm)	Dy (ppm)	Ho (ppm)	Er (ppm)	Tm (ppm)	Yb (ppm)	Lu (ppm)	ΣREE (ppm)
1	03504	hill	03S2028FG01	CM01	5,149	Manganes nodule	pebble,2×3.5cm,balk	***	***	***	***	***	***	***	***	***	***	***	***	***	***	***
2	03506	flat	03S1929FG01	CM01	5,412	Manganes nodule	0-2cm,balk	***	***	***	***	***	***	***	***	***	***	***	***	***	***	***
3				CM02	5,412	Manganes nodule	2-4cm,balk	***	***	***	***	***	***	***	***	***	***	***	***	***	***	***
4			03S1929FG02	CM01	5,396	Manganes nodule	0-2cm,balk	***	***	***	***	***	***	***	***	***	***	***	***	***	***	***
5				CM02	5,396	Manganes nodule	2-4cm,balk	***	***	***	***	***	***	***	***	***	***	***	***	***	***	***
6				CM03	5,396	Manganes nodule	2-4cm,core-less	174.5	1061.0	44.1	176.5	39.9	9.3	43.6	6.8	41.0	8.3	24.0	3.0	23.0	3.7	1659
7			03S1929FG03	CM01	5,391	Manganes nodule	0-2cm,balk	***	***	***	***	***	***	***	***	***	***	***	***	***	***	***
8				CM02	5,391	Manganes nodule	2-4cm,balk	***	***	***	***	***	***	***	***	***	***	***	***	***	***	***
9	03507	flat	03S2029FG02	CM01	5,260	Manganes nodule	0-2cm,balk	***	***	***	***	***	***	***	***	***	***	***	***	***	***	***
10	03509	hill	03S2028AD01	CM01	5,165	Manganes nodule	0-2cm,balk	***	***	***	***	***	***	***	***	***	***	***	***	***	***	***
11				CM02	5,165	Manganes nodule	2-4cm,core-less	226.5	1745.0	58.5	228.5	51.5	11.8	54.8	8.4	48.0	9.3	26.5	3.4	24.5	3.9	2501
12				CM03	5,165	Manganes nodule	4-6cm,core-less	231.5	1632.5	58.5	231.5	51.2	11.6	53.8	8.2	47.3	9.1	25.7	3.2	23.3	3.6	2391
13				CM04	5,165	Manganes nodule	6-8cm,core-less	227.5	1715.5	58.9	229.5	52.1	11.8	55.3	8.4	48.3	9.3	26.6	3.4	24.6	3.8	2475
14				CM05	5,165	Manganes nodule	8cm<,core-less	237.5	1644.5	62.5	246.5	55.2	12.7	58.3	8.8	51.3	9.8	27.9	3.5	25.4	3.9	2448
15				CM06	5,165	Manganes nodule	cylinder-shape,core-less	225.5	1787.0	58.2	228.5	51.8	11.8	54.8	8.3	54.8	9.3	26.6	3.4	24.6	3.8	2548
16				CM07	5,165	Manganes nodule	crust-type	247.5	1717.0	64.9	257.5	57.4	12.9	59.8	9.1	52.4	10.0	28.0	3.5	25.5	3.9	2549
17				CM08	5,165	Manganes nodule	polysynthetic.nodul.balk	***	***	***	***	***	***	***	***	***	***	***	***	***	***	***
18	03511	hill	03S2227AD01	CM01	1,791	Manganes nodule	0-2cm,core-less	219.5	1685.5	56.9	219.5	50.7	11.5	54.1	8.1	47.9	9.4	27.0	3.5	25.5	4.0	2423
19				CM02	1,791	Cobble-type crust	core-less	208.0	678.0	34.6	149.5	28.8	7.4	37.4	5.6	37.0	8.4	26.2	3.3	25.5	4.1	1254
20				CM03	1,791	Crust		234.5	1035.5	39.0	165.5	32.0	8.1	41.5	6.0	39.6	8.9	27.7	3.6	26.4	4.3	1673
21	03513	flat	03S2327SC01	CM01	5,569	Manganes nodule	0-2cm.balk,buried-type	***	***	***	***	***	***	***	***	***	***	***	***	***	***	***
22				CM02	5,569	Manganes nodule	0-2cm,core-less,buried-type	156.5	1025.5	41.7	168.5	39.1	9.0	42.7	6.7	39.8	7.8	22.7	2.8	21.8	3.5	1588

Table 3-5-2 Chemical Properties of Manganese Nodule and Crust

Whole

	Co	Ni	Cu	Mn	Fe	Mn/Fe	Pb	Zn	Ti	Mo	V	Si	Al	Ca	Na	K	P	Ba	Sr	Pt	Ig-loss	H2O+	H2O-	La	Ce	Pr	Nd	Sm	Eu	Gd	Tb	Dy	Ho	Er	Tm	Yb	Lu
	(%)	(%)	(%)	(%)	(%)		(%)	(%)	(%)	(%)	(ppm)	(%)	(%)	(%)	(%)	(%)	(%)	(ppm)	(ppm)	(ppm)	(%)	(%)	(%)	(ppm)	(ppm)	(ppm)	(ppm)	(ppm)	(ppm)	(ppm)	(ppm)	(ppm)	(ppm)	(ppm)	(ppm)	(ppm)	(ppm)
Samples	22	22	22	22	22	22	11	11	11	11	11	11	11	11	11	11	11	11	11	11	22	22	22	11	11	11	11	11	11	11	11	11	11	11	11	11	11
Min.	0.28	0.14	0.05	14.03	14.85	0.72	0.09	0.04	1.23	0.01	514	4.16	1.13	1.72	1.83	0.48	0.35	800	877	0.05	13.01	7.18	3.36	156.5	678.0	34.6	149.5	28.8	7.4	37.4	5.6	37.0	7.8	22.7	2.8	21.8	3.5
Max.	0.89	0.53	0.29	22.94	19.76	1.32	0.14	0.07	1.47	0.04	635	8.45	3.51	4.04	2.00	0.60	0.53	1680	1415	0.30	19.45	13.39	6.33	247.5	1787.0	64.9	257.6	57.4	12.9	59.8	9.1	54.8	10.0	28.0	3.6	26.4	4.3
Renge	0.61	0.39	0.23	8.91	4.91	0.59	0.05	0.03	0.24	0.03	121	4.28	2.39	2.32	0.17	0.12	0.18	880	538	0.25	6.44	6.21	2.97	91.0	1109.0	30.3	108.1	28.6	5.6	22.4	3.5	17.9	2.2	5.2	0.7	4.6	0.8
Ave.	0.54	0.33	0.15	19.27	17.96	1.08	0.12	0.05	1.29	0.03	587	5.74	2.12	2.40	1.91	0.56	0.41	1082	1130	0.13	15.48	9.55	4.57	217.2	1429.7	52.5	209.2	46.3	10.7	50.6	7.7	46.1	9.1	26.3	3.3	24.5	3.8
Med.	0.51	0.31	0.11	19.56	18.47	1.08	0.12	0.04	1.27	0.04	588	5.77	2.07	2.10	1.90	0.56	0.41	930	1133	0.10	15.17	9.64	4.41	226.5	1644.5	58.2	228.4	51.2	11.6	54.1	8.2	47.9	9.3	26.6	3.4	24.6	3.9
S.D.	0.20	0.11	0.09	2.06	1.39	0.14	0.01	0.01	0.07	0.01	33	1.10	0.68	0.80	0.05	0.04	0.05	295	168	0.08	1.77	1.34	0.66	27.7	395.4	10.5	37.0	9.7	1.9	7.7	1.2	5.9	0.7	1.6	0.2	1.3	0.2
V.a.r	0.04	0.01	0.01	4.23	1.94	0.02	0.00	0.00	0.00	0.00	1076	1.21	0.46	0.64	0.00	0.00	0.00	86836	28290	0.01	3.14	1.81	0.44	769.3	156376.5	110.7	1370.4	94.1	3.6	59.2	1.4	34.7	0.5	2.7	0.1	1.8	0.1
C.V	37.32	34.05	57.58	10.67	7.76	12.91	11.82	23.31	5.42	27.51	5.59	19.15	32.05	33.18	2.58	6.28	11.31	27.24	14.88	57.82	11.45	14.09	14.50	12.77	27.66	20.03	17.69	20.94	17.82	15.22	15.55	12.77	7.40	6.21	6.90	5.50	6.17

Plain Province

	Co	Ni	Cu	Mn	Fe	Mn/Fe	Pb	Zn	Ti	Mo	V	Si	Al	Ca	Na	K	P	Ba	Sr	Pt	Ig-loss	H2O+	H2O-	La	Ce	Pr	Nd	Sm	Eu	Gd	Tb	Dy	Ho	Er	Tm	Yb	Lu
	(%)	(%)	(%)	(%)	(%)		(%)	(%)	(%)	(%)	(ppm)	(%)	(%)	(%)	(%)	(%)	(%)	(ppm)	(ppm)	(ppm)	(%)	(%)	(%)	(ppm)	(ppm)	(ppm)	(ppm)	(ppm)	(ppm)	(ppm)	(ppm)	(ppm)	(ppm)	(ppm)	(ppm)	(ppm)	(ppm)
Samples	10	10	10	10	10	10	2	2	2	2	2	2	2	2	2	2	2	2	2	2	10	10	10	2	2	2	2	2	2	2	2	2	2	2	2	2	2
Min.	0.28	0.20	0.19	14.03	14.85	0.72	0.09	0.05	1.29	0.01	514	6.58	3.17	1.72	1.84	0.59	0.35	1170	877	0.10	13.01	7.18	3.98	156.5	1025.5	41.7	168.5	39.1	9.0	42.7	6.7	39.8	7.8	22.7	2.8	21.8	3.5
Max.	0.41	0.53	0.29	19.56	19.76	1.32	0.10	0.06	1.35	0.03	596	8.45	3.51	1.91	1.91	0.60	0.39	1210	899	0.22	16.01	13.39	5.40	174.5	1061.0	44.1	176.5	39.9	9.3	43.6	6.8	41.0	8.3	24.0	3.0	23.0	3.7
Renge	0.13	0.33	0.10	5.53	4.91	0.59	0.01	0.01	0.06	0.02	82	1.87	0.34	0.19	0.08	0.01	0.04	40	22	0.12	3.00	6.21	1.42	18.0	35.5	2.4	8.0	0.8	0.3	0.8	0.1	1.2	0.4	1.2	0.1	1.1	0.2
Ave.	0.36	0.41	0.24	17.76	17.04	1.06	0.10	0.06	1.32	0.02	555	7.51	3.34	1.81	1.88	0.60	0.37	1190	888	0.16	14.08	9.17	4.51	165.5	1043.3	42.9	172.5	39.5	9.2	43.2	6.8	40.4	8.0	23.4	2.9	22.4	3.6
Med.	0.37	0.45	0.24	18.37	16.88	1.09	0.10	0.06	1.32	0.02	555	7.51	3.34	1.81	1.88	0.60	0.37	1190	888	0.16	13.88	8.97	4.43	165.5	1043.3	42.9	172.5	39.5	9.2	43.2	6.8	40.4	8.0	23.4	2.9	22.4	3.6
S.D.	0.04	0.11	0.04	1.85	1.60	0.19	0.01	0.01	0.05	0.01	58	1.32	0.24	0.14	0.05	0.01	0.03	28	16	0.08	0.91	1.66	0.47	12.7	25.1	1.7	5.7	0.6	0.2	0.6	0.1	0.9	0.3	0.9	0.1	0.8	0.2
V.a.r	0.00	0.01	0.00	3.42	2.55	0.03	0.00	0.00	0.00	0.00	3334	1.74	0.06	0.02	0.00	0.00	0.00	800	252	0.01	0.82	2.76	0.22	162.0	630.1	2.8	32.0	0.3	0.0	0.3	0.0	0.7	0.1	0.8	0.0	0.6	0.0
C.V	12.19	27.18	15.69	10.42	9.38	17.69	7.80	13.21	3.46	70.98	10.40	17.55	7.17	7.51	2.87	0.85	7.50	2.38	1.79	50.74	6.44	18.13	10.46	7.69	2.41	3.88	3.28	1.45	1.93	1.36	1.42	2.14	3.94	3.75	2.84	3.57	4.40

Hilly Province (Manganese nodule)

	Co	Ni	Cu	Mn	Fe	Mn/Fe	Pb	Zn	Ti	Mo	V	Si	Al	Ca	Na	K	P	Ba	Sr	Pt	Ig-loss	H2O+	H2O-	La	Ce	Pr	Nd	Sm	Eu	Gd	Tb	Dy	Ho	Er	Tm	Yb	Lu
	(%)	(%)	(%)	(%)	(%)		(%)	(%)	(%)	(%)	(ppm)	(%)	(%)	(%)	(%)	(%)	(%)	(ppm)	(ppm)	(ppm)	(%)	(%)	(%)	(ppm)	(ppm)	(ppm)	(ppm)	(ppm)	(ppm)	(ppm)	(ppm)	(ppm)	(ppm)	(ppm)	(ppm)	(ppm)	(ppm)
Samples	10	10	10	10	10	10	7	7	7	7	7	7	7	7	7	7	7	7	7	7	10	10	10	7	7	7	7	7	7	7	7	7	7	7	7	7	7
Min.	0.39	0.14	0.05	19.06	17.55	1.00	0.12	0.04	1.23	0.03	554	4.96	1.69	1.99	1.83	0.53	0.39	800	1064	0.05	14.55	7.36	3.36	219.5	1632.5	56.9	219.3	50.7	11.5	53.8	8.1	47.3	9.1	25.7	3.2	23.3	3.6
Max.	0.89	0.34	0.08	22.94	19.19	1.31	0.13	0.04	1.27	0.04	635	5.82	2.12	2.29	2.00	0.60	0.42	1090	1166	0.10	18.47	11.05	6.33	247.5	1787.0	64.9	257.6	57.4	12.9	59.8	9.1	54.8	10.0	28.0	3.5	25.5	4.0
Renge	0.50	0.20	0.02	3.87	1.64	0.31	0.01	0.00	0.04	0.01	81	0.86	0.43	0.30	0.17	0.07	0.03	290	101	0.05	3.92	3.68	2.97	28.0	154.5	8.1	38.3	6.7	1.5	6.0	1.0	7.5	0.9	2.3	0.4	2.2	0.4
Ave.	0.69	0.25	0.07	20.53	18.77	1.10	0.13	0.04	1.25	0.04	596	5.60	2.01	2.12	1.92	0.56	0.40	901	1120	0.09	16.26	9.81	4.69	230.8	1703.9	59.8	234.5	52.8	12.0	55.8	8.5	50.0	9.5	26.9	3.4	24.7	3.8
Med.	0.71	0.25	0.08	20.00	18.95	1.06	0.12	0.04	1.25	0.04	588	5.77	2.07	2.10	1.91	0.56	0.41	890	1133	0.10	16.28	9.90	4.37	227.5	1715.5	58.5	229.4	51.8	11.8	54.8	8.4	48.3	9.3	26.6	3.4	24.6	3.9
S.D.	0.13	0.05	0.01	1.31	0.49	0.09	0.01	0.00	0.01	0.00	28	0.30	0.15	0.10	0.06	0.03	0.01	98	37	0.02	1.17	1.03	0.87	9.2	54.6	2.9	13.0	2.5	0.6	2.3	0.4	2.9	0.3	0.8	0.1	0.8	0.1
V.a.r	0.02	0.00	0.00	1.70	0.24	0.01	0.00	0.00	0.00	0.00	793	0.09	0.02	0.01	0.00	0.00	0.00	9614	1367	0.00	1.38	1.07	0.77	84.9	2977.6	8.3	169.8	6.2	0.3	5.2	0.1	8.2	0.1	0.7	0.0	0.6	0.0
C.V	19.03	20.43	10.76	6.36	2.63	8.64	4.08	0.35	1.10	9.83	4.73	5.45	7.41	4.79	2.87	4.71	2.39	10.88	3.30	19.98	7.21	10.53	18.64	3.99	3.20	4.82	5.56	4.70	4.66	4.09	4.21	5.72	3.45	3.01	3.49	3.20	3.52

Hilly Province (Crust)

	Co	Ni	Cu	Mn	Fe	Mn/Fe	Pb	Zn	Ti	Mo	V	Si	Al	Ca	Na	K	P	Ba	Sr	Pt	Ig-loss	H2O+	H2O-	La	Ce	Pr	Nd	Sm	Eu	Gd	Tb	Dy	Ho	Er	Tm	Yb	Lu
	(%)	(%)	(%)	(%)	(%)		(%)	(%)	(%)	(%)	(ppm)	(%)	(%)	(%)	(%)	(%)	(%)	(ppm)	(ppm)	(ppm)	(%)	(%)	(%)	(ppm)	(ppm)	(ppm)	(ppm)	(ppm)	(ppm)	(ppm)	(ppm)	(ppm)	(ppm)	(ppm)	(ppm)	(ppm)	(ppm)
Samples	2	2	2	2	2	2	2	2	2	2	2	2	2	2	2	2	2	2	2	2	2	2	2	2	2	2	2	2	2	2	2	2	2	2	2	2	2
Min.	0.61	0.35	0.11	19.85	18.42	1.07	0.13	0.06	1.27	0.03	583	4.16	1.13	3.93	1.89	0.48	0.46	1530	1404	0.23	17.68	9.56	4.20	208.0	678.0	34.6	149.5	28.8	7.4	37.4	5.6	37.0	8.4	26.2	3.3	25.5	4.1
Max.	0.89	0.37	0.11	21.14	18.52	1.15	0.14	0.07	1.47	0.03	597	4.81	1.51	4.04	1.90	0.56	0.53	1680	1415	0.30	19.45	10.75	4.42	234.5	1035.5	39.0	165.5	32.0	8.1	41.5	6.0	39.6	8.9	27.7	3.6	26.4	4.3
Renge	0.28	0.02	0.00	1.29	0.10	0.08	0.01	0.01	0.20	0.00	14	0.65	0.38	0.11	0.01	0.07	0.06	150	11	0.07	1.78	1.18	0.22	26.5	357.5	4.3	16.0	3.2	0.7	4.1	0.4	2.6	0.6	1.6	0.2	0.9	0.1
Ave.	0.75	0.36	0.11	20.50	18.47	1.11	0.14	0.07	1.37	0.03	590	4.49	1.32	3.98	1.90	0.52	0.50	1605	1410	0.27	18.56	10.16	4.31	221.3	856.8	36.8	157.5	30.4	7.7	39.4	5.8	38.3	8.7	26.9	3.4	25.9	4.2
Med.	0.75	0.36	0.11	20.50	18.47	1.11	0.14	0.07	1.37	0.03	590	4.49	1.32	3.98	1.90	0.52	0.50	1605	1410	0.27	18.56	10.16	4.31	221.3	856.8	36.8	157.5	30.4	7.7	39.4	5.8	38.3	8.7	26.9	3.4	25.9	4.2
S.D.	0.20	0.02	0.00	0.91	0.07	0.05	0.01	0.01	0.14	0.00	10	0.46	0.27	0.08	0.01	0.05	0.04	106	8	0.05	1.26	0.84	0.16	18.7	252.8	3.1	11.3	2.3	0.5	2.9	0.3	1.9	0.4	1.1	0.2	0.7	0.1
V.a.r	0.04	0.00	0.00	0.83	0.00	0.00	0.00	0.00	0.02	0.00	100	0.21	0.07	0.01	0.00	0.00	0.00	11250	57	0.00	1.58	0.70	0.02	351.1	63903.1	9.4	127.8	5.1	0.3	8.6	0.1	3.4	0.2	1.2	0.0	0.4	0.0
C.V	26.24	4.52	0.36	4.44	0.37	4.81	5.60	11.23	10.27	0.36	1.69	10.18	20.32	1.98	0.44	9.97	9.02	6.61	0.54	18.60	6.78	8.24	3.61	8.47	29.51	8.33	7.18	7.43	6.83	7.44	5.32	4.85	4.49	4.08	4.52	2.57	2.06

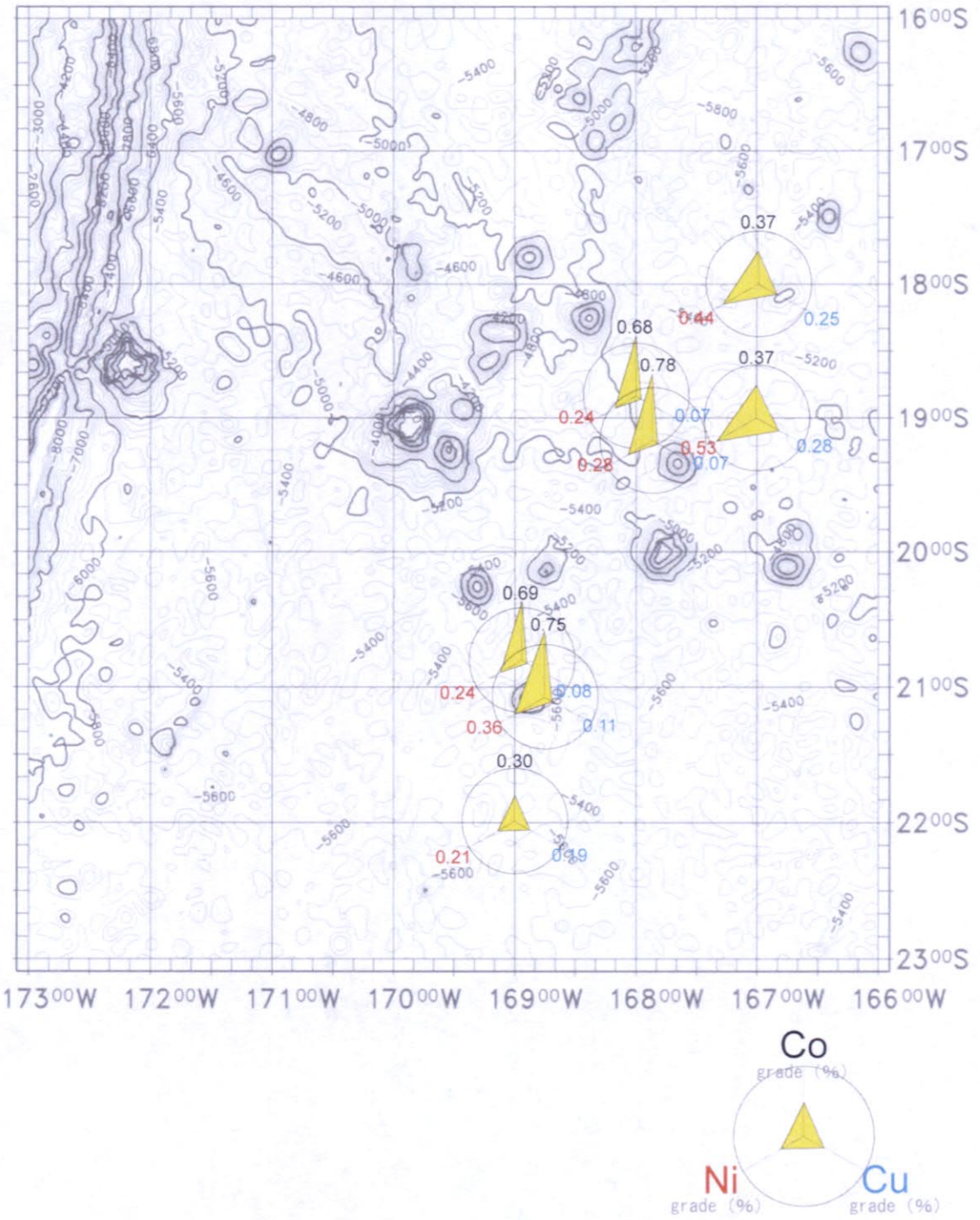

Fig. 3-5-8 Distribution Map of Co, Ni, Cu Grades

Comparing the nodules of the Plain Province and the Hilly Province, there is a significant difference on the concentration of Co, the former (0.28 to 0.41%, average0.36%) is lower compared with the latter (0.39 to 0.89%, average 0.69%). The crust samples collected in the Hilly Province show 0.69% and 0.89%, similar value to manganese nodules in the Hilly Province.

- Ni of all the sample ranges from 0.14 to 0.53% with an average of 0.33%. Comparison between the Plain and the Hilly Provinces shows a reverse relation with Co, the former (0.20 to 0.53%) is higher than the latter (0.14 to 0.34 %). The manganese crusts of the Hilly Province are 0.35% and 0.37%, similar to those of manganese nodules in the Plain Province.
- Cu of all the sample ranges from 0.05 to 0.29% with an average of 0.15% . There is a clear difference between manganese nodules of the Plain Province and the Hilly Province, the former (0.19 to 0.29%) is higher than the latter (0.05 to 0.08%). The crust samples of the Hilly Province are 0.11% and close to nodule samples of that area.
- Mn of all the samples ranges from 14.03 to 22.94% with an average of 19.27%. Same as Cu, there is clear difference between the Plain Province and the Hilly Province, the former (14.03 to 19.56%) is lower than the latter (19.06 to 22.94%). The crusts in the Hilly Province are 19.85% and 21.14%, similar to those of manganese nodules of the Hilly Province.
- Fe of all the samples ranges from 14.85 to 19.76% with an average of 17.96%. Comparison of manganese nodules of the Plain Province and the Hilly Province does not show clear difference, the former is slightly lower than the latter. The ratio of Mn/Fe is similar for both areas and shows 0.72 to 1.32%.

The average chemical compositions of manganese nodules in this survey area are given on Table 3-5-3 with existing data of the Cook Islands area, the Central Pacific Basin, and the East Pacific area (Clarion-Clipperton area).

Comparison of chemical composition of manganese nodules in the Hilly Province and the Plain Province in the survey area shows that the contents of Co and Mn are higher in the former area and Ni and Cu are lower than the latter. The manganese nodules of the Hilly Province show similar chemical composition to that of the associated manganese crust, moreover, similar to cobalt rich manganese crust distributed over the seamounts in the Northwest Pacific (e.g. seamounts of the Marshall Islands area). On the other hand, chemical composition of manganese nodules in the Plain Province resembles to that of manganese nodules in the South Area of the Cook Islands, adjacent

Table 3-5-3 Average Chemical Composition of Manganese Nodules

	This Survey			2001 the Cook Islands Area (South Area)[1]	Central Pacific Basin[2]			Clarion-Clipperton Area[3]	The Marshall Islands Area Crust[4]
	Manganese Nodules of Plain Province	Manganese Nodules of Hilly Province	Crust of Hilly Province		S type	Mix type	R type		
Sample Numbers	10	10	2	49	314	35	86	308	22
Co (%)	0.36	0.69	0.75	0.46	0.32	0.20	0.14	0.26	0.89
Ni (%)	0.41	0.25	0.36	0.32	0.56	1.10	1.39	1.21	0.40
Cu (%)	0.24	0.07	0.11	0.19	0.38	0.99	1.32	1.00	0.04
Mn (%)	17.76	20.53	20.50	13.76	19.30	25.50	27.50	26.20	20.60
Fe (%)	17.04	18.77	18.47	18.79	14.50	10.30	6.60	6.60	12.40
Mn/Fe	1.06	1.10	1.11	0.73	1.48	2.62	4.63	4.10	1.66
Ni+Cu+Co	1.01	1.01	1.22	0.97	1.26	2.29	2.85	2.47	1.33

Source 1: JICA/MMAJ (2001)
2: Usui and Moritani (1992)
3: Hallbach and others ed.(1988)
4: Hein et al. (1992)

to the east of the survey area, where the survey was conducted in the fiscal year 2000.

Comparison of chemical composition of manganese nodules of the Plain Province of this area and the South Area of Cook Islands with Clarion-Clipperton area (known as the area of typical manganese nodules distribution in the East Pacific) shows that Ni and Cu are clearly lower and Co is slightly higher. Mn is lower and Fe is higher, accordingly, the ratios of Mn/Fe are clearly lower compared with that of the Clarion-Clipperton area.

Usui and Moritani (1992) studied the mode of occurrences and chemical composition of the manganese nodules of the Central Pacific Basin and showed that nodules can be classified into s-type of hydrogenous origin and r-type of diagenetic origin. The s-type nodules have relatively smooth surface and they glow from the seawater on the surface of seafloor, while the r-type has rough irregular surface and formed surrounded by sediments several centimeter below the seafloor. These two types have significantly different chemical characteristics: namely the s-type has clearly lower Ni and Cu contents while Co is somewhat higher than those of r-type nodules. Further, Mn is lower and Fe is higher in s-type than in r-type and thus Mn/Fe ratio is lower in s-type nodule. The manganese nodules of both of the Plain and Hilly Provinces have chemical compositions similar to s-type nodule, while chemical composition of r-type is similar to that of the Clarion-Clipperton area.

The results of chemical analysis of manganese nodules and crust of the area are shown in the Fe-(Cu+Ni)-Mn triangular diagram (Fig. 3-5-9). All the samples are plotted near the area of hydrogenous manganese nodules, the area represented by poor Cu+Ni, closer to the Fe-Mn side, and Mn/Fe ratio is close to 1. The samples of the Plain Province and the Hilly Province occupy slightly different domains in the diagram. The former is plotted slightly closer position to the area of diagenetic manganese nodule, and the latter occupies the area closer to the area of hydrogenous manganese nodules. The manganese nodule samples collected at 03513 station in the Plain Province are buried nodule found at 30cm below the surface, and they show low Mn content of 14.03% and 15.01%, and they occupy slightly different domain from the other samples, close to Fe rich side.

Manganese nodules of the survey area has chemical composition close to that of hydrogenous nodule, and when it is compared with that of the Clarion-Clipperton area, Co and Fe is high, but Ni, Cu, Mn is low. In the survey area, chemical composition is different from the Plain Province to the Hilly Province, and the composition of the Hilly Province is close to that of manganese oxides of hydrogenous origin and shows similar composition to that of cobalt-rich manganese crust with high Co, which is commonly

found being distributed over seamounts in the Pacific Ocean.

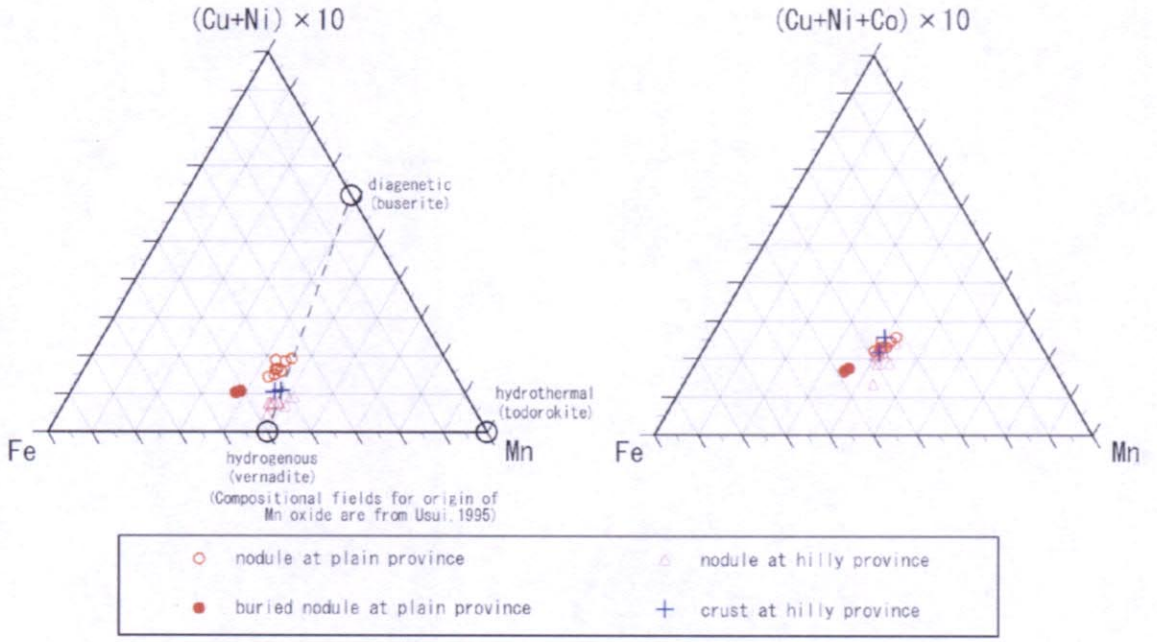

Fig. 3-5-9 Fe−(Cu+Ni)−Mn Triangular Diagram

2) Characteristics of Chemical Composition

For eleven samples of manganese nodules without nuclei and manganese crust samples, the chemical analyses of 36 elements were conducted. From results of these, in order to investigate the correlation among elements, correlation coefficient was calculated (Table3-5-4). Combinations of elements showing strong positive correlation (correlation coefficient >0.7) and strong negative correlation (correlation <-0.7) are as follows.

- combination of elements showing strong positive correlation
  Co-Mn-Pb, Ni-Zn-Pt, Si-Al, Ca-P-Ba-Sr
- combination of elements showing strong negative correlation
  Co-Cu, Al, Si, Ni-Fe, Mn-Si-Al

The group of elements Co-Mn-Pb and that of Ni-Zn-Pt have high positive correlation coefficient respectively and each group is considered to show similar behavior. Si and Al have high positive correlation coefficient, but have high negative correlation with Co and Mn, and they are elements reflecting impure inclusion such as clay minerals. The group of elements such as Ca-P-Ba-Sr has high positive correlation

Table 3-5-4 Correlation Coefficient(1)

Correlation Coefficient (Manganes nodule+Crust; n=11)

	Co	Ni	Cu	Mn	Fe	Pb	Zn	Ti	Mo	V	Si	Al	Ca	Na	K	P	Ba	Sr	Pt	Ig-loss	H_2O^+	H_2O^-	La	Ce	Pr	Nd	Sm	Eu	Gd	Tb	Dy	Ho	Er	Tm	Yb	Lu
Co	1.000																																			
Ni	0.035	1.000																																		
Cu	-0.785	0.509	1.000																																	
Mn	0.772	0.229	-0.601	1.000																																
Fe	-0.168	-0.849	-0.277	-0.495	1.000																															
Pb	0.779	-0.042	-0.753	0.714	-0.015	1.000																														
Zn	-0.145	0.741	0.585	-0.164	-0.320	0.007	1.000																													
Ti	0.087	0.368	0.346	-0.215	0.012	0.050	0.782	1.000																												
Mo	0.665	-0.063	-0.702	0.816	-0.322	0.651	-0.481	-0.516	1.000																											
V	0.286	-0.594	-0.567	0.237	0.513	0.445	-0.330	-0.041	0.239	1.000																										
Si	-0.834	-0.314	0.605	-0.823	0.316	-0.888	-0.180	-0.094	-0.617	-0.184	1.000																									
Al	-0.881	-0.101	0.738	-0.715	0.089	-0.931	-0.093	-0.135	-0.568	-0.352	0.951	1.000																								
Ca	0.378	0.449	-0.123	0.229	-0.115	0.591	0.696	0.518	-0.042	0.079	-0.686	-0.709	1.000																							
Na	0.473	-0.159	-0.442	0.378	-0.051	0.138	-0.335	-0.062	0.177	0.309	-0.171	-0.283	-0.029	1.000																						
K	-0.232	-0.089	0.360	-0.288	-0.011	-0.535	-0.137	0.153	-0.104	-0.116	0.559	0.565	-0.634	-0.021	1.000																					
P	0.495	0.100	-0.325	0.223	0.210	0.719	0.527	0.626	-0.009	0.366	-0.659	-0.753	0.869	-0.008	-0.465	1.000																				
Ba	-0.046	0.567	0.402	-0.161	-0.104	0.101	0.920	0.774	-0.458	-0.074	-0.239	-0.226	0.789	-0.191	-0.180	0.656	1.000																			
Sr	0.624	0.170	-0.512	0.507	0.004	0.857	0.354	0.278	0.316	0.384	-0.856	-0.908	0.890	0.120	-0.651	0.879	0.528	1.000																		
Pt	0.067	0.801	0.425	0.043	-0.425	0.164	0.960	0.730	-0.299	-0.382	-0.384	-0.281	0.769	-0.211	-0.203	0.580	0.882	0.476	1.000																	
Ig-loss	0.552	0.055	-0.591	0.512	0.012	0.781	0.090	-0.073	0.356	0.089	-0.794	-0.806	0.675	0.134	-0.838	0.620	0.158	0.799	0.271	1.000																
H_2O^+	0.259	-0.534	-0.659	0.240	0.455	0.463	-0.429	-0.405	0.217	0.315	-0.304	-0.408	0.137	0.341	-0.624	0.233	-0.305	0.370	-0.315	0.730	1.000															
H_2O^-	-0.050	0.129	0.074	0.040	-0.154	-0.271	-0.162	-0.269	-0.136	-0.511	0.032	0.169	-0.245	-0.033	-0.247	-0.356	-0.326	-0.328	-0.111	0.141	0.198	1.000														
La	0.820	-0.252	-0.882	0.822	0.025	0.882	-0.370	-0.221	0.832	0.560	-0.776	-0.804	0.211	0.258	-0.294	0.419	-0.259	0.605	-0.204	0.573	0.455	-0.164	1.000													
Ce	0.425	-0.585	-0.660	0.407	0.145	0.232	-0.874	-0.556	0.678	0.279	-0.068	-0.112	-0.613	0.285	0.269	-0.344	-0.861	-0.234	-0.776	-0.035	0.291	0.106	0.598	1.000												
Pr	0.318	-0.594	-0.624	0.443	0.134	0.220	-0.895	-0.667	0.699	0.391	-0.049	-0.064	-0.635	0.226	0.205	-0.392	-0.874	-0.232	-0.827	-0.058	0.300	0.079	0.612	0.961	1.000											
Nd	0.350	-0.584	-0.652	0.490	0.126	0.277	-0.873	-0.650	0.725	0.451	-0.099	-0.117	-0.584	0.244	0.171	-0.338	-0.839	-0.168	-0.804	-0.026	0.313	0.031	0.659	0.946	0.996	1.000										
Sm	0.216	-0.618	-0.543	0.348	0.155	0.104	-0.916	-0.683	0.622	0.346	0.072	0.057	-0.723	0.209	0.268	-0.484	-0.910	-0.346	-0.870	-0.151	0.265	0.108	0.510	0.953	0.992	0.981	1.000									
Eu	0.261	-0.618	-0.585	0.388	0.160	0.174	-0.902	-0.671	0.662	0.386	0.013	-0.005	-0.674	0.196	0.233	-0.426	-0.884	-0.280	-0.852	-0.106	0.279	0.073	0.567	0.955	0.998	0.991	0.997	1.000								
Gd	0.327	-0.626	-0.643	0.430	0.182	0.252	-0.885	-0.638	0.690	0.416	-0.060	-0.085	-0.613	0.204	0.195	-0.344	-0.860	-0.205	-0.820	-0.035	0.325	0.060	0.632	0.963	0.997	0.995	0.987	0.995	1.000							
Tb	0.230	-0.624	-0.560	0.362	0.167	0.141	-0.905	-0.675	0.645	0.372	0.047	0.029	-0.698	0.189	0.264	-0.449	-0.892	-0.310	-0.858	-0.133	0.269	0.066	0.541	0.953	0.995	0.987	0.998	0.999	0.992	1.000						
Dy	0.337	-0.596	-0.645	0.421	0.119	0.323	-0.838	-0.594	0.697	0.354	-0.069	-0.118	-0.552	0.267	0.130	-0.303	-0.854	-0.168	-0.762	0.041	0.379	-0.024	0.612	0.937	0.939	0.938	0.930	0.939	0.945	0.935	1.000					
Ho	0.554	-0.485	-0.795	0.655	0.157	0.661	-0.626	-0.460	0.801	0.503	-0.468	-0.476	-0.182	0.101	-0.127	0.095	-0.581	0.248	-0.511	0.367	0.483	-0.026	0.893	0.808	0.849	0.874	0.787	0.827	0.871	0.811	0.836	1.000				
Er	0.686	-0.261	-0.793	0.690	0.141	0.918	-0.227	-0.140	0.710	0.495	-0.763	-0.781	0.313	0.004	-0.400	0.544	-0.146	0.663	-0.088	0.673	0.519	-0.147	0.941	0.465	0.483	0.529	0.383	0.446	0.521	0.421	0.516	0.869	1.000			
Tm	0.680	-0.260	-0.770	0.623	0.211	0.916	-0.148	-0.045	0.616	0.447	-0.765	-0.799	0.389	0.014	-0.412	0.628	-0.050	0.709	0.002	0.734	0.573	-0.147	0.893	0.389	0.379	0.421	0.277	0.340	0.422	0.316	0.425	0.799	0.981	1.000		
Yb	0.578	-0.081	-0.610	0.532	0.153	0.904	0.099	0.080	0.469	0.307	-0.795	-0.802	0.582	-0.148	-0.550	0.741	0.164	0.797	0.233	0.818	0.530	-0.118	0.760	0.129	0.123	0.166	0.020	0.085	0.170	0.061	0.191	0.622	0.916	0.956	1.000	
Lu	0.442	0.171	-0.340	0.386	0.071	0.777	0.431	0.316	0.218	0.136	-0.760	-0.740	0.777	-0.212	-0.548	0.834	0.510	0.854	0.549	0.796	0.382	-0.149	0.515	-0.223	-0.240	-0.196	-0.338	-0.277	-0.197	-0.298	-0.176	0.293	0.705	0.790	0.918	1.000

Test of Correlation (t-Test,Manganes nodule+Crust; n=11)

	Co	Ni	Cu	Mn	Fe	Pb	Zn	Ti	Mo	V	Si	Al	Ca	Na	K	P	Ba	Sr	Pt	Ig-loss	H_2O^+	H_2O^-	La	Ce	Pr	Nd	Sm	Eu	Gd	Tb	Dy	Ho	Er	Tm	Yb	Lu
Co	0.00																																			
Ni	-6.47	0.00																																		
Cu	-8.13	-9.06	0.00																																	
Mn	33.97	32.59	32.08	0.00																																
Fe	70.57	70.69	75.45	-2.04	0.00																															
Pb	-10.72	-7.24	0.80	-32.78	-77.06	0.00																														
Zn	-11.32	-12.04	-3.66	-32.70	-77.05	-13.57	0.00																													
Ti	11.23	40.72	53.00	-30.47	-72.04	54.70	66.89	0.00																												
Mo	-12.12	-11.21	-3.65	-32.88	-77.17	-26.66	-2.59	-55.34	0.00																											
V	59.39	59.25	59.29	58.07	58.20	59.36	59.35	59.23	59.36	0.00																										
Si	13.47	16.07	17.55	-15.87	-37.47	16.75	17.14	13.34	17.13	-58.39	0.00																									
Al	5.77	8.79	10.47	-23.26	-54.61	9.56	10.10	4.01	10.10	-58.71	-24.09	0.00																								
Ca	7.72	9.14	9.45	-29.27	-45.14	9.59	9.89	4.85	9.85	-59.22	-6.35	0.68	0.00																							
Na	25.86	56.17	65.37	-29.97	-69.29	119.94	114.21	23.48	128.27	-59.20	-11.47	-1.04	-2.06	0.00																						
K	-1.74	10.56	26.83	-31.73	-75.16	32.48	44.28	-32.88	46.69	-59.30	-15.91	-7.84	-7.45	-73.07	0.00																					
P	-5.10	4.94	11.92	-32.29	-76.70	25.59	28.89	-53.06	26.34	-59.35	-15.62	-7.91	-8.71	-72.56	-6.87	0.00																				
Ba	12.24	12.24	12.25	12.00	12.03	12.24	12.25	12.23	12.25	5.52	12.17	12.22	12.24	12.22	12.24	12.24	0.00																			
Sr	22.29	22.29	22.29	22.03	21.93	22.29	22.29	22.27	22.29	11.37	22.06	22.17	22.34	22.26	22.28	22.29	0.65	0.00																		
Pt	0.94	0.98	1.00	-1.20	-1.04	1.00	1.01	0.87	1.01	-55.78	0.38	0.78	0.75	0.81	0.95	0.97	-11.83	-21.94	0.00																	
Ig-loss	34.77	33.63	33.23	-6.22	-3.51	34.16	34.09	31.41	34.17	-57.86	14.05	21.89	38.48	30.37	32.43	33.92	-12.07	-22.13	0.82	0.00																
H_2O^+	50.13	47.21	48.30	-16.84	-37.06	51.73	51.20	43.12	51.82	-58.70	9.99	23.68	26.64	43.02	47.29	50.43	-12.12	-22.12	0.09	-17.83	0.00															
H_2O^-	23.12	27.30	28.28	-24.74	-45.49	27.90	28.48	19.95	28.60	-58.41	-3.15	10.42	6.88	16.79	24.91	25.40	-12.19	-22.18	-0.51	-24.56	-24.23	0.00														
La	25.99	25.88	25.87	25.01	23.72	25.93	25.92	25.77	25.94	-42.69	24.49	25.18	25.79	25.72	25.86	25.90	-9.52	-19.80	19.35	24.74	24.99	25.30	0.00													
Ce	11.99	11.99	11.99	11.85	11.84	11.99	11.99	11.98	11.99	7.21	11.94	11.97	11.96	11.97	11.99	11.99	1.74	2.14	12.04	11.85	11.91	11.95	10.60	0.00												
Pr	16.43	16.40	16.46	10.98	10.78	16.52	16.52	16.08	16.55	-58.55	14.59	15.79	15.05	15.97	16.39	16.40	-11.30	-20.91	5.02	11.07	13.61	15.15	-23.84	-11.85	0.00											
Nd	18.72	18.70	18.72	17.39	17.13	18.74	18.74	18.61	18.75	-34.09	18.17	18.51	18.30	18.58	18.70	18.70	-8.91	-17.15	16.95	17.22	17.94	18.34	-0.94	-11.22	19.58	0.00										
Sm	15.67	15.67	15.75	9.46	9.58	15.80	15.81	15.32	15.84	-58.19	13.90	15.14	14.16	15.20	15.66	15.66	-11.38	-20.93	4.29	9.77	12.59	14.33	-23.31	-11.88	-13.65	-19.60	0.00									
Eu	17.83	17.68	18.10	-14.27	-13.36	18.43	18.43	15.99	18.62	-59.53	7.53	14.04	10.96	15.38	17.72	17.71	-12.05	-22.01	0.17	-7.50	1.19	10.44	-25.61	-11.96	-16.09	-18.74	-15.14	0.00								
Gd	21.66	21.53	21.64	14.29	13.98	21.75	21.74	21.11	21.79	-58.50	18.96	20.64	19.46	20.99	21.57	21.56	-11.41	-21.08	4.81	14.19	17.88	19.84	-23.35	-11.79	-2.25	-17.92	5.76	22.79	0.00							
Tb	19.97	19.74	20.46	-21.16	-27.41	21.03	21.02	17.07	21.35	-59.36	4.04	13.57	9.50	16.14	19.92	19.82	-12.11	-22.09	-0.17	-13.98	-6.64	8.01	-25.59	-11.96	-15.93	-18.65	-15.06	-14.02	-21.84	0.00						
Dy	25.84	25.61	25.74	16.09	15.62	25.91	25.89	25.06	25.97	-57.49	22.07	24.28	22.78	24.94	25.67	25.67	-11.52	-21.24	4.23	16.16	21.06	23.23	-23.05	-11.77	-3.94	-17.14	-0.14	28.28	-5.10	26.59	0.00					
Ho	47.12	40.98	41.36	-21.92	-32.97	44.82	44.09	36.55	45.13	-59.05	7.19	19.82	19.53	35.54	41.69	42.93	-12.13	-22.13	-0.02	-16.73	-4.93	17.13	-25.40	-11.93	-14.47	-18.22	-13.46	-3.90	-19.33	6.10	-23.00	0.00				
Er	56.10	52.18	51.75	13.71	14.94	53.63	53.26	50.48	53.59	-58.08	26.49	36.34	50.27	49.55	51.84	53.42	-11.94	-21.91	1.91	24.26	38.16	40.24	-24.12	-11.79	-8.85	-16.77	-7.23	27.45	-11.53	39.44	-12.57	51.96	0.00			
Tm	52.02	38.83	38.52	-29.35	-65.06	49.13	46.98	27.75	48.79	-59.21	-6.30	4.48	4.05	19.94	37.21	47.48	-12.21	-22.25	-0.65	-30.38	-41.04	-7.10	-25.73	-11.97	-15.64	-18.50	-14.80	-13.33	-20.62	-12.69	-24.49	-37.62	-54.12	0.00		
Yb	63.10	59.25	58.48	8.41	13.58	60.60	60.24	57.31	60.43	-57.57	26.85	38.34	66.88	55.29	58.09	60.85	-11.98	-21.95	1.70	28.04	41.87	43.91	-23.87	-11.79	-8.89	-16.64	-7.40	20.42	-11.38	32.02	-12.38	47.96	-8.58	62.14	0.00	
Lu	47.00	49.95	47.20	-27.62	-60.17	54.62	54.16	37.71	53.73	-59.03	-4.89	6.54	7.56	25.46	42.19	56.97	-12.21	-22.24	-0.59	-29.62	-34.67	-4.13	-25.59	-11.96	-15.26	-18.38	-14.40	-11.47	-20.00	-9.90	-23.62	-26.96	-50.50	11.77	-60.44	0.00

: non-correlation

Table 3-5-4 Correlation Coefficient(2)

Correlation Coefficient (Manganes nodule: n=9)

	Co	Ni	Cu	Mn	Fe	Pb	Zn	Ti	Mo	V	Si	Al	Ca	Na	K	P	Ba	Sr	Pt	Ig-loss	H_2O^+	H_2O^-	La	Ce	Pr	Nd	Sm	Eu	Gd	Tb	Dy	Ho	Er	Tm	Yb	Lu
Co	1.000																																			
Ni	-0.125	1.000																																		
Cu	-0.874	0.563	1.000																																	
Mn	0.785	0.203	-0.612	1.000																																
Fe	-0.159	-0.927	-0.276	-0.493	1.000																															
Pb	0.774	-0.355	-0.884	0.759	0.022	1.000																														
Zn	-0.780	0.710	0.978	-0.465	-0.459	-0.801	1.000																													
Ti	-0.694	0.099	0.722	-0.803	0.148	-0.884	0.611	1.000																												
Mo	0.803	0.033	-0.712	0.863	-0.342	0.879	-0.571	-0.880	1.000																											
V	0.270	-0.703	-0.571	0.224	0.523	0.477	-0.662	-0.281	0.253	1.000																										
Si	-0.883	-0.062	0.759	-0.937	0.341	-0.850	0.619	0.911	-0.913	-0.184	1.000																									
Al	-0.960	0.250	0.939	-0.816	0.062	-0.913	0.850	0.837	-0.873	-0.398	0.926	1.000																								
Ca	0.876	0.004	-0.767	0.765	-0.298	0.802	-0.643	-0.790	0.827	0.225	-0.878	-0.902	1.000																							
Na	0.570	-0.131	-0.442	0.402	-0.058	0.219	-0.442	0.056	0.164	0.321	-0.280	-0.427	0.288	1.000																						
K	-0.417	0.210	0.534	-0.443	-0.045	-0.588	0.486	0.605	-0.315	-0.201	0.549	0.543	-0.628	-0.063	1.000																					
P	0.489	-0.881	-0.848	0.250	0.669	0.738	-0.915	-0.534	0.406	0.747	-0.397	-0.644	0.417	0.206	-0.477	1.000																				
Ba	-0.708	0.377	0.818	-0.562	-0.102	-0.827	0.759	0.741	-0.620	-0.259	0.714	0.809	-0.763	-0.234	0.754	-0.712	1.000																			
Sr	0.831	-0.407	-0.928	0.769	0.095	0.952	-0.871	-0.841	0.857	0.619	-0.846	-0.937	0.781	0.335	-0.493	0.758	-0.710	1.000																		
Pt	-0.435	0.880	0.780	-0.121	-0.711	-0.585	0.875	0.373	-0.264	-0.840	0.264	0.554	-0.399	-0.249	0.433	-0.927	0.541	-0.678	1.000																	
Ig-loss	0.707	-0.283	-0.777	0.644	0.052	0.815	-0.700	-0.771	0.621	0.115	-0.787	-0.798	0.668	0.222	-0.752	0.614	-0.885	0.721	-0.398	1.000																
H_2O^+	0.468	-0.670	-0.726	0.326	0.494	0.633	-0.760	-0.450	0.261	0.389	-0.429	-0.573	0.311	0.360	-0.622	0.799	-0.756	0.587	-0.619	0.832	1.000															
H_2O^-	0.056	0.306	0.084	0.083	-0.181	-0.152	0.128	-0.096	-0.202	-0.515	-0.171	-0.002	0.100	-0.064	-0.528	-0.240	-0.172	-0.195	0.266	0.370	0.206	1.000														
La	0.825	-0.348	-0.908	0.817	0.036	0.963	-0.837	-0.903	0.886	0.554	-0.890	-0.942	0.787	0.285	-0.521	0.735	-0.765	0.984	-0.607	0.770	0.606	-0.133	1.000													
Ce	0.875	-0.457	-0.965	0.676	0.160	0.933	-0.910	-0.793	0.817	0.434	-0.822	-0.949	0.762	0.352	-0.467	0.783	-0.823	0.934	-0.639	0.830	0.702	-0.109	0.935	1.000												
Pr	0.770	-0.441	-0.909	0.757	0.137	0.960	-0.858	-0.883	0.842	0.619	-0.834	-0.908	0.732	0.251	-0.520	0.798	-0.760	0.981	-0.671	0.756	0.645	-0.176	0.993	0.927	1.000											
Nd	0.748	-0.432	-0.889	0.765	0.122	0.952	-0.840	-0.868	0.837	0.659	-0.819	-0.891	0.719	0.266	-0.506	0.787	-0.730	0.979	-0.670	0.717	0.618	-0.216	0.988	0.902	0.997	1.000										
Sm	0.742	-0.489	-0.909	0.724	0.187	0.956	-0.868	-0.864	0.812	0.646	-0.802	-0.889	0.702	0.248	-0.524	0.829	-0.764	0.973	-0.699	0.753	0.674	-0.192	0.984	0.922	0.998	0.995	1.000									
Eu	0.729	-0.482	-0.899	0.716	0.182	0.959	-0.857	-0.869	0.821	0.650	-0.797	-0.882	0.705	0.213	-0.519	0.822	-0.744	0.977	-0.700	0.736	0.645	-0.212	0.982	0.915	0.997	0.995	0.998	1.000								
Gd	0.734	-0.502	-0.910	0.705	0.206	0.957	-0.871	-0.869	0.809	0.631	-0.796	-0.885	0.696	0.216	-0.525	0.838	-0.771	0.969	-0.702	0.762	0.680	-0.186	0.981	0.928	0.996	0.991	0.999	0.998	1.000							
Tb	0.712	-0.496	-0.890	0.703	0.199	0.950	-0.851	-0.860	0.815	0.652	-0.781	-0.867	0.673	0.206	-0.482	0.828	-0.738	0.966	-0.692	0.725	0.648	-0.240	0.977	0.912	0.995	0.993	0.998	0.998	1.000							
Dy	0.685	-0.456	-0.846	0.637	0.109	0.960	-0.786	-0.736	0.773	0.500	-0.705	-0.825	0.694	0.290	-0.533	0.776	-0.827	0.877	-0.605	0.773	0.690	-0.271	0.879	0.893	0.890	0.886	0.899	0.897	0.899	0.895	1.000					
Ho	0.665	-0.433	-0.843	0.712	0.154	0.956	-0.788	-0.913	0.807	0.535	-0.805	-0.842	0.668	0.091	-0.579	0.787	-0.775	0.929	-0.612	0.806	0.683	-0.101	0.960	0.890	0.976	0.967	0.978	0.979	0.982	0.979	0.888	1.000				
Er	0.651	-0.436	-0.835	0.681	0.167	0.951	-0.779	-0.918	0.800	0.491	-0.796	-0.831	0.664	0.035	-0.585	0.783	-0.781	0.914	-0.602	0.819	0.681	-0.078	0.946	0.890	0.961	0.948	0.964	0.966	0.972	0.966	0.882	0.997	1.000			
Tm	0.632	-0.500	-0.837	0.617	0.254	0.918	-0.795	-0.864	0.740	0.448	-0.750	-0.802	0.582	0.055	-0.540	0.808	-0.776	0.879	-0.598	0.850	0.758	-0.051	0.912	0.901	0.933	0.911	0.939	0.937	0.951	0.942	0.866	0.977	0.984	1.000		
Yb	0.522	-0.435	-0.735	0.555	0.223	0.870	-0.685	-0.868	0.689	0.323	-0.706	-0.714	0.533	-0.114	-0.584	0.738	-0.765	0.786	-0.504	0.854	0.726	0.043	0.837	0.821	0.860	0.833	0.867	0.868	0.884	0.872	0.812	0.944	0.963	0.979	1.000	
Lu	0.373	-0.321	-0.553	0.471	0.187	0.716	-0.502	-0.759	0.582	0.147	-0.605	-0.548	0.323	-0.219	-0.422	0.562	-0.550	0.640	-0.300	0.772	0.640	0.109	0.692	0.684	0.712	0.681	0.717	0.721	0.738	0.730	0.644	0.827	0.855	0.899	0.943	1.000

Test of Correlation (Manganes nodule: n=9)

	Co	Ni	Cu	Mn	Fe	Pb	Zn	Ti	Mo	V	Si	Al	Ca	Na	K	P	Ba	Sr	Pt	Ig-loss	H_2O^+	H_2O^-	La	Ce	Pr	Nd	Sm	Eu	Gd	Tb	Dy	Ho	Er	Tm	Yb	Lu
Co	0.00																																			
Ni	-5.43	0.00																																		
Cu	-6.73	-7.75	0.00																																	
Mn	27.66	26.62	26.21	0.00																																
Fe	57.86	57.60	61.25	-1.55	0.00																															
Pb	-9.26	-5.81	0.55	-26.79	-62.61	0.00																														
Zn	-9.67	-10.05	-3.17	-26.72	-62.62	-11.17	0.00																													
Ti	9.13	37.85	74.95	-24.81	-59.02	70.88	115.41	0.00																												
Mo	-10.61	-9.69	-2.90	-26.88	-62.63	-36.33	-1.74	-82.06	0.00																											
V	48.25	48.15	48.18	47.16	47.30	48.24	48.23	48.13	48.24	0.00																										
Si	13.89	17.10	18.63	-13.14	-34.70	17.48	18.00	14.73	17.77	-47.49	0.00																									
Al	6.38	10.24	12.03	-19.27	-46.85	10.54	11.25	5.37	11.01	-47.73	-22.58	0.00																								
Ca	48.60	29.02	26.24	-25.51	-52.28	36.79	34.75	11.90	37.78	-48.12	-10.34	-0.99	0.00																							
Na	24.59	50.37	53.08	-24.50	-56.23	100.45	95.97	30.31	104.12	-48.11	-12.13	-1.87	-2.64	0.00																						
K	-1.11	12.12	25.04	-25.92	-60.96	36.07	63.84	-72.09	49.85	-48.19	-16.59	-8.75	-23.78	-64.08	0.00																					
P	-4.31	3.94	10.40	-26.35	-62.66	57.40	37.63	-61.79	55.50	-48.23	-16.71	-9.19	-30.87	-83.29	-12.37	0.00																				
Ba	18.90	18.93	18.94	18.39	18.56	18.93	18.93	18.91	18.93	6.85	18.90	18.95	18.88	18.89	18.92	18.92	0.00																			
Sr	29.84	29.81	29.80	29.74	29.32	29.82	29.82	29.78	29.82	16.13	29.42	29.60	29.80	29.77	29.80	29.81	1.27	0.00																		
Pt	0.95	0.98	1.00	-0.79	-0.67	1.00	1.01	0.90	1.01	-45.77	0.47	0.80	0.83	0.84	0.96	0.97	-17.64	-30.90	0.00																	
Ig-loss	36.45	33.57	33.25	-6.62	-4.34	34.72	34.47	31.37	34.77	-47.08	13.46	21.72	32.80	30.86	32.99	34.16	-18.46	-29.65	0.45	0.00																
H_2O^+	47.66	41.53	42.41	-14.14	-32.07	46.13	45.47	39.24	46.08	-47.74	8.54	20.72	38.50	38.33	42.32	45.41	-18.68	-29.65	-0.11	-19.93	0.00															
H_2O^-	20.69	24.05	24.26	-20.36	-36.86	24.01	24.55	17.88	24.46	-47.48	-3.31	8.51	13.67	14.46	21.16	22.42	-18.83	-29.66	-0.59	-26.60	-20.90	0.00														
La	21.49	21.40	21.39	20.69	19.61	21.44	21.44	21.30	21.45	-34.74	20.25	20.82	21.33	21.27	21.38	21.42	-12.69	-32.82	15.92	20.56	20.72	20.93	0.00													
Ce	15.82	15.82	15.82	15.70	15.64	15.82	15.82	15.81	15.82	10.35	15.72	15.77	15.81	15.80	15.82	15.82	4.12	7.38	15.81	15.72	15.75	15.77	15.06	0.00												
Pr	21.50	21.18	21.17	17.03	14.41	21.36	21.34	20.81	21.38	-49.42	17.21	19.14	20.92	20.68	21.12	21.27	-17.16	-30.44	4.23	17.38	18.49	19.30	-21.40	-15.64	0.00											
Nd	22.38	22.29	22.29	21.53	20.53	22.34	22.33	22.19	22.35	-39.19	21.14	21.71	22.23	22.16	22.27	22.31	-12.71	-32.32	17.17	21.41	21.62	21.78	2.91	-14.91	22.66	0.00										
Sm	24.06	23.60	23.59	18.28	15.22	23.86	23.82	23.14	23.88	-49.13	18.53	20.93	23.32	23.00	23.54	23.74	-17.40	-30.14	3.64	19.06	20.43	21.18	-20.70	-15.62	-11.14	-21.90	0.00									
Eu	26.28	24.01	24.00	-16.38	-14.67	25.27	25.07	21.96	25.36	-48.45	7.20	14.26	22.62	21.21	23.76	24.72	-18.59	-29.87	0.02	-14.56	3.81	12.83	-21.25	-15.77	-20.55	-22.20	-23.46	0.00								
Gd	27.06	26.49	26.48	21.34	17.75	26.79	26.74	26.02	26.81	-48.43	20.86	23.47	26.27	25.88	26.44	26.67	-17.37	-29.94	3.94	22.29	23.39	23.91	-20.02	-15.57	-4.46	-21.17	21.48	27.22	0.00							
Tb	32.03	27.50	27.46	-20.28	-29.22	29.87	29.44	24.24	30.00	-48.27	3.63	12.63	25.47	23.06	27.27	28.99	-18.70	-29.81	-0.28	-24.71	-9.22	9.38	-21.20	-15.78	-20.38	-22.13	-22.96	-18.23	-26.30	0.00						
Dy	29.56	28.86	28.84	21.46	17.94	29.23	29.17	28.30	29.25	-47.14	22.16	25.19	28.65	28.15	28.79	29.08	-17.53	-29.67	3.40	24.14	25.29	25.44	-19.40	-15.57	-5.89	-20.43	-2.11	29.19	-5.86	28.41	0.00					
Ho	42.70	36.14	35.82	-18.04	-27.15	39.35	38.60	32.20	39.42	-47.98	5.80	16.33	35.35	31.08	35.85	38.32	-18.69	-29.75	-0.19	-22.71	-4.88	14.26	-21.00	-15.76	-19.58	-21.92	-21.87	-9.83	-25.07	16.59	-27.00	0.00				
Er	46.87	43.68	43.44	11.04	12.43	45.13	44.77	42.02	45.14	-47.16	23.10	31.43	44.17	41.73	43.60	44.73	-18.26	-29.53	1.37	29.63	34.91	34.37	-19.94	-15.64	-14.45	-20.86	-15.44	79.32	-18.93	55.28	-18.77	48.78	0.00			
Tm	42.50	32.01	32.38	-23.91	-53.65	42.22	39.92	22.45	42.35	-48.11	-6.93	3.59	18.81	17.06	32.10	39.22	-18.85	-29.79	-0.72	-32.16	-40.69	-6.68	-21.27	-15.80	-20.70	-22.17	-23.12	-21.49	-26.13	-24.25	-28.41	-37.25	-45.42	0.00		
Yb	59.39	54.89	54.66	6.75	12.24	57.26	56.67	52.73	57.23	-46.75	25.94	37.31	55.71	52.20	54.95	56.75	-18.34	-29.42	1.19	32.53	46.32	42.76	-19.73	-15.63	-14.03	-20.62	-14.79	56.76	-17.83	70.02	-17.96	69.09	-9.23	60.18	0.00	
Lu	47.73	50.62	51.28	-22.54	-51.16	67.81	63.87	37.56	67.72	-47.97	-6.10	6.09	25.97	29.18	52.02	63.15	-18.85	-29.75	-0.67	-29.32	-33.63	-4.74	-21.15	-15.79	-20.25	-22.05	-22.50	-18.54	-25.43	-18.59	-27.54	-28.43	-41.97	13.02	-55.03	0.00

: non-correlation

coefficient each other, and they are elements reflecting impure inclusion such as calcareous or phosphatic minerals.

Among metallic elements other than five major elements, such as Pb, Zn, Ti, Mo, and V, neither of them shows significantly high concentration and spatial difference in concentration of these elements between the Plain Province and the Hilly Province is not observed. Pt ranges from 0.05 to 0.30ppm with an average of 0.13ppm, and it is low compared to the average of manganese crust of seamounts in the Pacific Ocean, 0.777ppm (Usui and Someya, 1997). Average concentration of Pt is 0.16ppm in the Plain Province and 0.09ppm in the Hilly Province, and that of crust in the Hilly Province is slightly higher, 0.27ppm. None of the elements of Si, Al, Ca, Na, K and P, reflecting accessory minerals of manganese nodules such as quarts, feldspar, clay minerals, phosphates and so on, shows high concentration. In comparison of the Plain Province and the Hilly Province, the former shows higher concentration in Si and Al and lower in Ca and Sr.

The analytical results of rare earth element (La, Ce, Pr, Nd, Sm, Eu, Gd, Tb, Dy, Ho, Er, Tm, Yb, Lu) were normalized to the values of chondrite and North American shale standard and normalized patterns are shown in Fig. 3-5-10. The sum of the value of rare earth elements widely ranges from 1,254 to 2,549ppm, and this is controlled by wide range of Ce from 678 to 1,787ppm. In the figure of chondrite normalized patterns, all the sample show similar pattern declining to the right, with light rare earths of 500 to 700 times higher to chondrite and heavy rare earths of 100 times of chondrite, and clear positive anomaly of Ce is observed.

The concentration of rare earth elements of manganese nodules and crust is known to show large difference between those of hydrogenous origin and hydrothermal origin. The former has significantly high concentration of total REE and Ce often shows positive anomaly (Usui and Someya, 1997). The chondrite normalized pattern of rare earth elements of the survey area shows similar pattern to those of hydrogenous manganese oxides. The concentration of Ce is known to be largely affected by the oxidation-reduction condition on the formation of manganese nodules (De Carlo and McMurty, 1992). Since the concentration of Ce in the survey area is high (average 1,430ppm), the manganese nodules in the area is assumed to have grown under oxidation environment of deepwater.

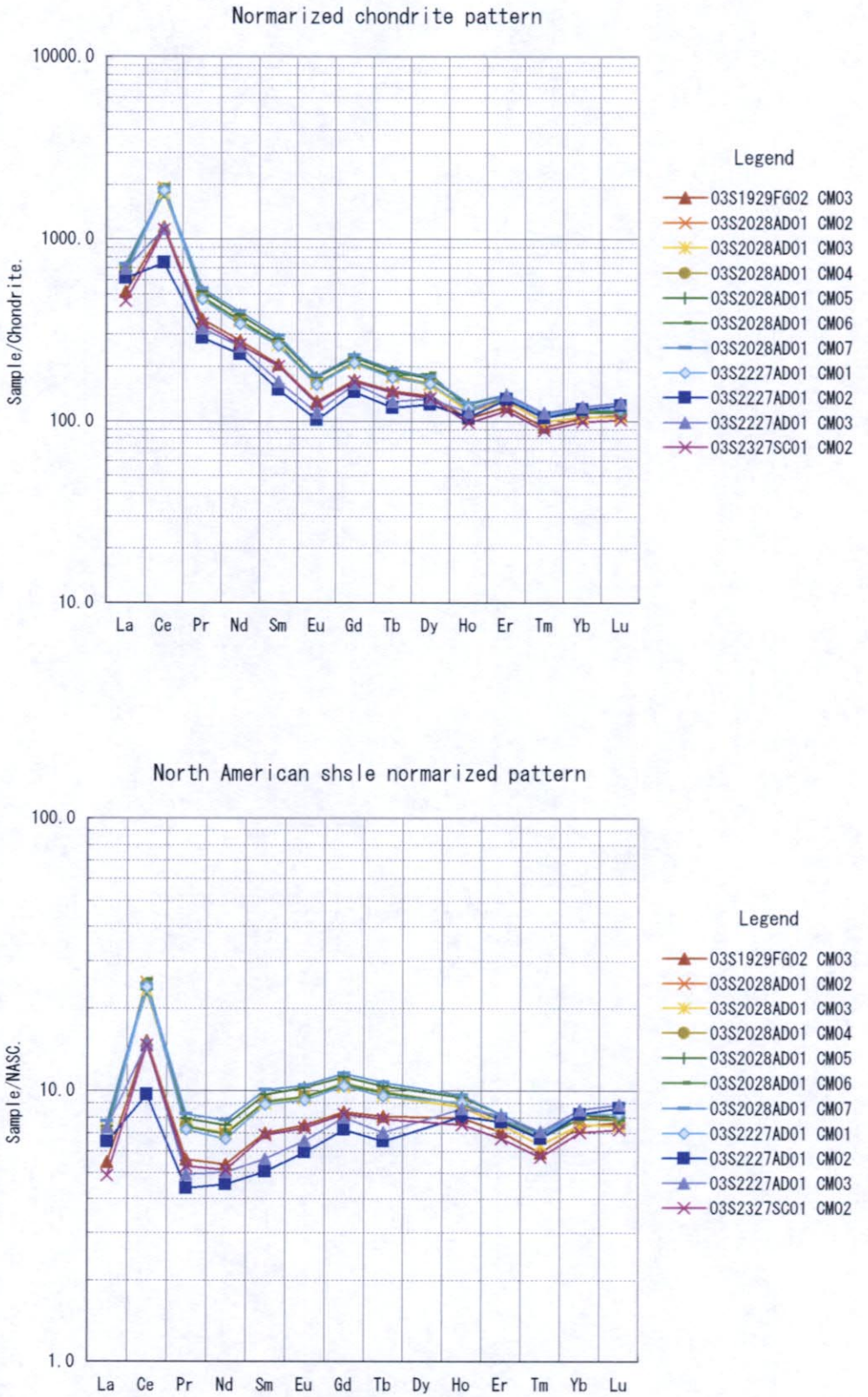

Fig. 3－5－10 REE Normalized Pattern

3 - 6 Environmental Survey

(1) Survey Area

Surveys were conducted at three stations in the survey area within the EEZ of the Niue. The station 03S2027SC01 is located at the foot of a seamount in the central part of the survey area. The water depth is ca. 4,800 m at this station. Stations 03S2326SC01 and 03S2327SC01 are located in the southern part of the survey area on an almost flat seafloor with a depth of ca. 5,600 m.

(2) Sediments Properties

1) Water Content

The vertical distributions of water content of sediments of each station are shown in Fig. 3-6-1 and Appendix Table 2. Investigation of the vertical distribution of water content at 03S2027SC01 showed an average value of 72.2 % in the double cores at the 0-1 cm layer. Water content tended to decrease with depth from the surface to the 4-5 cm layer and was 66 to 67 % in layers deeper than 10 cm. On the other hand, it was 35.1% and 36.5 % on average in the 0-1 cm layer at 03S2326SC01 and 03S2327SC01, respectively. It was observed that there were minimum values of less than 30 % in the 1-2 cm and 2-3 cm layers at 03S2326SC01. These values increased toward the 4-5 cm layer and were 56 to 61 % in the layers deeper than 10 cm. At 03S2327SC01, water content increased from the surface to the 4-5 cm layer and was 60 to 67 % in the layers deeper than 10 cm.

Water content decreased from the surface, then was similar in the layers deeper than 10 cm at 03S2027SC01. At 03S2326SC01 and 03S2327SC01, water content in the surface layers was also lower than that of deeper layers.

2) Specific Sediment Gravity

Vertical distributions of specific sediment gravity at each station are shown in Fig. 3-6-2 and Appendix Table 2. The specific sediment gravities were 2.63 to 2.69 (average: 2.67) in each layer at 03S2027SC01 and only a little variation was observed vertically. On the other hand, the value from the surface to the 3-4cm layer at 03S2326SC01, which was 2.77 to 2.78 (average: 2.78), was higher than that at 03S2027SC01. At 03S2327SC01, the highest value of 2.79 was found in the 0-1 cm layer, and sediment gravities decreased from the surface to a depth of approximately 4 cm. Sediment gravities were considerably higher in the layers deeper than 5 cm at 03S2327SC01.

3) Total Organic Carbon

Vertical distributions of total organic carbon concentrations of each station are shown in Fig. 3-6-3 and Appendix Table 2. At 03S2027SC01, the concentration in the 0-1 cm layer was 2.37 mg/g(D) on average, and was similar down to the 3-4 cm layer. But in the 4-5cm layer, it was 1.83 mg/g(D) on average, which was lower than the upper layers. At 03S2326SC01, the concentration from the surface to the 2-3 cm layers were 0.59～0.22 mg/g(D) on average, and at 03S2327SC01, the concentration from the surface to the 1-2 cm layers were 0.59～0.71 mg/g(D) on average. In the deeper layers at 03S2326SC01 and 03S2327SC01, the concentrations were higher than at each surface layer.

Thus, the total organic carbon concentrations showed a tendency to increase from the surface to deeper layers at the southern two stations, and vertical distributions were different from the central station.

4) Total Nitrogen

Vertical distributions of total nitrogen concentrations of each station are shown in Fig. 3-6-4 and Appendix Table 2. At 03S2027SC01, the concentration in the 0-1 cm layer was 0.40 mg/g(D) on average, and was similar down to the 3-4 cm layer. But in the 4-5cm layer, it was 0.27 mg/g(D) on average, which was lower than the upper layers. At 03S2326SC01, the concentration from the surface to the 2-3 cm layers were 0.05～0.10 mg/g(D) on average, and at 03S2327SC01, the concentration from the surface to the 1-2 cm layers were 0.10～0.14 mg/g(D) on average.

At the southern two stations, the total nitrogen concentrations showed a tendency to increase from the surface to deeper layers as seen for total organic carbon.

5) Sediment Particle Size Distribution

The sediment particle size distributions of each layer of each station are shown in Fig. 3-6-5 and Appendix Table 3.

At 03S2027SC01, each layer from the surface to the bottom showed bimodal distributions. It was observed, that particles with a diameter of 48~57μm showed the highest frequency and a second frequency peak was found for the particle diameter of 3.3μm in every layer of this station. On the other hand, each layer from the surface to the 3-4 cm layer at 03S2326SC01 showed a frequency peak similar to a normal distribution with the highest frequency at the particle diameter of 40~80μm. All layers deeper than 4 cm showed bimodal distributions, where both frequencies of particles with 40~160μm as well as 3~4μm diameter increased. At 03S2327SC01, the 0-1 cm and 1-2 layers showed distributions similar to a normal distributions with the highest frequency

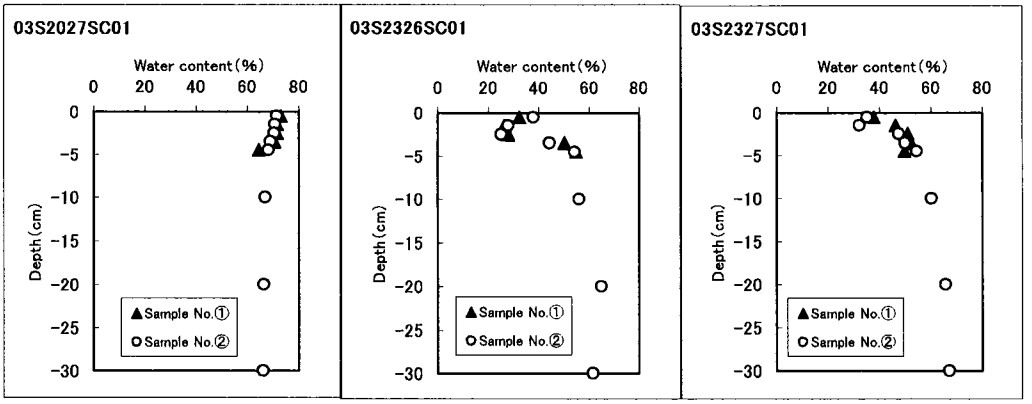

Fig. 3-6-1 Vertical Profiles of Water Content at Each Station

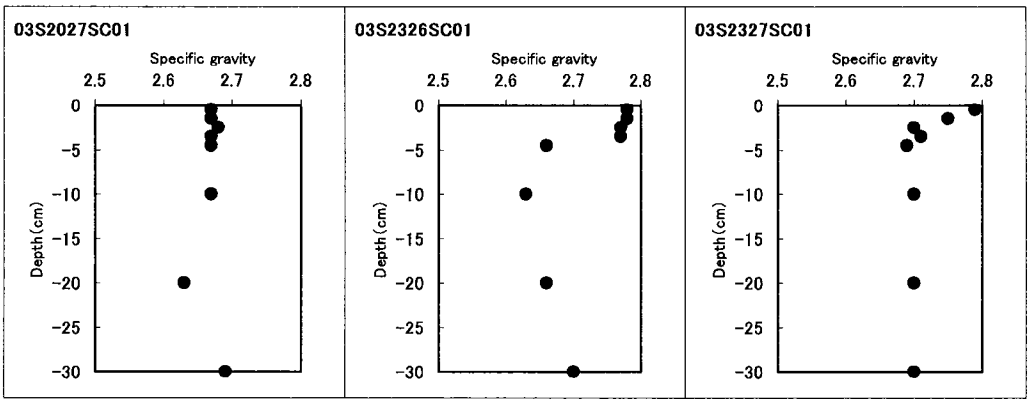

Fig. 3-6-2 Vertical Profiles of Specific Sediment Gravity at Each Station

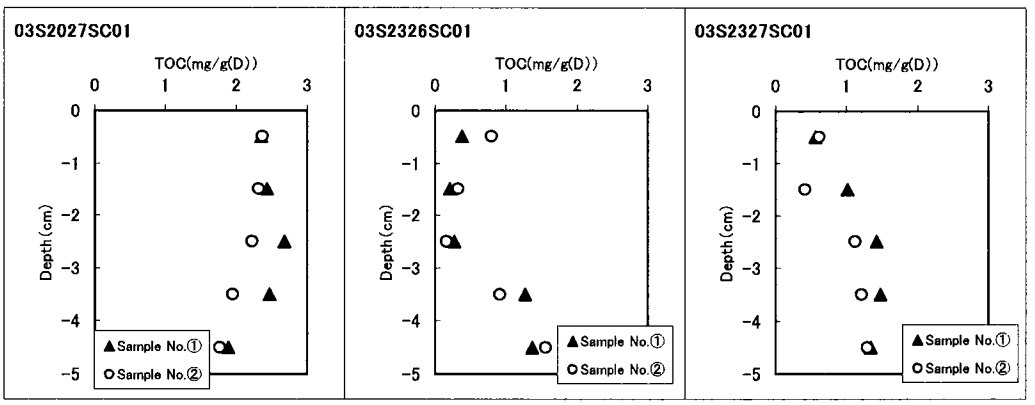

Fig. 3-6-3 Vertical Profiles of Total Organic Carbon at Each Station

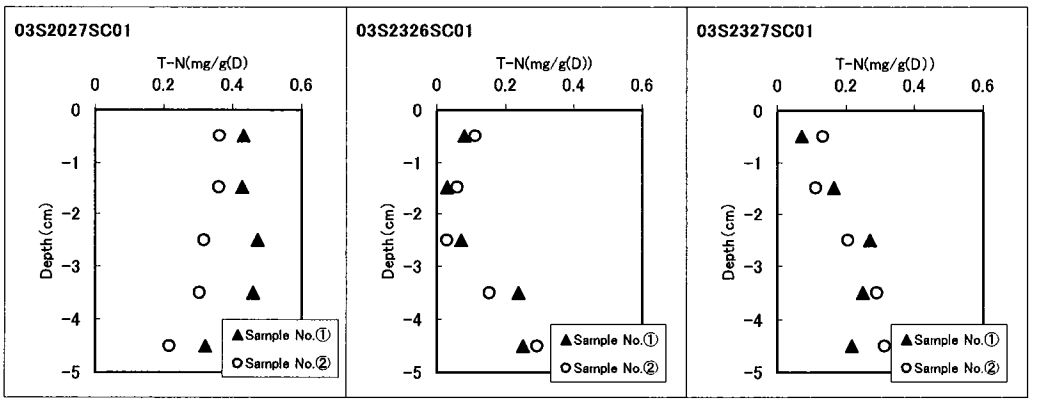

Fig. 3-6-4 Vertical Profiles of Total Nitrogen at Each Station

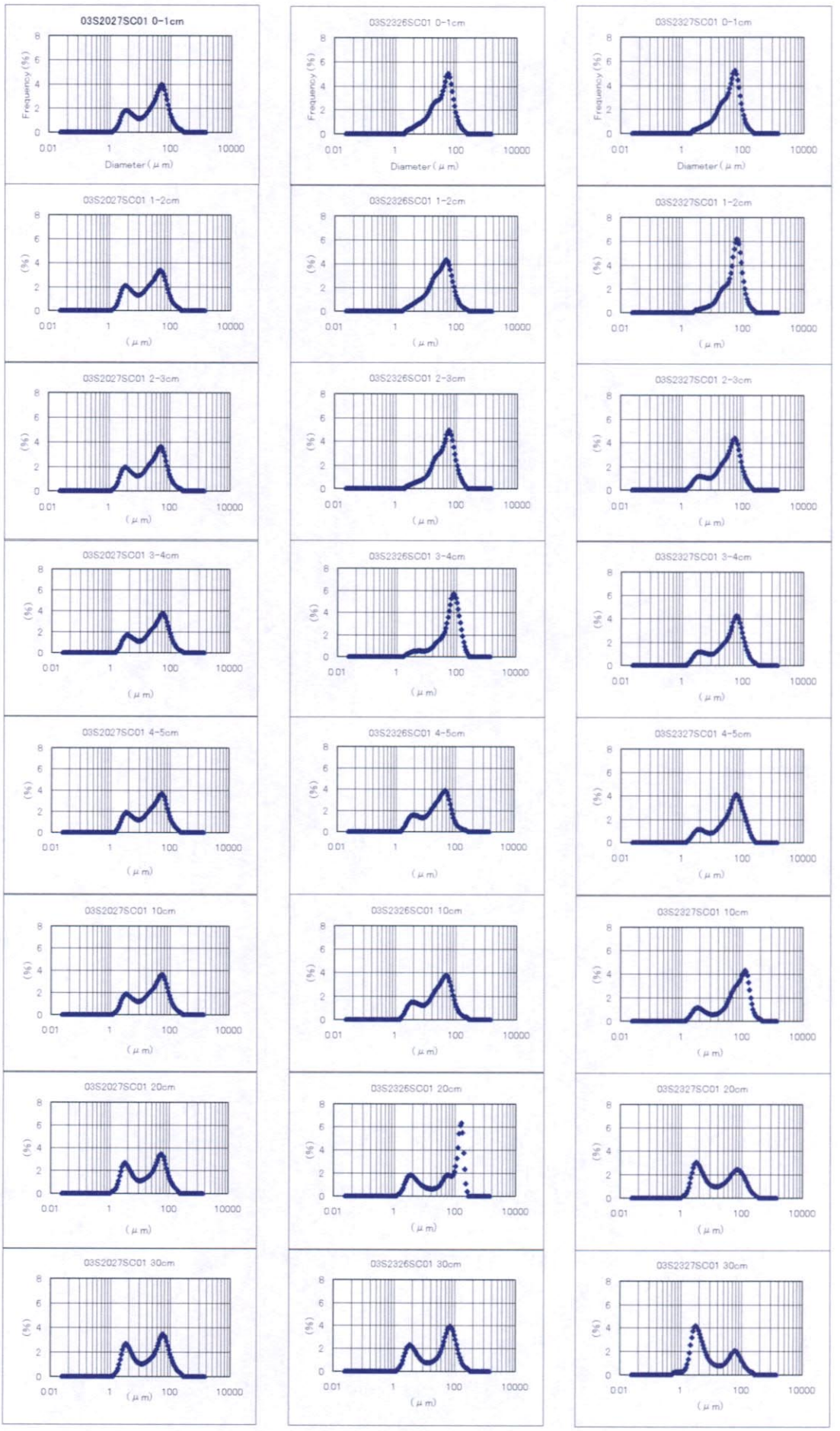

Fig. 3-6-5 Sediment Particle Size Distribution at Each Station

at the particle diameter of 57~62μm. All layers deeper than 2 cm showed bimodal distributions, where the frequency of 50~60μm diameter particles decreased and the frequency of 3~4μm diameter particles increased with increasing sediment depth.

Overall, bimodal distributions were found in all layers at the central station, while normal distributions were found in the upper layers at the southern two stations, followed by bimodal distributions in the layers deeper than 4 cm and 2 cm at 03S2326SC01 and 03S2327SC01, respectively.

(3) Benthic Organisms

1) Meiobenthos

Abundance and vertical distribution of metazoan meiobenthos at each station are shown in Table 3-6-1.

i. Fauna

Five taxa were identified from the meiobenthos samples, including Nematoda (two taxa), Annelida (one taxon) and Arthropoda (two taxa). Nematoda were found at all stations, while Annelida were only found at station 03S2326SC01, and Arthropoda were found at two stations, 03S2326SC01 and 03S2327SC01. Although Protozoa (Foraminifera) were observed at all stations, this phylum was excluded from the table.

ii. Abundance

The total metazoan meiobenthos abundance was 2.3 inds./10cm^2 on average at 03S2027SC01, 14.9 inds./10cm^2 at 03S2326SC01 and 28.8 inds./10cm^2 at 03S2327SC01. At 03S2027SC01, total abundance was lower than at the southern two stations. The most dominant organisms were nematodes which accounted for more than 84% of the abundance at every station, with the highest abundance of 27.7 inds./10cm^2 at 03S2327SC01. Comparing the samples from two cores at each station, no differences in nematode abundance were observed in the two cores.

iii. Vertical Distribution

At station 03S2027SC01, metazoan meiobenthos was observed in the 0-1 cm and 1-2 cm layers, while at the two southern stations (03S2326SC01 and 03S2327SC01) meiobenthos was only found in the 0-1 cm layer. Nevertheless, the abundance was much higher at the two southern stations than at the central station.

Table 3-6-1 Abundance and Vertical Distribution of Metazoan Meiobenthos at Each Station

inds. ／10cm^2

No.	Phylum	Class	Taxa	03S2027SC01-1					03S2027SC01-2					03S2027SC01 average					
				0-1cm	1-2cm	2-3cm	3-4cm	4-5cm	0-1cm	1-2cm	2-3cm	3-4cm	4-5cm	0-1cm	1-2cm	2-3cm	3-4cm	4-5cm	total
1	NEMATODA	ADENOPHOREA	Desmoscolecidae																
2			NEMATODA	1.1	1.1				2.3					1.7	0.6				2.3
3	ANNELIDA	POLYCHAETA	Cirratulidae																
4	ARTHROPODA	CRUSTACEA	Harpacticoida																
5			nauplius larvae																
			total	1.1	1.1	0	0	0	2.3	0	0	0	0	1.7	0.6	0.0	0.0	0.0	2.3

No.	Phylum	Class	Taxa	03S2326SC01-1					03S2326SC01-2					03S2326SC01 average					
				0-1cm	1-2cm	2-3cm	3-4cm	4-5cm	0-1cm	1-2cm	2-3cm	3-4cm	4-5cm	0-1cm	1-2cm	2-3cm	3-4cm	4-5cm	total
1	NEMATODA	ADENOPHOREA	Desmoscolecidae																
2			NEMATODA	10.2					14.7					12.5					12.5
3	ANNELIDA	POLYCHAETA	Cirratulidae	1.1										0.6					0.6
4	ARTHROPODA	CRUSTACEA	Harpacticoida	2.3										1.2					1.2
5			nauplius larvae						1.1					0.6					0.6
			total	13.6	0	0	0	0	15.8	0	0	0	0	14.9	0.0	0.0	0.0	0.0	14.9

No.	Phylum	Class	Taxa	03S2327SC01-1					03S2327SC01-2					03S2327SC01 average					
				0-1cm	1-2cm	2-3cm	3-4cm	4-5cm	0-1cm	1-2cm	2-3cm	3-4cm	4-5cm	0-1cm	1-2cm	2-3cm	3-4cm	4-5cm	total
1	NEMATODA	ADENOPHOREA	Desmoscolecidae	1.1										0.6					0.6
2			NEMATODA	28.2					26.0					27.1					27.1
3	ANNELIDA	POLYCHAETA	Cirratulidae																
4	ARTHROPODA	CRUSTACEA	Harpacticoida																
5			nauplius larvae	1.1					1.1					1.1					1.1
			total	30.4	0	0	0	0	27.1	0	0	0	0	28.8	0.0	0.0	0.0	0.0	28.8

2) Macrobenthos

Abundance and vertical distribution of metazoan macrobenthos at each station are shown in Table 3-6-2.

i. Fauna

Seven taxa were identified from the macrobenthos samples, including Nematoda (one taxon), Mollusca (one taxon), Annelida (three taxa) and Arthropoda (two taxa). These taxa were all present at station 03S2327SC01, but at stations 03S2027SC01 and 03S2326SC01 only Annelida were found. Although Protozoa (Foraminifera) were observed at all stations, this phylum was excluded from the table.

ii. Abundance

Abundance of the total metazoan macrobenthos was highest at station 03S2327SC01 with 564 inds./m^2. About 40% of these organisms were arthropods, making it the most abundant phyla at this station. A much lower abundance of 71 inds./m^2 was found at stations 03S2027SC01 and 03S2326SC01.

iii. Vertical Distribution

At 03S2027SC01 and 03S2326SC01, metazoan macrobenthos was only observed in the 0-1 cm layer. In contrast, at station 03S2327SC01 meibenthos was found down to 3 cm, with a decreasing abundance from 353 inds./m^2 in the 0-1 cm layer to 71 inds./m^2 in the 2-3 cm layer.

Table 3-6-2 Abundance and Vertical Distribution of Metazoan Macrobenthos at Each Station

inds. / m^2

No.	Phylum	Class	Taxa	03S2027SC01-1					03S2027SC01-2					03S2027SC01 average					
				0-1cm	1-2cm	2-3cm	3-4cm	4-5cm	0-1cm	1-2cm	2-3cm	3-4cm	4-5cm	0-1cm	1-2cm	2-3cm	3-4cm	4-5cm	total
1	NEMATODA		NEMATODA																
2	MOLLUSCA	BIVALVIA	BIVALVIA																
3	ANNELIDA	POLYCHAETA	Paraonidae	141										71					71
4			Cirratulidae																
5			Sabellidae																
6	ARTHROPODA	CRUSTACEA	Harpacticoida																
7			Isopoda																
			total	141	0	0	0	0	0	0	0	0	0	71	0	0	0	0	71

No.	Phylum	Class	Taxa	03S2326SC01-1					03S2326SC01-2					03S2326SC01 average					
				0-1cm	1-2cm	2-3cm	3-4cm	4-5cm	0-1cm	1-2cm	2-3cm	3-4cm	4-5cm	0-1cm	1-2cm	2-3cm	3-4cm	4-5cm	total
1	NEMATODA		NEMATODA																
2	MOLLUSCA	BIVALVIA	BIVALVIA																
3	ANNELIDA	POLYCHAETA	Paraonidae																
4			Cirratulidae	141										71					71
5			Sabellidae																
6	ARTHROPODA	CRUSTACEA	Harpacticoida																
7			Isopoda																
			total	141	0	0	0	0	0	0	0	0	0	71	0	0	0	0	71

No.	Phylum	Class	Taxa	03S2327SC01-1					03S2327SC01-2					03S2327SC01 average					
				0-1cm	1-2cm	2-3cm	3-4cm	4-5cm	0-1cm	1-2cm	2-3cm	3-4cm	4-5cm	0-1cm	1-2cm	2-3cm	3-4cm	4-5cm	total
1	NEMATODA		NEMATODA	141										71					71
2	MOLLUSCA	BIVALVIA	BIVALVIA						141					71					71
3	ANNELIDA	POLYCHAETA	Paraonidae		141										71				71
4			Cirratulidae																
5			Sabellidae	141										71					71
6	ARTHROPODA	CRUSTACEA	Harpacticoida	141	141				141					141	71				212
7			Isopoda								141					71			71
			total	423	282	0	0	0	282	0	141	0	0	353	141	71	0	0	564